MHD-CONJUGATE MIXED CONVECTION OVER A VERTICAL HOLLOW CYLINDER EMBEDDED IN A SATURATED POROUS MEDIUM

By

Yaser Abdo Al-kablawi

Suppervisor

Dr. Hamzeh M. Duwairi

This Thesis was Submitted in Partial Fulfillment of the Requirements

For the Master's Degree of Science

In

Mechanical Engineering

Faculty of Graduate Studies

The University of Jordan

April,2005

This Thesis (MHD-Conjugate mixed convection over a vertical hollow cylinder embedded in a saturated porous medium) was successfully defended and approved on April 20-2005.

Examination Committee	**Signature**
Dr. Hamzeh Duwairi (Chairman of the committee)	.....
Prof. Mahmoud Hammad (Member of the committee)	.....
Dr. Ali-Al-shawabkeh (Member of the committee)	.....
Prof. Mahmoud Alhusein (Mu'tah University, Member of the committee)	.....

The University of Jordan
Authorization Form

I, Yaser Alkablawi, authorize the University of Jordan to supply copies of my Thesis to libraries or establishments or individuals on request.

Signature:

Date: April 20, 2005

DEDICATION

- *To my father, who has given his unlimited and unconditional love and care, without his support, I could not succeed.*
- *To my loving mother, whose presence has been my motivation.*
- *To my wife Rasha, and my kid; Abed Alhaleem.*
- *To my brothers and sisters: Ali, Fadi, Fadia, Maies, Lara, Reem, and Lina.*
- *To my niece, nephew: Rawa , Mhammad.*

ACKNOWLEDGEMENT

I would like to express my sincere gratitude and deepest appreciation to my advisor Dr. Hamzeh Dwiari for his substantial inspiration and technical guidance throughout this study.

Also my thanks extended to the members of the committee: Prof. Mahmoud Hammad, Prof. Mahmoud Al-Husein, Dr. Ali Al-Shawabkeh. For their support, help and valuable advises in writing this thesis.

Great thanks to my friends, and all who have contributed in bringing out this work.

LIST OF CONTENTS

LIST OF TABLES

LIST OF FIGURES

LIST OF SYMBOLS

B_o	Magnetic field flux density, wb/m^2
Cf_x	Local skin friction factor
c_p	Specific heat at constant pressure, J/kg.K^o
D_o	Particle diameter, m
$\vec{E}$	Electric field vector, volt/m
f	Dimensionless stream function
F_e	Electrical force, N
F_m	Magnetic force, N
Ge_x	Gebhart number (g βx/ c_p).
$\overset{*}{Ge}_x$	Modify Gebhart number (Ge_x/(1-ζ)^2)
g	Acceleration of the gravity, m/s^2
h_x	Local heat transfer coefficient, w/m^2.K^o.
$\bar{h}$	Average heat transfer coefficient, w/m^2.K^o
Ha_x	Hartman number $\left(B\sqrt{K\sigma/\mu}\right)$
H	Magnetic field influence (1+(Ha_x)^2/ ε)
K	Permeability coefficient of the porous medium, m^2
K'	Coefficient of Forchheimer, m
.k	Effective thermal conductivity, w/m.K^o
L	Length of the cylinder, m
Nu_x	Local Nusselt number (h_x.x/k)
$\bar{N}u$	Average Nusselt number ($\bar{h}$ .x/k)

Pr	Prantdle number (ν/α)
Pe_x	Local Peclet number $(u_\infty x/\alpha)$
P	Pressure, N/m^2
P^*	Conjugate conduction parameter
J	Current density, ampere/area
Re	Reynolds number ($K' u / \nu$)
Re^*	Modify Reynolds number (Re/ζ^2)
Ra_x	Local Rayleigh number $(Kg\beta\Delta Tx/\alpha\upsilon)$
r_o, r_i	Outer and inner radii of the cylinder, m
T	Temperature, K^o
ΔT	Reference temperature, K^o
u , v	Velocity components in x- and r- directions,m/s
x, r	Axial and radial coordinates

Greek symbols

α	Effective thermal diffusivity of saturated porous medium, m^2/s
μ	Dynamic viscosity, $N.s/m^2$
υ	Kinematical viscosity, m^2/s
ε	Porosity
ρ	Fluid density, kg/m^3
σ	Electrical conductivity, mho/m
μ_o	Magnetic permeability

ρ_e	Charge density
β	Volumetric coefficient of thermal expansion , $1/K^o$
θ	Dimensionless temperature
ψ	Stream function
ζ	Non-similarity parameter
η	Similarity parameter
λ	Curvature parameter
δ	Thickness of the boundary layer, m
τ_w	Local wall shear stress, N/m^2
χ	Non-similarity parameter

Subscripts

∞	Free stream condition
w	Wall condition
s	Solid condition
m	Fluid
b	Inner surface of the cylinder

MHD-CONJUGATE MIXED CONVECTION OVER A VERTICAL HOLLOW CYLINDER EMBEDDED IN A SATURATED POROUS MEDIUM

By

Yaser Abdo Al-kablawi

Supervisor

Dr. Hamzeh Mustafa Duwairi

ABSTRACT

In this study, the combined effect of forced and natural convection heat transfer in presence of transverse magnetic field over a vertical slender, hollow cylinder embedded in a saturated porous medium with viscous dissipation effects included in the energy equation are studied. Both cases of the mixed convection heat transfer problem namely: the buoyancy aiding and the buoyancy opposing flows are investigated. The governing equations are solved using Keller box methods, and the solutions are obtained for two different nonsimilarity parameters. The first one is $\zeta = \frac{Pe_x^{1/2}}{Pe_x^{1/2} + Ra_x^{1/2}}$, which covers the entire mixed convection regime, where ζ=0 corresponds to pure free convection, and ζ=1 corresponds to pure forced convection. The second nonsimilarity parameter is $\chi = \frac{g\beta x}{c_p}$, which covers the mixed convection regime. The effects of the characteristic parameters on the velocity, temperature, local coefficient of friction and heat transfer rates are found and drawn for both cases of nonsimilarity parameters.

INTRODUCTION

1. Introduction:

It is very important to get better understanding of the flow in porous media. Many processes in nature involve transport processes in such media. In many parts of the world water that has been stored for thousands of years in large volumes of porous rock is an important asset. Similarly the world supply of oil was formed and stored, under rather special circumstances in porous rock formations. Other processes, which involve flow in porous media, are frost heaves, filtration or straining and sewage purification in sand beds. The flow of homogeneous fluids through porous media is sufficiently wide in scope to find application in many branches of applied science. By the term homogeneous fluid is meant essentially a single-phase fluid. This may be either a gas or a liquid. The study of fluid, which is electrically conducted and moves in a magnetic field, is known as a magnetohydrodynamics (MHD). The simplest of this kind of the fluid is liquid metals for example mercury. However, the study of MHD flow in a porous media becomes very important in recent studies, specially when we cant neglect the effect of MHD, such that in the nuclear reactor, where the MHD effect is very dangerous and very important.

In addition to that, the heat transfer through a porous media, for two centuries, had been a subject of extensive investigations, geothermal operations, and refrigeration cycles insulation. On the other hand, conjugate heat transfer plays a great rule in determining the thermal behavior of most engineering systems, as in heat exchangers. In general, the natures of the porous media with which deal are:

1- Porosity, which is a measure of the pore space and hence of the fluid capacity of the medium.

2- Permeability, which is a measure of the ease with which fluids may transfer the medium under the influence of a driving pressure.

2. Darcy and Non-Darcy Models:

The bulk resistance to flow of a fluid through a solid matrix was first measured by Darcy (1856). Darcy experiment used nearly uniform-size particles that where randomly and closely packed, i.e., a non-consolidated, uniform, rigid and isotropic solid matrix (Nield and Bejan, 1999)

The macroscopic flow was steady, one-dimensional and driven by gravity. The mass flow rate of the liquid was measured and the filtration or filter velocity was determined by dividing the mass flow rate by the product of fluid density and the cross sectional area of the channel. In applying volumetric force balance to this flow. He discovered that the bulk resistance can be characterized by the viscosity of the Newtonian fluid μ and the permeability of the solid matrix K . such that:

$$-\frac{dp}{dx}=\frac{\mu}{K}u_p \tag{1.1}$$

Where u_p the Darcy velocity in the porous medium, dimension of K is in square of length, the experimental measurements have shown that the equation (1.1) is valid as long as the flow is slow enough or the pores are small enough so that O(Re)< 1, where Reynolds number is defined as:

$$\mathrm{Re} = \frac{u\ K^{1/2}}{\upsilon} \tag{1.2}$$

In other words, the formulation of Darcy's law completely neglects the viscous force action along the impermeable surface and effects of the solid boundary. Accounts for the inertia effect Forchheimer's modification of the Darcy's law is presented as (Bejan,1972):

$$u + \frac{K'}{\upsilon} u^2 = -\frac{K}{\mu}\left(\frac{dp}{dx}\right) \tag{1.3}$$

Where K' is empirical constant correlated as(Plumb and Huenefeld,1981):

$$K' = 1.75\ D_o / (150\ (1-\varepsilon)) \tag{1.4}$$

The order of Darcy's law is lower than the Navier-Stokes equation, so that, the no slip boundary condition is not required to be imposed on the impermeable boundary.To account for noslip condition effects Brinkman model has been used(Hsu and heng,1985)

$$u = \frac{K}{\varepsilon}\nabla^2 u - \frac{K}{\mu}(\nabla p + \rho g) \tag{1.5}$$

Recently, to combine two effects of non-Darcy model, the Brinkman Forchheimer's extension has been used(Nield,1991). The governing equation becomes:

$$u + \frac{K'}{\upsilon} u^2 = \frac{K}{\varepsilon}\nabla^2 u - \frac{K}{\mu}(\nabla p + \rho g) \tag{1.6}$$

In this model, it is assumed that the flow velocity is large enough or the pores are big enough so that:

$$O\left(\frac{uK^{\frac{1}{2}}}{\upsilon}\right) > 1 \tag{1.7}$$

3. Mixed convection (Natural convection versus forced convection):

In the context of heat transfer, convection means the process of carrying the thermal energy away from a solid surface to an adjacent moving fluid in the presence of temperature differences. The convection process has two contributing mechanisms:

1- The conduction of heat from a solid surface to a thin layer of adjacent fluid.

2- The movement of hot fluid particles a way from the solid surface.

Where the movement of the fluid particles can be attributed to pressure changes, to buoyancy, or to a combination of both. Thus, the study of convective heat transfer is intimately related to the study of fluid flow.

In general, the discussion of convective heat transfer can be divided into two areas, namely, forced convection and natural convection, mixed convection occurs when both modes of convection act together.

The forced convection is very important rather than natural convection, because of it is industrial applications, Most of industrial heating or cooling devices such as, heat exchangers, condensers and boilers, etc. Natural convection, on the other hand, plays an important role in thermal pollution, and in ecological problems.

Mixed convection heat transfer is combination of natural and forced convection, the extreme limits of mixed convection satisfies pure forced convection and pure natural convection limits.

4. Conjugate heat transfer:

Conjugate heat transfer refers to the heat transfer processes involving an interaction of conduction in a solid body and convection in the fluid surrounding it. Thus the analysis of this type of heat transfer processes necessitates, and coupling of the conduction in solid tube wall is greatly influenced by the convection in fluid flowing over it. Another example of practical importance of conjugate heat transfer is found in fins. The conduction within the fin and convection in the fluid surrounding it, must be simultaneously analyzed to obtain vital design information.

5. Heat transfer in magneto hydrodynamic (MHD) system:

Magneto hydrodynamics (MHD) is a relatively new but important branch of fluid dynamics. It is concerned with the interaction of electrically conducting and electromagnetic fluids. When a conducting fluid moves through a magnetic field, an electric field and consequently a current may be induced and, in turn, the current interacts with the magnetic field to produce a body force on the fluid. MHD flow occurs

in the sun, the earths interior, the ionosphere, and the stars and their atmosphere, and many new devices have been made which utilize the fluid electromagnetic field interactions, such as traveling wave tubes, electrical discharges, and many others.

Holman (1990) had examined some basic electromagnetic concept as follows:

For a neutrally charged system the current density $\vec{J}$ is given by:

$$\vec{J} = \sigma.\vec{E} \tag{1.8}$$

Where σ is the electrical conductive and $\vec{E}$ is the electric field vector. The magnetic field strength $\vec{B}$ is expressed by (Holman ,1990):

$$\vec{B} = \mu_o.\vec{H} \tag{1.9}$$

Where μ_0 is called the magnetic permeability and $\vec{H}$ is the Magnetic field intensity. The force exerted on a system of charged particles by an electric field is given by (Holman,1990):

$$\vec{F}_e = \rho_e.\vec{E} \tag{1.10}$$

Where ρ_e is the charge density. The magnetic force exerted on a current carrying conduction is (Holman,1990):

$$\vec{F}_m = \vec{J} \,\mathrm{X}\, \vec{B} \tag{1.11}$$

The total electromagnetic force is given by (Holman,1990):

$$\vec{F}_{em} = \rho_e.\vec{E} + \vec{J} \,\mathrm{X}\, \vec{B} \tag{1.12}$$

The work done on the system per unit time by the electromagnetic force is (Holman,1990):

$$W_{em} = \vec{F}_{em}.\vec{V} \tag{1.13}$$

Where $\vec{V}$ is the velocity of the conductor.

The magnetic field induces a current in the conductor Holman (1990):

$$\vec{J}_{ind} = \sigma(\vec{V} \times \vec{B}) \tag{1.14}$$

Then, the conduction current is defined as Holman (1990):

$$\vec{J}_c = \sigma(\vec{E} + \vec{V} \times \vec{B}) \tag{1.15}$$

And the total current flow is Holman (1990):

$$\vec{J} = \vec{J}_c + \rho_e . \vec{V}$$

For the electromagnetic work Holman (1990) :

$$W_{em} = \vec{E} . \vec{J} - \frac{\vec{J}_c . \vec{J}_c}{\sigma} \tag{1.17}$$

The fluid dynamical aspects of MHD are handled by adding the electromagnetic force and work to non-Darcy equations and energy equation respectively.

The momentum equation in x-direction (Kaviany, 1991):

$$u + \frac{K'}{\upsilon} u^2 = -\frac{K}{\mu}\left(\frac{dp}{dx} + \rho g\right) - \frac{K \sigma B_0^2}{\mu \varepsilon} \tag{1.18}$$

Where the term $\left(\frac{K\sigma B_0^2}{\mu\varepsilon}\right)$ represents the effect of magnetic field force on the fluid velocity. And the energy equation becomes(Kaviany, 1991):

$$u \frac{\partial T}{\partial x} + v \frac{\partial T}{\partial r} = \frac{\alpha}{r} \frac{\partial}{\partial r}\left(r \frac{\partial T}{\partial r}\right) + \frac{u}{K C_p}\left(u + K' u^2\right) + \frac{\sigma B_0^2}{\rho C_p} u^2 \tag{1.19}$$

Where the term $(\sigma B_0^2 u^2)$ represents the work done by the magnetic field force on the fluid.

REVIEW OF LITERATURE

1. Introduction:

Since the early work of Darcy in the 19th century, extensive investigation have been conducted on flow and heat transfer through porous media, covering range of different fields and application such as geothermal operation, nuclear reactors, transpiration cooling, and building thermal insulation.

2. Magneto hydrodynamic flow:

Magneto hydrodynamics has been a subject for many researchers in the field. Henoch and Meng (1991) used the magnetic force to retard the transition to the turbulent boundary layer and reduce the frictional Darcy force. Kim and Lee (2000) set up an experiment using a circular cylinder where electrodes and magnets are installed in an alternative sequence in axial direction of the cylinder to generate magnetic force in the circumferential direction. Many authors had studied the effects of magnetic on mixed, natural and force convection heat transfer problems. Chandra and Gosh (2001) studied the effect of magnetic field on electrically conducted visco-elastic fluid; they found in such a flow that the velocity field decreases with increase of magnetic field strength.

In the following a review of the works and the results of some researchers on this field is addressed.

2.1 Effect of MHD on natural convection:

Sparrow and Cess (1961) investigated the free convection heat transfer due to the simultaneous action of buoyancy and induced magnetic forces, the analysis is carried out for laminar boundary-layer flow about an isothermal vertical plate. They found that the free convection heat transfer to liquid metals may be significantly affected by the presence of magnetic field, but that very small effects are experienced by other fluid.

Raptis and Singh (1983) studied the effect of a uniform transform transverse magnetic field on the free convection flow of an electrically conducting fluid past an infinite vertical plate for both the classes of impulsive as well as uniformly accelerated motion of the plate. They found that the effect of the magnetic field is to increase the velocity field on both cases.

Jha (2001) discussed the combined effect of natural convection and uniform transverse magnetic field on the quette flow of an electrically conducting fluid between two parallel plates for impulsive motion of one plate, Comparative study is made between the velocity field for magnetic field fixed with respect to plate and a fixed magnetic field with respect to the fluid

Hossain (1992). had studied the effect of viscous and joule heating on the flow of an electrically conducting and viscous incompressible fluid past a semi-infinite plate of which temperature varies linearly with the distance from the leading edge and in the presence of uniform transverse magnetic field. The equations governing the flow are solved numerically applying the finite difference method along with Newton's linearization approximation.

Duwairi and Damseh (2004,a) studied the effects of MHD-natural convection heat transfer from rading vertical porous surfaces, they found nonsimilarity parameter to

solve this problem with fluid suction or injection along the stream wise coordinate. Three dimensionless parameters had been found to describe the problem, and they found that increasing the magnetic field strength decreases the velocity and the heat transfer rates inside the boundary layer.

Recently, Duwairi and Duwairi (2004) studied the thermal radiation heat transfer effects on the Rayleigh flow of gray viscous fluids under the effect of a transverse magnetic field. The free convection heat transfer problem from constant surface heat flux moving plate is selected for study. It is found that the increasing of the magnetic field strength decreased the velocity inside the boundary layer

2.2 Effect of MHD on mixed convection heat transfer:

The combined effects of forced and natural convection heat transfer in the presence of transverse magnetic field from vertical surfaces are studied by many Researchers. Garandet et al. (1992) had analyzed the equations of the magnetohydrodynamics that can be used to model the effect of a transverse magnetic field on the buoyancy driven convection in a two dimensional cavity.

Aldoss et al.(1995) Studied the effect of mixed convection heat transfer from a vertical plate embedded in a saturated porous medium and subjected to a uniform magnetic field. They found the strength of the magnetic field has an effect on the Nusselt number and wall shear stress, and increasing the magnetic field strength has the effect of decreasing the local Nusselt number in the mixed convection regime.

Tashtoush (2000) introduced a new analytical solution for the effect of viscous dissipation on mixed convection flow and heat transfer about an isothermal vertical wall embedded in Darcy and non-Darcy porous media with uniform free stream velocity, the effect of viscous dissipation on mixed convection in both regimes has been analyzed. A good agreement was found between the numerical and analytical solutions. It was found

from the Nusselt number results that viscous dissipation lowers the heat transfer rate in both Darcy and Forchheimer's flow regimes.

Recently, Dawairi and Damseh (2004,b). Studied the MHD-buoyancy aiding and opposing flows with viscous dissipation effects from radiate vertical surfaces. They found that increasing the Hartman number had decreased the velocity inside the boundary layer and the heat transfer rates from the porous plate, and increasing the Eckert number or the viscous dissipation effect is found to increase the conductive fluid temperature and consequently decrease the heat transfer rates.

3. Conjugate heat transfer:

The conjugate heat transfer from vertical surfaces has attracted many researchers because of its importance in many applications, such as in the nuclear reactor, exchangers. Luikov et al.(1971) studied the conjugate heat transfer problem of laminar forced convection along a flat plate and they solved the problem by means of the generalized Fourier sine transformation and a series expansion in terms of the Fourier variable.

Karvinen (1978) presented an approximate method for solving the conjugated heat transfer from a flat plate in the presence of uniform internal heat generation. The results have been compared with a variable experimental data.

Sparrow and Chyu (1982) carried out a conjugate heat transfer analysis for a vertical plate fin washed by laminar forced convection boundary layer flow. They assumed the heat conduction in the fin to be one dimensional, and the results have been compared with those from the conventional methods.

Huang and Chen (1984) have studied a vertical thin circular pin fin in forced convection flow. They have considered one dimensional heat conduction, the governing equations have been solved by an efficient implicit difference method. And the results

are presented for a range of values of conjugated convection conduction parameter and the transverse curvature parameter.

Velusamy and Garg (1988) have obtained the heat transfer characteristics for a vertical cylindrical fin washed by a combined forced and free convective flow. The effects of various parameters have been analyzed numerically by treating one-dimensional heat conduction in the fin. The conjugate heat transfer from vertical or horizontal surfaces as well as horizontal cylinders embedded in porous media have extensively investigated by Kimura and Pop(1991, a and b), Kimura and Pop (1992), Kimura and Pop(1994), Vynnycky and Kimura(1994), Pop et al..(1995), Lesnic et al.(1995), Kimura et al.(1997).

recently, Jilani et al.(2002) had studied the problem of conjugate forced convection. Taking into account conduction heat transfer over a vertical cylinder with heat generation they found that higher length to diameter ratio corresponds to higher flow Reynolds number which in turn gives rise to higher convective heat transfer.

4. Cylindrical geometry:

Aldoss et al.(1996) analyzed the problem of non-Darcian mixed convection about a vertical cylinder embedded in a porous medium. They found nonsimilarity solutions for the case of variable wall temperature and variable surface heat flux. They found that the Non-Darcian model results are much different than those obtained using Darcian model alone. A boundary parameter has the effect of reducing the heat transfer rates in the entire regime, while the inertia parameter decreases the heat transfer rates in the natural convection regime and increases it in the forced convection regime.

Pop and Na (2000) made a numerical study of the conjugate free convection over a vertical slender, hollow, circular cylinder with the inner surface at constant temperature and embedded in porous medium, and by using a nonsimilarity

transformation. They solved the problem and found the effects of the conjugate parameter on the velocity and heat transfer rates inside the boundary layer. Also they found that the convection heat transfer rates increase with increasing in the radius of the cylinder, the temperature of the fluid will increase as the axial distance increases. And the temperature of the outer surface of the cylinder will decrease as the conjugate parameter increases.

Takhar et al.(2000) studied the problem of mixed convection flow over a continuous moving vertical cylinder under the combined buoyancy effect of thermal and mass diffusion, the surface skin friction and heat transfer rates increase with the increase of buoyancy forces, and the heat transfer rate was found to increase with the increase in the cylinder curvature.

Jilani et al.(2002) had studied the problem of the conjugate force convection taking into account conduction heat transfer over a vertical cylinder with heat generation, they found that higher length to diameter ratio corresponds to higher flow Reynolds number which in turn gives rise to higher convective heat transfer.

Recently, Duwairi and Al-araj (2004) had studied the combined effects of forced and natural convection heat transfer in the presence of transverse magnetic field from a vertical cylinder with radiation heat transfer effects from its surface. The buoyancy aiding and the buoyancy-opposing flows are investigated with viscous dissipation effects included in the governing equations they found that the increasing of the mixed parameter increases the velocity and temperature gradients for the buoyancy- aiding flow, and decreases the velocity and heat rates for the buoyancy-opposing flow.

5. Present contributions to the previous work:

In the present study we propose a mathematical model to investigate the conjugate problem of mixed convection over the out side surface of a vertical slender, hollow, circular cylinder which is embedded in a porous medium with MHD and viscous dissipation effects included in the governing equations, the temperature of the inner surface of the cylinder is kept at a constant value T_b and the temperature of the outer surface is determined by the conjugate boundary condition on the outer surface of the cylinder, The viscous dissipation effects include in the energy equation and the MHD effects are included in both energy and momentum equations. The boundary layer equations outside the cylinder and the one dimensional heat conduction equation for the hollow cylinder are simultaneously solved. these equations are solved by finite difference method known as Keller-box Scheme.The results obtained in terms of velocity, temperature, skin friction coefficient and local Nmussel number for different dimensionless groups are presented and drawn.

PROBLEM FORMULATION

1. Introduction:

Several analytical studies have been performed in recent years relating to the problem of steady two-dimensional convection about an infinite long vertical cylinder. In most of these studies a linear orthogonal coordinate system is used. Further more, it is assumed that Darcy's law and the boundary layer approximation are applicable. However, the inertial and boundary effects are expected to play significant roles in momentum and heat transfer rates where the Reynolds number is large. This is especially true for the case of either the high Rayleigh number regime or for the high porosity media.

2. Analysis:

The geometry considered is vertical slender, hollow circular cylinder with inner and outer radii r_i and r_0, respectively, which embedded in a fluid- saturated porous medium as shown in fig. (3.1).

To combine natural and forced convection, the fluid is viscous and electrically conducted so the influence of transversely magnetic field is considered on such a flow. The following important assumptions are made in order to obtain the governing equations:

1- The flow is steady, laminar, incompressible and two-dimensional.

2- The Boussinesq approximation is valid. Which is a two part approximations:(a) it neglects all variable property effects in the three governing equations, excepct

for density in the momentum equations, and (b) it approximates the density difference term with a simplified equation of state

$$\rho = \rho_{\infty}(1-\beta(T-T_{\infty})) \tag{3.1}$$

Where β is the volumetric coefficient of thermal expansion.

3- The fluid and solid matrix are everywhere in local thermodynamic equilibrium.

4- The Thermo physical properties of the fluid are homogeneous and isotropic.

5- The temperature of the fluid is everywhere below the boiling point.

6- The cylinder surface is impermeable, with no injection at the wall.

7- The saturated porous medium considered as a continuum.

8- The magnetic field is uniform throughout the boundary layer.

9- The heat flux by conduction inside the cylinder is one-dimensional.

10- The flow field a round the cylinder is assumed to be axsymmetric.

Under these assumptions the governing equations which describing the problem are (Kaviany, 1991):

Continuity equation:

$$\frac{\partial(ru)}{\partial x}+\frac{\partial(rv)}{\partial r}=0 \tag{3.2}$$

X-momentum equation:

$$u+\frac{K'}{\upsilon}u^2+\frac{\sigma B_0^2}{\mu\varepsilon}u=-\frac{K}{\mu}(\frac{dp}{dx}+\rho g) \tag{3.3}$$

Energy equation:

$$u\frac{\partial T}{\partial x}+v\frac{\partial T}{\partial r}=\frac{\alpha}{r}\frac{\partial}{\partial r}(r\frac{\partial T}{\partial r})+\frac{u}{KC_p}(\upsilon u+K'u^2)+\frac{\sigma B_0^2}{\rho C_p}u^2 \tag{3.4}$$

Where x and r are the axial and radial coordinates, and the corresponding velocities are u and v respectively, the gravitational acceleration g is acting downward in the direction opposite to the x coordinate. The non-Darcy effects are introduced through the

term ($\frac{K'}{\upsilon}u^2$) in the momentum equation. This term represents the effect of inertial forces, while in this study had neglected the term ($\frac{\mu}{\varepsilon}\frac{\partial^2 u}{\partial r^2}$), this term represents boundary layer effects, so that the no-slip velocity boundary condition is not needed.

The viscous dissipation effect is introduced by the two terms ($\frac{\upsilon}{KC_p}u^2 + \frac{K'}{KC_p}u^3$), in the energy equation (Murthy and Singh,1997). In addition, the magnetic effect is introduced into the governing equations through two terms:($\frac{\sigma B_0^2}{\mu\varepsilon}u$) In the momentum equation, which represent the effect of magnetic force, and ($\frac{\sigma B_0^2}{\rho c_p}u^2$) in the energy equation, which represent the magnetic work on the viscous fluid.

3. Boundary condition:

The system of equation (3.3. -3.4.) are constrained to the following boundary conditions:

Conduction boundary condition: as shown in Fig (3.1) the inner surface of the cylinder is held at a constant temperature T_b, while the temperature of the ambient fluid is T_∞, where $T_b > T_\infty$. The outer surface of the cylinder is held at a variable temperature $T(x,r_o)$,which is determined from the heat conduction equation inside the cylinder as following:

$$\frac{1}{r}\frac{\partial}{\partial r}\left(r\frac{\partial T_s}{\partial r}\right) + \frac{\partial^2 T_s}{\partial x^2} = 0 \qquad (3.5)$$

Where, Ts is the temperature inside the solid cylinder.

If equation (3.5) is normalized by introducing the dimensionless variables:

$$\bar{r} = \frac{r}{r_o} \quad , \qquad \bar{x} = \frac{x}{L}, \qquad \theta_s = \frac{T_s - T}{\Delta T} \tag{3.6}$$

Where $\Delta T = T_b - T_\infty$ and by substitution equation (3.6):

$$\frac{1}{\bar{r}} \frac{\partial}{\partial \bar{r}} (\bar{r} \frac{\partial \theta_s}{\partial \bar{r}}) + (\frac{r_o}{L})^2 \frac{\partial^2 \theta_s}{\partial \bar{x}^2} = 0 \tag{3.7}$$

Assuming that $\frac{r_o}{L} << 1$, then the axial conduction temperature, $\frac{\partial^2 T_s}{\partial x^2}$, can be neglected, so that equation (3.7) becomes

$$\frac{1}{\bar{r}} \frac{\partial}{\partial \bar{r}} (\bar{r} \frac{\partial \theta_s}{\partial \bar{r}}) = 0 \tag{3.8}$$

Subject to the conditions:

At $r = r_i$: $T_s = T_b$ (3.9)

At $r = r_o$: $T_s = T(x, r_0)$

The solution of equation (3.8), with respect to the conditions (3.9), is:

$$T_s = T_b + (T(x, r_o) - T_b) \frac{\ln(r / r_i)}{\ln(r_0 / r_i)} \tag{3.10}$$

On the other hand, at the outer surface of the cylinder the heat flux from the solid and fluid-porous medium interface are equal:

At $r = r_0$: $-k_s \frac{dT_s(r_o)}{dr} = -k_m \frac{\partial T(x, r_o)}{\partial r}$ (3.11)

Substitute equation (3.10) in equation (3.11) this yield:

At $r = r_0$: $v = 0$, $T = T(x, ro)$

Where $T(x, r_o) = T_b + \frac{k_m}{k_s} r_o \ln\left(\frac{r_o}{r_i}\right) \frac{\partial T(x, r_o)}{\partial r}$ (3.12)

And when $r \to \infty$: $u = u_\infty$, $T = T_\infty$

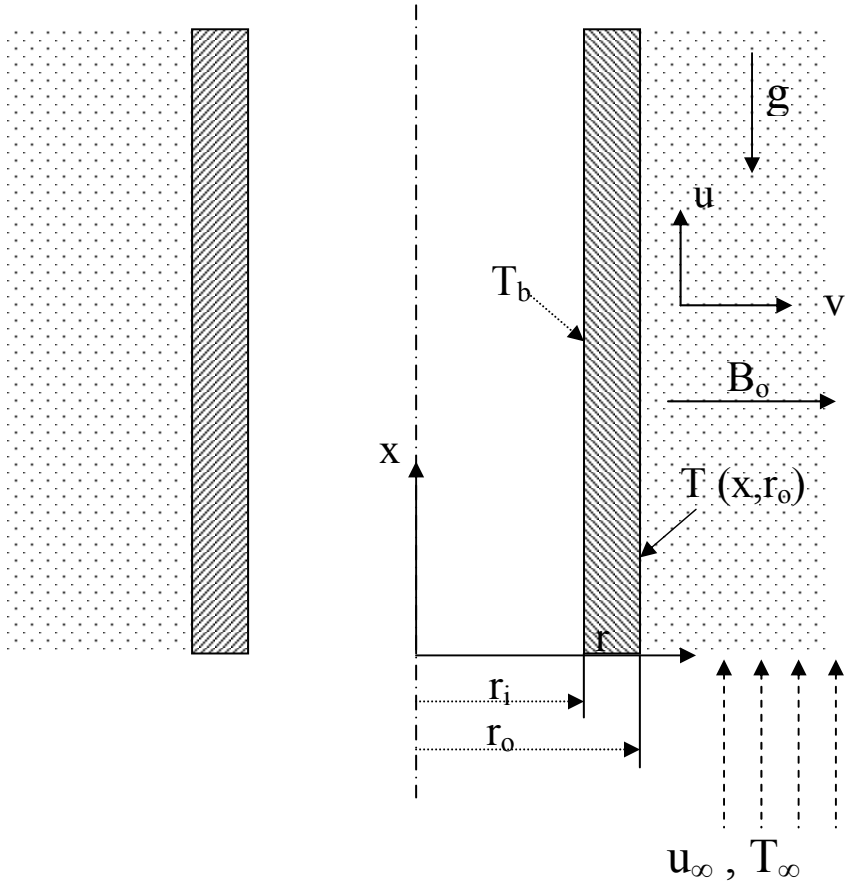

Figure.1 Schematic of physical model and coordinate system

4. Non-similarity approach:

4.1 Introduction:

When the similarity solution is not available in some problems, the non-similarity solution will be used. To solve a non-similar boundary layer problem by non-similarity method, it is necessary to execute a definite succession of steps. First, the cylindrical coordinate (x,r) are placed with properly selected dimensionless coordinate (ζ,η) appropriate for the problem. The η variable depends on both x and r, while the non similarity variable ζ is function of x only, the dependent variables in the governing equations are also transformed in terms of new variables, velocity components are replaced by a reduced stream function f(ζ,η), and for the thermal field a dimensionless temperature Θ(ζ,η), is introduced. Second, the conservation equations and their boundary conditions are transformed in terms of the new variable. The end results of the transformation yield a system of partial differential equations of f(ζ,η), and Θ(ζ,η),and their partial derivatives.

4.2 Performing the case of study by nonsimilar method:

In this system of equations (3.2-3.4) two cases will study as following:

A: In the system of equations (3.2-3.4) and in order to satisfy the continuity equation define the stream function ψ as following:(Aldoss et al., 1995)

$$u = \frac{r_o}{r}\frac{\partial \psi}{\partial r}$$

$$v = -\frac{r_o}{r}\frac{\partial \psi}{\partial x} \tag{3.14}$$

And introduce the following dimensionless variables in the transformations:

$$\zeta = \frac{Pe_x^{1/2}}{Pe_x^{1/2} + Ra_x^{1/2}} \tag{3.15}$$

$$\eta = \frac{1}{x} Pe_x^{1/2} \left(\frac{r^2}{2r_o} - \frac{r_o}{2} \right) \zeta^{-1} \tag{3.16}$$

$$\psi(\zeta, \eta) = \alpha Pe_x^{1/2} f(\zeta, \eta) \zeta^{-1} \tag{3.17}$$

$$\theta(\zeta, \eta) = \frac{T - T_\infty}{T_b - T_\infty} \tag{3.18}$$

Where ζ is the nonsimilar mixed convection parameter, the case of ζ=0 corresponds to pure free convection and ζ =1 corresponds to pure forced convection.

B: In the system of equations (3.2-3.4) and in order to satisfy the continuity equation define another stream function ψ as following:

$$u = \frac{r_o}{r} \frac{\partial \psi}{\partial r}$$

$$v = -\frac{r_o}{r} \frac{\partial \psi}{\partial x} \tag{3.19}$$

And introduce the following dimensionless variables in the transformations:

$$\chi = \frac{g\beta x}{C_p} \tag{3.20}$$

$$\eta = \frac{1}{x} Pe_x^{1/2} \left(\frac{r^2}{2r_o} - \frac{r_o}{2} \right) \tag{3.21}$$

$$\psi(\chi, \eta) = \alpha Pe_x^{1/2} f(\chi, \eta) \tag{3.22}$$

$$\theta(\chi, \eta) = \frac{T - T_\infty}{T_b - T_\infty} \tag{3.23}$$

Where χ is the nonsimilar and viscous dissipation parameter, $\chi \equiv Ge_x = g\beta x/C_p$. where χ=0,corresponds to no heat transfer by viscous dissipation**,** for the two cases, by differentiate the above system of equations and substitute it in momentum and energy equations (3.3-3.4) this yields to:

A:

Momentum equation:

$$Hf'' + \overset{*}{\mathrm{Re}}\left\{(f')^2\right\}' = \pm(1-\zeta)^2\theta' \tag{3.24}$$

and energy equation:

$$(1+\lambda\eta\zeta)\theta'' + \lambda\zeta\theta' + \frac{1}{2}f\theta' + \overset{*}{Ge}\left\{1+\varepsilon(H-1)\right\}\left(f^{\backslash}\right)^2 + \overset{*}{Ge}\,\overset{*}{\mathrm{Re}}\left(f^{\backslash}\right)^3 = 0 \tag{3.25}$$

B:

Momentum equation:

$$Hf'' + \mathrm{Re}\left\{(f')^2\right\}' = \pm\frac{Ra_x}{Pe_x}\theta' \tag{3.26}$$

and energy equation:

$$(1+\lambda\eta)\theta'' + \lambda\theta' + \frac{1}{2}f\theta' + \frac{Pe_x}{Ra_x}\chi\left[\left\{1+\varepsilon(H-1)\right\}(f')^2 + \mathrm{Re}\,(f')^3\right] = \chi\left(f'\frac{\partial\theta}{\partial\chi} - \theta'\frac{\partial f}{\partial\chi}\right) \tag{3.27}$$

Note that: in the case A, where $\zeta = \dfrac{Pe_x^{1/2}}{Pe_x^{1/2} + Ra_x^{1/2}}$ is identified as the mixed convection parameter. For the case B: $\chi = \dfrac{g\beta x}{C_p}$ corresponds to the viscous dissipation effects on mixed convection regime, the case of χ=0 corresponds to no viscous dissipation effects, note that $\dfrac{Ra_x}{Pe_x}$ is the mixed convection parameter and the case of $\dfrac{Ra_x}{Pe_x}$=0 corresponds to pure forced convection while the case of $\dfrac{Ra_x}{Pe_x} \to \infty$ corresponds to pure natural convection, and the plus and minus signs correspond to buoyancy aiding and buoyancy opposing flows respectively.

These two systems of equations (3.24-3.27) are solved with the following boundary conditions

A:

$$\begin{aligned} f(\zeta,0)&=0 \qquad & \theta(\zeta,0)-1&=p^{*}\theta^{\backslash}(\zeta,0)\\ f^{\backslash}(\zeta,\infty)&=\zeta^{2} \qquad & \theta(\zeta,\infty)&=0 \end{aligned} \tag{3.28}$$

where P^{*} represents the conjugate conduction parameter, define as:

$$p^{*}=2\frac{k_m}{k_s}\ln\left(\frac{r_o}{r_i}\right)\frac{1}{\lambda\zeta} \tag{3.29}$$

B:

$$\begin{aligned} f(\chi,0)&=0 \qquad & \theta(\chi,0)-1&=P^{*}\theta'(\chi,0)\\ f'(\chi,\infty)&=1 \qquad & \theta(\chi,\infty)&=0 \end{aligned} \tag{3.30}$$

where P^{*} represents the conjugate conduction parameter for the B case, define as:

$$P^{*}=2\frac{k_m}{k_s}\ln\left(\frac{r_o}{r_i}\right)\frac{1}{\lambda} \tag{3.31}$$

Noting that in the previous system of equations the primes denote to the partial differentiations with respect to η, while H represents the effects of the magnetic field in the boundary layer, where these effects are absent from the problem when $H=1$

The viscous dissipation heat transfer effects are represented by the local Gebhart number $Ge_{x,}$ where the viscous dissipation heat transfer effects are absent when $Ge_x=0$.

Also, the inertial effects are introduced by the Forchheimer coefficient dependent Reynolds number defined as: $\mathrm{Re}=\frac{K'u_{\infty}}{\upsilon}$, where Re=0 corresponds to Darcy mixed convection region. In addition to that, the effects of the curvature cylindrical surface are presented in these equations by the curvature parameter λ, which is defined as: $\lambda=\frac{2x}{r_o Pe_x^{1/2}}$. Where it is possible to reduce the problem to the mixed convection heat transfer over a flat plate by putting λ=0.

Some of the physical quantities of interest include the velocity component u and v in the x and r directions respectively, the local nusselt number Nu_x which is defined as $Nu_x=hx/k$, where k is the effective thermal conductivity of the porous matrix fluid. $k=(1-\varepsilon).k_s+\varepsilon.k_m$ (Nield and Bejan,1999). and h_x is the local heat transfer coefficient, and the wall shear stress (τ_w) which is defined as: $\tau_w=\mu(\partial u/\partial r)|_{r=ro}$.

A:

$$u = u_\infty \zeta^{-2} f'(\zeta,\eta) \tag{3.32}$$

$$v = \frac{\alpha}{r}\lambda^{-1}\zeta^{-1}\left(\eta f' - f\right) \tag{3.33}$$

$$\frac{Nu_x}{\left[Pe_x^{1/2} + Ra_x^{1/2}\right]} = -\frac{\theta'(\zeta,0)}{\theta(\zeta,0)} \tag{3.34}$$

$$\frac{Cf_x Pe_x}{\left[Pe_x^{1/2} + Ra_x^{1/2}\right]^3} = 2.\Pr.f''(\zeta,0) \tag{3.35}$$

B:

$$u = u_\infty f'(\chi,\eta) \tag{3.36}$$

$$v = -\frac{1}{2}\frac{r_o}{r}\left(\frac{\alpha u_\infty}{x}\right)^{1/2}\left(f + 2\chi\frac{\partial f}{\partial \chi} - \eta f'\right) \tag{3.37}$$

$$\frac{Nu_x}{Pe_x^{1/2}} = -\frac{\theta'(\chi,0)}{\theta(\chi,0)} \tag{3.38}$$

$$Cf_x Pe_x^{1/2} = 2.\Pr.f''(\chi,0) \tag{3.39}$$

a) Aiding flow

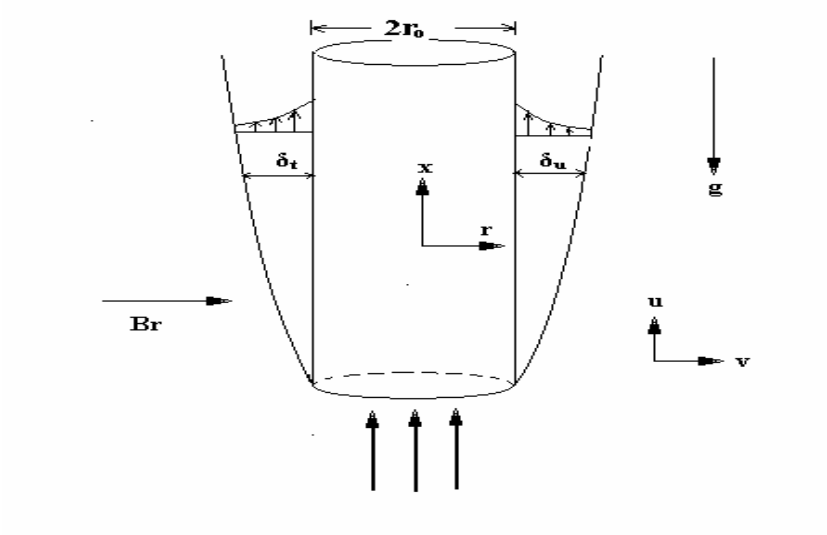

b) Opposing flow

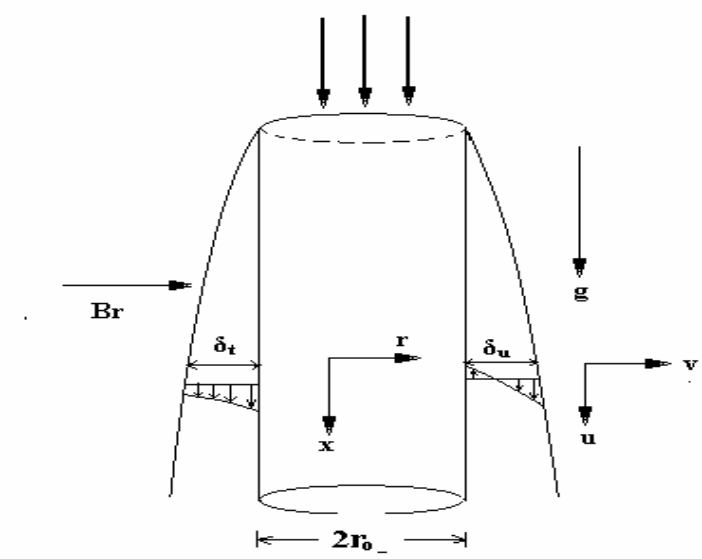

Figure.2 Schematic of MHD-conjugate cylinder. a) Aiding flow. b) Opposing flow

NUMERICAL SOLUTION

1. Introduction:

In recent years a large number of numerical methods have been developed for the solving of boundary layer equations. Such as the finite difference method, Galerkin method, and finite element method. Of these, the finite difference method is at present the most common for the boundary layer equations.

In the finite difference approach, the dependent variables are considered to exist only at discrete points. Derivatives are approximated by finite difference resulting in an algebraic representation of the partial differential equation. Many different finite difference representations are possible for any given partial differential equation

There are two different ways to convert a differential equation into finite difference equation, namely Implicit and Explicit methods. In an explicit method the unknown values may be found directly at a grid points in terms of the known values at previous step. However, in the implicit method, the unknown values at a grid point are not only a function of the previous known values but also a function of unknown values at the same step. This requires solution of a set of simultaneous algebraic equations, which are resulted when the difference equations are written for all interior points and the boundary points if the boundary conditions have a derivative forms. In most cases, implicit finite difference techniques tend to be numerically stable and significantly larger steps, on the other hand, explicit finite difference techniques tend to be less stable, less calculations and then less time and storage by the computer.

2. Solution of mass, momentum and energy equations:

To solve these systems of equations (3.24-3.27) with it is boundary conditions Keller box methods as described by (Cebeci and Bradshow, 1977,a) had used. The solution of an equation by this method can be obtained by the following:

1- Reduce the equation to a first order system.

2-Write the difference equations by using central differences.

3-Linearize the resulting algebraic equations if they are nonlinear and write them in a matrix vector form.

4-Solve the linear system by block-elimination method.

2.1 Numerical Formulation:

In this chapter, an iterative implicit method due to Keller (1978). is now described and is referred to as the Box-method. This method has several desirable features that make it appropriate for the solution of all parabolic partial differential equations. (Anderson et al., 1984).

2.1_A Finite-Difference scheme:

The system of coupled partial differential equations (3.24-3.27) and their boundary conditions (3.28) and (3.30) can be written as following:

A:

Momentum equation:

$$m_1 f'' + m_2 \left\{ (f')^2 \right\}' = m_3 \theta' \tag{4.1}$$

Energy equation:

$$\theta'' + m_3 \eta \theta'' + m_3 \theta' + \frac{1}{2} f\theta' + m_4 (f')^2 + m_5 (f')^3 = 0 \tag{4.2}$$

with the following boundary conditions:

$$\begin{aligned} f(\zeta,0) &= 0 \qquad & \theta(\zeta,0) - 1 &= P^* \theta'(\zeta,0) \\ f'(\zeta,\infty) &= \zeta^2 \qquad & \theta(\zeta,\infty) &= 0 \end{aligned} \tag{4.3}$$

B:

Momentum equation:

$$m_1 f'' + m_2 \left\{ (f')^2 \right\}' = m_3 \theta' \tag{4.4}$$

Energy equation:

$$\theta'' + m_4 \eta \theta'' + m_4 \theta' + m_5 f \theta' + m_6 (f')^2 + m_7 (f')^3 = m_8 \left(f' \frac{\partial \theta}{\partial \chi} - \theta' \frac{\partial f}{\partial \chi} \right) \tag{4.5}$$

with the following boundary conditions:

$$\begin{aligned} f(\chi,0) &= 0 \qquad & \theta(\chi,0) - 1 &= P^* \theta'(\chi,0) \\ f'(\chi,\infty) &= 1 \qquad & \theta(\chi,\infty) &= 0 \end{aligned} \tag{4.6}$$

where the values of the coefficients m_1, $m_2 \ldots m_8$ are given in appendix (A).

First will write equations (4.1-4.2) in case A, and equations (4.4-4.5) in second case B with their boundary conditions in terms of first order systems. For this purpose introduced new dependent variables U and V. So that the transformed momentum and energy equations can be written as:

A:

$$f' = U \tag{4.7}$$

$$\theta = V \tag{4.8}$$

$$m_1 u' + m_2 \left((U)^2 \right)' = m_3 V \tag{4.9}$$

$$V' + m_3 \eta V' + m_3 V + \frac{1}{2} f V + m_4 (U)^2 + m_5 (U)^3 = 0 \tag{4.10}$$

with the boundary condition equations (4.3), which can be written as:

$$\begin{aligned} f(\zeta,0) &= 0 \qquad & \theta(\zeta,0) - 1 &= P^* V(\zeta,0) \\ U(\zeta,\infty) &= \zeta^2 \qquad & \theta(\zeta,\infty) &= 0 \end{aligned} \tag{4.11}$$

B:

$$f' = U \tag{4.12}$$

$$\theta' = V \tag{4.13}$$

$$m_1 U' + m_2 \left\{ (U)^2 \right\}' = m_3 V \tag{4.14}$$

$$V' + m_4 \eta V' + m_4 V + m_5 f V + m_6 (U)^2 + m_7 (U)^3 = m_8 \left(U \frac{\partial \theta}{\partial \chi} - V \frac{\partial f}{\partial \chi} \right) \tag{4.15}$$

with the boundary condition equations (4.6), which can be written as:

$$\begin{aligned} f(\chi,0) &= 0 \qquad & \theta(\chi,0) - 1 &= P^* V(\chi,0) \\ u(\chi,\infty) &= 1 \qquad & \theta(\chi,\infty) &= 0 \end{aligned} \tag{4.16}$$

Next consider the rectangular system shown in figure (4.1), and denote the net points by:

$\zeta_0=0$ $\qquad \zeta_n= \zeta_{n-1}+k_n \qquad$ n=1,2,…N

$\eta_0=0 \qquad \eta_j= \eta_{j-1}+h_j \qquad$ j=1,2,…J

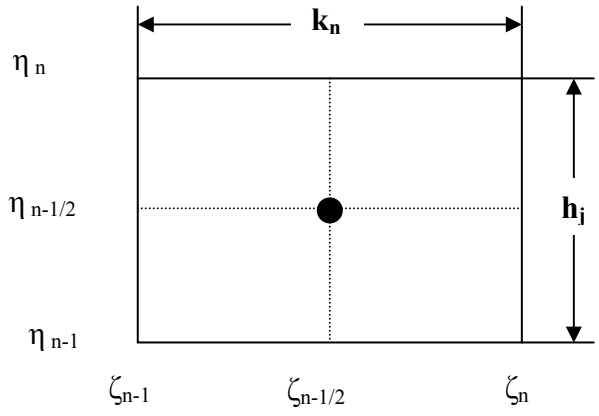

Figure 3 Rectangular net for difference approximation

Any quantity (g) at point (ζ_n, η_j) is written as (g_j^n). Quantities at the midpoints of grid segments are approximated to second order as:

$$g_j^{n-1/2} = \frac{1}{2}\left(g_j^n + g_j^{n-1}\right) \quad , \quad g_{j-1/2}^n = \frac{1}{2}\left(g_j^n + g_{j-1}^n\right)$$

And derivatives are approximated to second order as:

$$\left(\frac{\partial g}{\partial \zeta}\right)_j^{n-1/2} = k_n^{-1}\left(g_j^n - g_j^{n-1}\right) \quad , \quad \left(g^{\backslash}\right)_{j-1/2}^n = h_j^{-1}\left(g_j^n - g_{j-1}^n\right)$$

Quantity at the midpoints of the grid (n-1/2,j-1/2) are approximated as:

$$g_{j-1/2}^{n-1/2} = \frac{1}{2}\left(g_{j-1/2}^n + g_{j-1/2}^{n-1}\right)$$

And derivatives are approximated to second order as:

$$\left(\frac{\partial g}{\partial \zeta}\right)_{j-1/2}^{n-1/2} = k_n^{-1}\left(g_{j-1/2}^n - g_{j-1/2}^{n-1}\right) \quad , \quad \left(g^{\backslash}\right)_{j-1/2}^{n-1/2} = \frac{1}{2}\left(\left(g^{\backslash}\right)_{j-1/2}^n + \left(g^{\backslash}\right)_{j-1/2}^{n-1}\right)$$

The difference equations that are to approximate equations (4.7-4.8) and (4.12-4.13) are obtained about the midpoint (ζ_n, $\eta_{j-1/2}$), and those to approximate equations (4.9-4.10) and (4.14-4.15) are obtained by averaging about ($\zeta_{n-1/2}$, $\eta_{j-1/2}$), this will give the following system of equations:

A:

$$\left(f_j^n - f_{j-1}^n\right) - \frac{h_j}{2}\left(U_j^n + U_{j-1}^n\right) = 0 \tag{4.17}$$

$$\left(\theta_j^n - \theta_{j-1}^n\right) - \frac{h_j}{2}\left(V_j^n + V_{j-1}^n\right) = 0 \tag{4.18}$$

$$m_1 h_j^{-1}\left(U_j^n - U_{j-1}^n\right) + m_2\, h_j^{-1}\left\{\left(U^2\right)_j^n - \left(U^2\right)_{j-1}^n\right\} - \frac{m_3^n}{2}\left(V_j^n + V_{j-1}^n\right) = R_{j-1/2}^{n-1} \tag{4.19}$$

$$\begin{aligned}&\left(h_j^{-1} + m_4^n \eta_{j-1/2} h_j^{-1}\right)\left(V_j^n - V_{j-1}^n\right) + \frac{m_4^n}{2}\left(V_j^n + V_{j-1}^n\right) + \frac{1}{4}\left\{(fV)_j^n + (fV)_{j-1}^n\right\} + \\ &\frac{m_5^n}{2}\left\{\left(U^2\right)_j^n + \left(U^2\right)_{j-1}^n\right\} + \frac{m_6^n}{2}\left\{\left(U^3\right)_j^n + \left(U^3\right)_{j-1}^n\right\} = T_{j-1/2}^{n-1}\end{aligned} \tag{4.20}$$

where

$$R_{j-1/2}^{n-1}=\left[m_3V_{j-1/2}-h_j^{-1}\left(U_j-U_{j-1}\right)-m_2\,h_j^{-1}\left\{\left(U^2\right)_j-\left(U^2\right)_{j-1}\right\}\right]^{n-1} \tag{4.21}$$

and

$$T_{j-1/2}^{n-1}=\begin{Bmatrix}-\left(h_j^{-1}+m_4\eta_{j-1/2}h_j^{-1}\right)\left(V_j-V_{j-1}\right)-m_4V_{j-1/2}-\frac{1}{2}\left(fV\right)_{j-1/2}-m_5\left(U^2\right)_{j-1/2}\\-m_6\left(U^3\right)_{j-1/2}\end{Bmatrix}^{n-1} \tag{4.22}$$

B:

$$\left(f_j^n-f_{j-1}^n\right)-\frac{h_j}{2}\left(U_j^n+U_{j-1}^n\right)=0 \tag{4.23}$$

$$\left(\theta_j^n-\theta_{j-1}^n\right)-\frac{h_j}{2}\left(V_j^n+V_{j-1}^n\right)=0 \tag{4.24}$$

$$R_{j-1/2}^{n-1}=m_1h_j^{-1}\left(U_j^n-U_{j-1}^n\right)+m_2\,h_j^{-1}\left\{\left(U^2\right)_j^n-\left(U^2\right)_{j-1}^n\right\}-\frac{m_3}{2}\left(V_j^n+V_{j-1}^n\right) \tag{4.25}$$

and

$$\begin{aligned}T_{j-1/2}^{n-1}=&\left(h_j^{-1}+m_4\eta_{j-1/2}h_j^{-1}+\frac{m_4}{2}-\frac{\alpha}{2}f_{j-1/2}^{n-1}\right)V_j^n-\left(h_j^{-1}+m_4\eta_{j-1/2}h_j^{-1}-\frac{m_4}{2}+\frac{\alpha}{2}f_{j-1/2}^{n-1}\right)V_{j-1}^n\\&+\frac{\alpha_1}{2}\left\{\left(fV\right)_j^n+\left(fV\right)_{j-1}^n\right\}+\frac{m_6^n}{2}\left\{\left(U^2\right)_j^n+\left(U^2\right)_{j-1}^n\right\}+\frac{m_7^n}{2}\left\{\left(U^3\right)_j^n+\left(U^3\right)_{j-1}^n\right\}-\\&\frac{\alpha}{2}\left\{\left(U\theta\right)_j^n+\left(U\theta\right)_{j-1}^n\right\}+\frac{\alpha}{2}\theta_{j-1/2}^{n-1}\left(U_j^n+U_{j-1}^n\right)-\frac{\alpha}{2}U_{j-1/2}^{n-1}\left(\theta_j^n+\theta_{j-1}^n\right)+\\&\frac{\alpha}{2}V_{j-1/2}^{n-1}\left(f_j^n+f_{j-1}^n\right)\end{aligned} \tag{4.26}$$

where

$$\alpha=\frac{m_8^{n-1/2}}{k_n}$$

$$\alpha_1=\alpha+m_5$$

and

$$R_{j-1/2}^{n-1} = \left[m_3 V_{j-1/2} - m_1 h_j^{-1}(U_j - U_{j-1}) - m_2\, h_j^{-1}\left\{(U^2)_j - (U^2)_{j-1}\right\}\right]^{n-1} \tag{4.27}$$

$$T_{j-1/2}^{n-1} = \begin{Bmatrix} -\alpha\left\{(fV)_{j-1/2} - (U\theta)_{j-1/2}\right\} - \left(h_j^{-1} + m_4 \eta_{j-1/2} h_j^{-1}\right)\left(V_j - V_{j-1}\right) \\ -m_4 V_{j-1/2} - m_5 (fV)_{j-1/2} - m_6 \left(U^2\right)_{j-1/2} - m_7 \left(U^3\right)_{j-1/2} \end{Bmatrix}^{n-1} \tag{4.28}$$

Equations (4.17-4.28) are imposed for j=1,2,3,4…J at given n, and the transformed boundary layer thickness (η_∞) is required to be sufficiently large enough, that require Q (η_∞) is less than approximately 10^{-5}.

The boundary conditions given by equation (4.11) for the case A become:

$$\begin{aligned} f_o^n &= 0 & \theta_o^n - 1 &= P^* V_o^n \\ U_J^n &= \zeta^2 & \theta_J^n &= 0 \end{aligned} \tag{4.29}$$

And the boundary conditions given by equation (4.16) for the second case B becomes:

$$\begin{aligned} f_o^n &= 0 & \theta_o^n - 1 &= P^* V_o^n \\ U_J^n &= 1 & \theta_J^n &= 0 \end{aligned} \tag{4.30}$$

2.1.$_B$ Newton's Method:

Assume f_j^{n-1}, U_j^{n-1}, θ_j^{n-1} and V_j^{n-1} are known for $0 \le j \le J$ then the equations (4.17-4.20) for the first case, and equations (4.23-4.26) for the second case form systems of 4J+4 nonlinear equations. To solve these nonlinear systems of equations and its unknowns (f_j^n, U_j^n, θ_j^n, V_j^n) , j=0,1,2…J, will use Newton's method

and introduce the iteration $(f_j^i, U_j^i, \theta_j^i, V_j^i)$, i=0,1,2…I, with initial values equal to those at the previous ζ station.

For the higher iterates set:

$$f_j^{i+1} = f_j^i + \delta f_j^i$$
$$U_j^{i+1} = U_j^i + \delta U_j^i$$
$$\theta_j^{i+1} = \theta_j^i + \delta\theta_j^i$$
$$V_j^{i+1} = V_j^i + \delta V_j^i$$

then insert the right-hand sides of the above expression in places of $(f_j^i, U_j^i, \theta_j^i, V_j^i)$ in equations (4.17-4.20) and equations (4.23-4.26) and drop the terms that are quadratic in ($\delta f_j^i, \delta U_j^i, \delta\theta_j^i, \delta V_j^i$). With this procedure, equations (4.17-4.20), (4.23-4.26) and (4.29-4.30) become:(the subscript i in the δ quantities is dropped for simplicity)

A:

$$\delta f_j - \delta f_{j-1} - \frac{h_j}{2}\left(\delta U_j + \delta U_{j-1}\right) = \left(r_2\right)_{j-1} \tag{4.31}$$

$$\delta\theta_j - \delta\theta_{j-1} - \frac{h_j}{2}\left(\delta V_j + \delta V_{j-1}\right) = \left(r_4\right)_{j-1} \tag{4.32}$$

$$\left(S_1\right)_j \delta f_j + \left(S_2\right)_j \delta U_j + \left(S_3\right)_j \delta V_j + \left(S_4\right)_j \delta\theta_j + \left(S_5\right)_j \delta f_{j-1}$$
$$+ \left(S_6\right)_j \delta U_{j-1} + \left(S_7\right)_j \delta V_{j-1} + \left(S_8\right)_j \delta\theta_{j-1} = \left(r_1\right)_j \tag{4.33}$$

$$\left(B_1\right)_j \delta f_j + \left(B_2\right)_j \delta U_j + \left(B_3\right)_j \delta V_j + \left(B_4\right)_j \delta\theta_j + \left(B_5\right)_j \delta f_{j-1}$$
$$+ \left(B_6\right)_j \delta U_{j-1} + \left(B_7\right)_j \delta V_{j-1} + \left(B_8\right)_j \delta\theta_{j-1} = \left(r_3\right)_j \tag{4.34}$$

where the right hand sides of the above equations are given by:

$$(r_1)_j = R^{n-1}_{j-1/2} - \left[m_1 h_j^{-1}\left(U_j - U_{j-1}\right) + m_2 h_j^{-1}\left\{(U^2)_j - (U^2)_{j-1}\right\} - m_3^n V_{j-1/2}\right]^n \tag{4.35}$$

$$(r_2)_{j-1} = f_{j-1} - f_j + h_j U_{j-1/2} \tag{4.36}$$

$$(r_4)_{j-1} = \theta_{j-1} - \theta_j + h_j V_{j-1/2} \tag{4.37}$$

$$(r_3)_j = T^{n-1}_{j-1/2} - \begin{Bmatrix} \left(h_j^{-1} + \eta_{j-1/2} m_4^n h_j^{-1}\right)\left(V_j - V_{j-1}\right) + m_4^n V_{j-1/2} + \\ \frac{1}{2}(fV)_{j-1/2} + m_5^n (U^2)_{j-1/2} + m_6^n (U^3)_{j-1/2} \end{Bmatrix}^n \tag{4.38}$$

B:

$$\delta f_j - \delta f_{j-1} - \frac{h_j}{2}\left(\delta U_j + \delta U_{j-1}\right) = (r_2)_{j-1} \tag{4.39}$$

$$\delta\theta_j - \delta\theta_{j-1} - \frac{h_j}{2}\left(\delta V_j + \delta V_{j-1}\right) = (r_4)_{j-1} \tag{4.40}$$

$$\begin{aligned} &(S_1)_j \delta f_j + (S_2)_j \delta U_j + (S_3)_j \delta V_j + (S_4)_j \delta\theta_j + (S_5)_j \delta f_{j-1} \\ &+ (S_6)_j \delta U_{j-1} + (S_7)_j \delta V_{j-1} + (S_8)_j \delta\theta_{j-1} = (r_1)_j \end{aligned} \tag{4.41}$$

$$\begin{aligned} &(B_1)_j \delta f_j + (B_2)_j \delta U_j + (B_3)_j \delta V_j + (B_4)_j \delta\theta_j + (B_5)_j \delta f_{j-1} \\ &+ (B_6)_j \delta U_{j-1} + (B_7)_j \delta V_{j-1} + (B_8)_j \delta\theta_{j-1} = (r_3)_j \end{aligned} \tag{4.42}$$

where the right hand sides of the above equations are given by:

$$(r_1)_j = R^{n-1}_{j-1/2} - \left[m_1 h_j^{-1}\left(U_j - U_{j-1}\right) + m_2 h_j^{-1}\left\{(U^2)_j - (U^2)_{j-1}\right\} - m_3 V_{j-1/2}\right]^n \tag{4.43}$$

$$(r_2)_{j-1} = f_{j-1} - f_j + h_j U_{j-1/2} \tag{4.44}$$

$$(r_4)_{j-1} = \theta_{j-1} - \theta_j + h_j V_{j-1/2} \tag{4.45}$$

$$(r_3)_j = T^{n-1}_{j-1/2} - \left\{\begin{array}{l}\left(h_j^{-1} + \eta_{j-1/2} m_4 h_j^{-1}\right)\left(V_j - V_{j-1}\right) + \left(m_4 - \alpha f^{n-1}_{j-1/2}\right)V_{j-1/2} + \\ \alpha_1 (fV)_{j-1/2} + m_6^n (U^2)_{j-1/2} + m_7^n (U^3)_{j-1/2} - \\ \alpha\left((U\theta)_{j-1/2} - \theta^{n-1}_{j-1/2} U_{j-1/2} + U^{n-1}_{j-1/2}\theta_{j-1/2} - V^{n-1}_{j-1/2} f_{j-1/2}\right)\end{array}\right\}^n \tag{4.46}$$

Where $(S_k)_j$ (k=1 to 8) and $(B_k)_j$ (k=1 to 8) are the coefficients of the linearized momentum and energy equations. Their values are found in Appendix (A).

And the boundary conditions equations (4.29-4.30), for two cases can be written as following:

A:

$$\begin{array}{ll} \delta f_o = 0 & \delta\theta_o = 0 \\ \delta U_J = 0 & \delta\theta_J = 0 \end{array} \tag{4.47}$$

B:

$$\begin{array}{ll} \delta f_o = 0 & \delta\theta_o = 0 \\ \delta U_J = 0 & \delta\theta_J = 0 \end{array} \tag{4.48}$$

Note that: for the boundary condition $\theta_o^n - 1 = P^* V_o^n$, where put $\delta\theta_o = 0$, in equations (4.47) and (4.48) when linearized equations (4.29-4.30). That will be correct in the program, which will use to solve these equations by adding another condition to this program, which satisfy the required boundary condition for these cases. The solution of the linear system given by equations (4.31-4.34) for the first case A, and by

equations (4.39-4.42) for the second case B can be obtained by the block elimination method as described by Cebeci and Bradshow (1977). To introduce the solution procedure must define three-dimensional vectors δ_j and r_j for each value of j by:

$$\delta_j = \begin{pmatrix} \delta f_j \\ \delta U_j \\ \delta V_j \\ \delta \theta_j \end{pmatrix}, \qquad 0 \le j \le J \qquad , \; r_0 = \begin{pmatrix} 0 \\ (r_2)_j \\ 0 \\ (r_4)_j \end{pmatrix} \tag{4.49}$$

$$r_j = \begin{pmatrix} (r_1)_j \\ (r_2)_j \\ (r_3)_j \\ (r_4)_j \end{pmatrix}, \qquad 1 \le j \le J-1 \qquad , \; r_J = \begin{pmatrix} (r_1)_J \\ 0 \\ (r_3)_J \\ 0 \end{pmatrix} \tag{4.50}$$

And the 4x4matrices A_j, B_j, C_j by:

$$A_j = \begin{bmatrix} (S_1)_j & (S_2)_j & (S_3)_j & (S_4)_j \\ -1 & \frac{-h_{j+1}}{2} & 0 & 0 \\ (B_1)_j & (B_2)_j & (B_3)_j & (B_4)_j \\ 0 & 0 & \frac{-h_{j+1}}{2} & -1 \end{bmatrix} \tag{4.51}$$

$$A_0 = \begin{bmatrix} 1 & 0 & 0 & 0 \\ -1 & \frac{-h_1}{2} & 0 & 0 \\ 0 & 0 & 0 & 1 \\ 0 & 0 & \frac{-h_1}{2} & -1 \end{bmatrix} \tag{4.52}$$

$$A_J = \begin{bmatrix} (S_1)_J & (S_2)_J & (S_3)_J & (S_4)_J \\ 0 & 1 & 0 & 0 \\ (B_1)_J & (B_2)_J & (B_3)_J & (B_4)_J \\ 0 & 0 & 0 & 1 \end{bmatrix} \tag{4.53}$$

$$B_j = \begin{bmatrix} (S_5)_j & (S_6)_j & (S_7)_j & (S_8)_j \\ 0 & 0 & 0 & 0 \\ (B_5)_j & (B_6)_j & (B_7)_j & (B_8)_j \\ 0 & 0 & 0 & 0 \end{bmatrix} \qquad 1 \le j \le J \tag{4.54}$$

$$C_j = \begin{bmatrix} 0 & 0 & 0 & 0 \\ 1 & \frac{-h_{j+1}}{2} & 0 & 0 \\ 0 & 0 & 0 & 0 \\ 0 & 0 & \frac{-h_{j+1}}{2} & 1 \end{bmatrix} \qquad 1 \le j \le J-1 \tag{4.55}$$

Note that the first row and third one of A_o and C_o, and the second and the last rows of A_J and B_j are corresponding to the boundary conditions (equations 4.47and 4.48). it can be shown that the system of equations(4.31-4.48) can be written as:

$$[A]\,\boldsymbol{\delta} = \mathbf{r} \tag{4.56}$$

Where

$$[A] = \begin{bmatrix} A_o & C_o & & & & \\ B_1 & A_1 & C_1 & & 0 & \\ 0 & 0 & 0 & & & \\ & & B_j & A_j & C_j & \\ & 0 & & B_{j-1} & A_{j-1} & C_{j-1} \\ & & & & B_J & A_J \end{bmatrix}$$

$$\vec{\delta} = \begin{pmatrix} \delta_0 \\ \delta_1 \\ \delta_2 \\ . \\ . \\ \delta_{J-1} \\ \delta_J \end{pmatrix}, \qquad \vec{r} = \begin{pmatrix} r_0 \\ r_1 \\ r_2 \\ . \\ . \\ r_{J-1} \\ r_J \end{pmatrix}$$

Where A, B and C are 4x4 matrices, and δ and r are vectors as follows:

δ={ δf , δU , δV , δθ }

r={ r_1 , r_2 , r_3 , r_4 }

2.2 Numerical aspects of solution:

The convergence, grid spacing, and high-order accuracy of the computational scheme is a very important task to be considered. In the following are some notes concerning these aspects.

2.2.$_A$ Stability:

Since numerical solutions represent a subsequent operations, and when the errors in the procedure is not grow then the solution scheme is stable. These errors in the solution are known as descretization errors, these errors caused by replacing the continuous problem by a discrete one, also, it may be transitional errors corresponding to neglecting higher order terms in the Taylor series expansion or other errors result from the treatment of the governing equations and boundary conditions.

While for round off errors, the numerical solutions rounded to a finite number of digits in the arithmetic operations. And to reduce the effect of round off errors the double precision option has been used.

2.2.$_B$ Boundary layer Grid:

The Keller box scheme is unique in that various spacing in both the ζ and η directions can be used. A convenient and useful η net, which is recommended by Cebeci and Smith (1977), having the property that the ratio of lengths of any two adjacent intervals is a constant is used.

The value of $\Delta\eta$ and $\Delta\ \zeta$ spacing, have chosen are the values, which have not changed the solution.

2.2.$_C$ Boundary layer Thickness:

The choice of η_∞ is an important consideration. However, the chosen value of η_∞ has to be examined closely in each case to determine the validity of the choice. The value of η_∞ is varied and, in each case, the convergent solution is obtained. The value of η_∞ chosen finally is the one for which an increase beyond this value dose not alter the convergent solution significantly.

RESULT AND DISCUSION

1. Introduction:

The MHD-mixed convection heat transfer problems with conjugate conduction boundary effects across the hollow cylinder including the effects of viscous dissipation between fluids layers are analyzed. The buoyancy aiding and opposing flows have been studied, and the non-similar solutions are obtained using the finite difference scheme known as the Keller box method where, the solutions are generated for a range of values of the axial non-similar coordinate ζ and the conjugate conduction parameter p^*. The results are obtained in terms of Re, Re^*, λ, ε, p^*, Ge, $Ge^*$and H, where $H=1+Ha^2/\varepsilon$ represents the effect of the magnetic field strength, Re the inertial force parameter, $Re^*=Re/\zeta^2$ represents the modify inertial force parameter, λ the curvature surface effect, ε the effect of the porosity on the fluid, p^* the conjugate conduction effect, Ge is Gebhart number and represents the viscous dissipation effect, and $Ge^*=Ge/(1-\zeta)^2$ represents modifed Gebhart number effect.

The effects of all parameters above included in the final system of partial differential equations and there effects on the velocity and temperature profiles, rate of heat transfer and the local wall shear stress were computed and presented for both Darcian and non-Darcian models.

Note that for a hollow cylinder, where the temperature on the inner surface is maintained at a constant value of T_b, the temperature on the outer surface of cylinder given by equation (3.12) depends on the coupled solution of the conduction across the cylinder and the mixed convection of the fluid-saturated porous medium over the cylinder.

2. Magnetohydrodynamic effects:

The Magneto hydrodynamic effects can be studied by using different values of H in the momentum and energy equations, for both buoyancy aiding and opposing flows. Results for velocity and temperature profiles $f'(\zeta,\eta)$ and $\theta(\zeta,\eta)$ for different values of H are drawn.

For the mixed convection heat transfer problem it is noted as shown in figures (5.1-5.8), increasing the magnetic influence number H, had decreased the velocity inside the boundary layer and also increased the temperature of the flow inside the boundary layer for the buoyancy aiding flow; because the magnetic effect on this problem is found to retard the motion of the fluid and to heat it at the same time, this effect is analogous to the flow against an adverse pressure gradient which tend to reduce the velocity inside the boundary layer, and hence the heat transfer rates between the fluid layers. But for the buoyancy opposing flow increasing the magnetic influence number had increased the velocity inside the boundary layer because it reduces the effect of the buoyancy forces, and in this case the effect of the magnetic field is to increase the heat transfer rate, this results because the magnetic force acts like favorable pressure gradient on accelerating fluid which increases the velocity, so the motion of the fluid becomes more effective in moving the heat and hence the thermal boundary layer becomes thinner.

For the MHD-forced convection heat transfer problem (case A) as shown in figures (5.9-5.11) increasing the magnetic field parameter haven't any effect on the velocity inside the boundary layer with effect on the heat transfer rate, where the temperatures of the fluid inside the boundary layer increase, because the magnetic field acts to heat the fluid inside the boundary layer, where the fluid has a thermal resistance against the electrical current which has produced by the magnetic field inside the

boundary layer, this resistance will dissipate in the fluid as heat to increase its temperature.

For MHD-free convection heat transfer problem (case A) as shown in figures (5.12-5.13), increasing the magnetic field parameter H, had decreased the velocity inside the boundary layer and increased the temperature of the fluid. because of the magnetic field forces which act to retard the motion of the fluid and to heat it at same time.

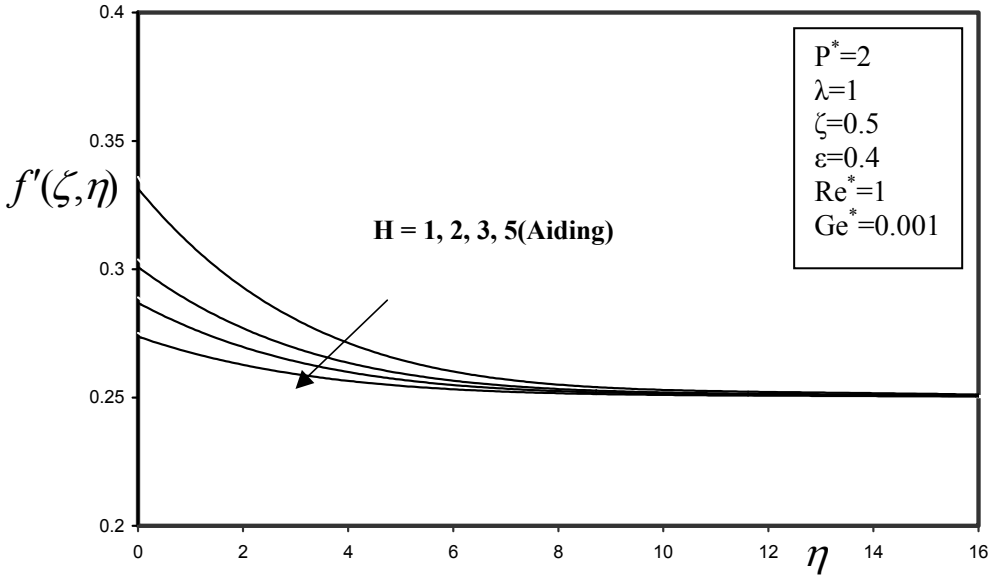

Fig 4 Dimensionless velocity profiles for different H
(mixed convection-A)

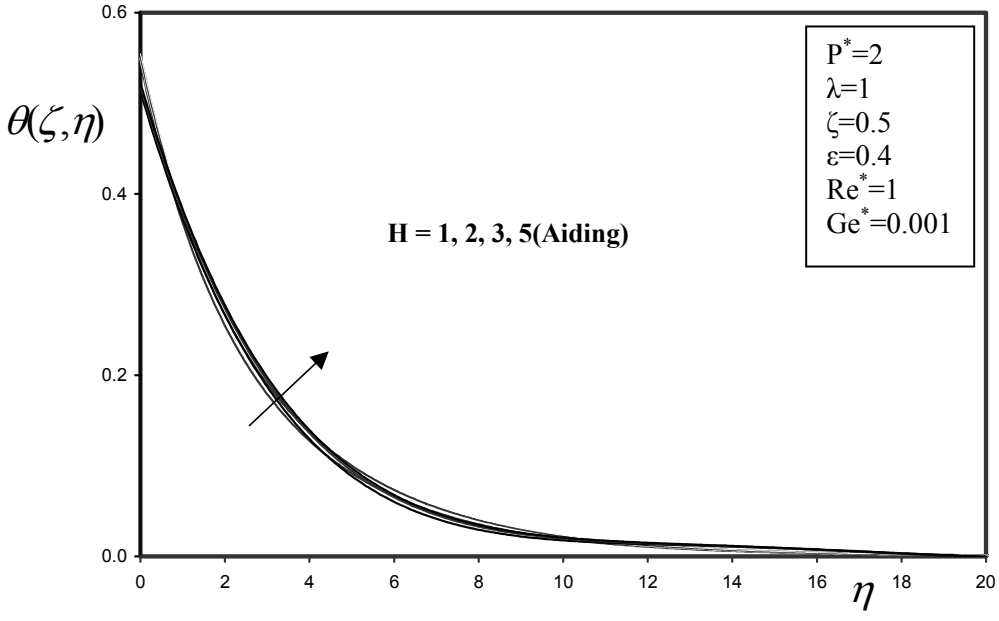

Fig 5 Dimensionless temperature profiles for different H
(mixed convection-A)

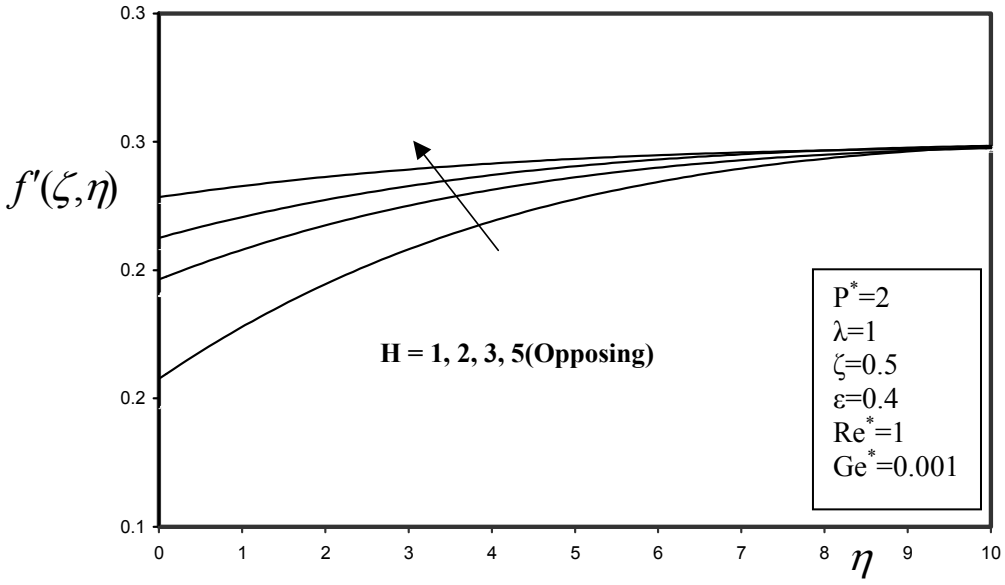

Fig 6 Dimensionless velocity profiles for different H
(mixed convection-A)

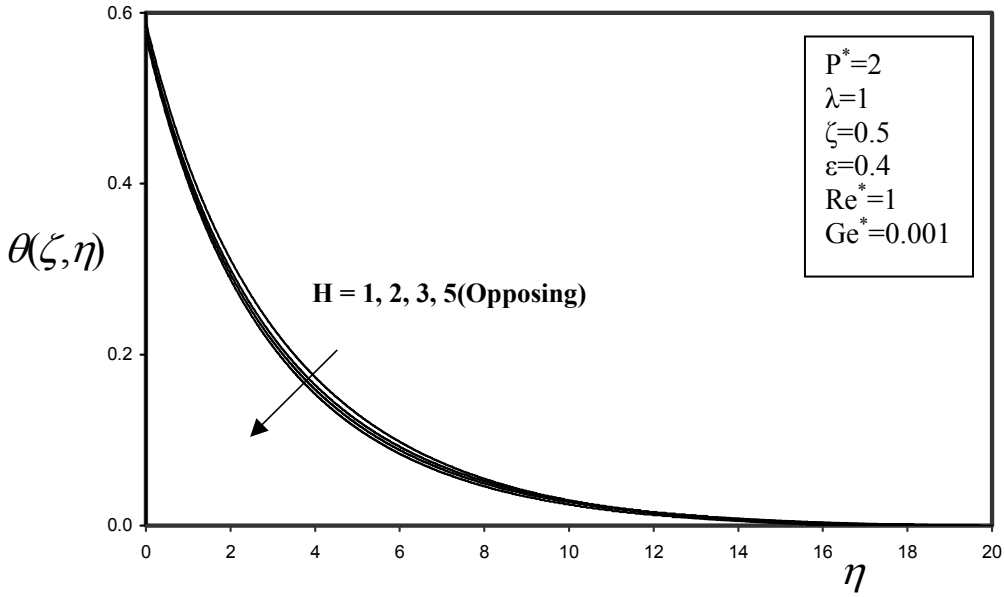

Fig 7 Dimensionless temperature profiles for different H
(mixed convection-A)

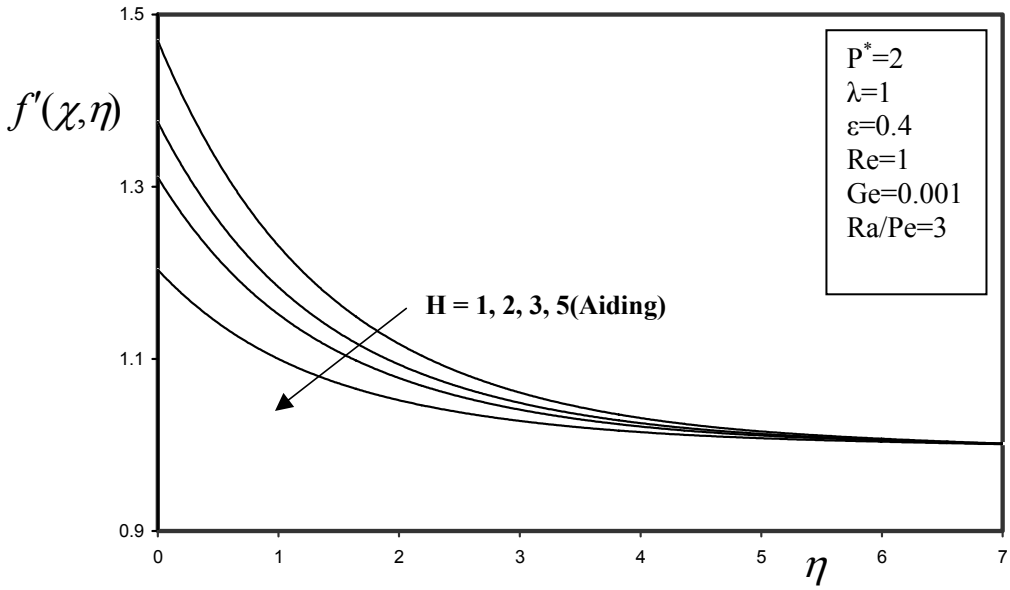

Fig 8 Dimensionless velocity profiles for different H
(mixed convection-B)

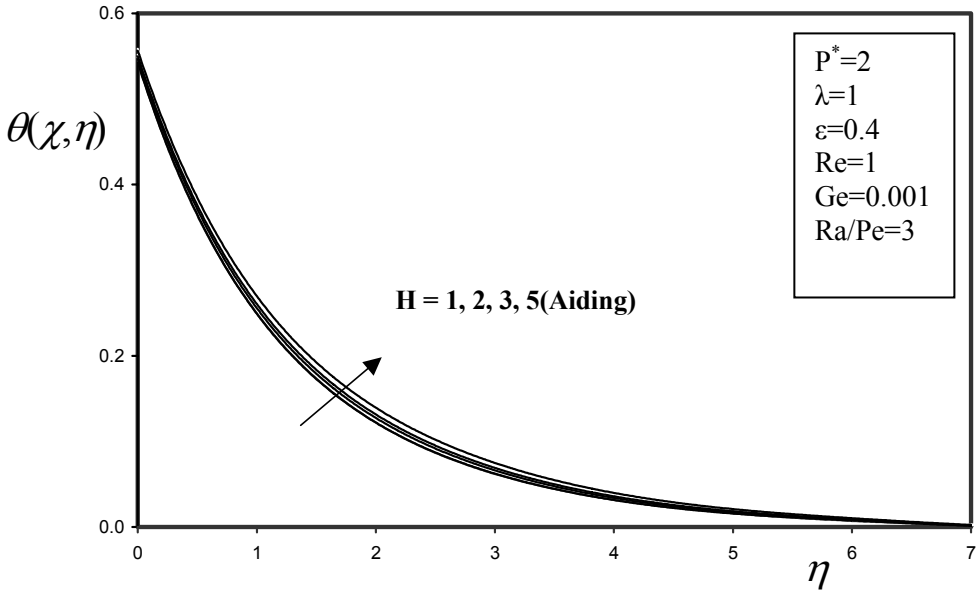

Fig 9 Dimensionless temperature profiles for different H
(mixed convection-B)

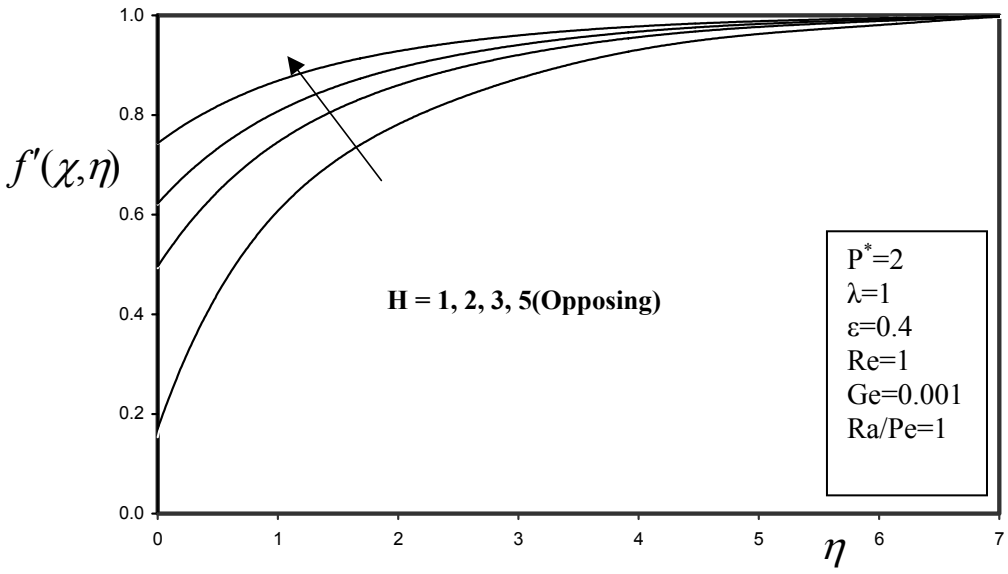

Fig 10 Dimensionless velocity profiles for different H
(mixed convection-B)

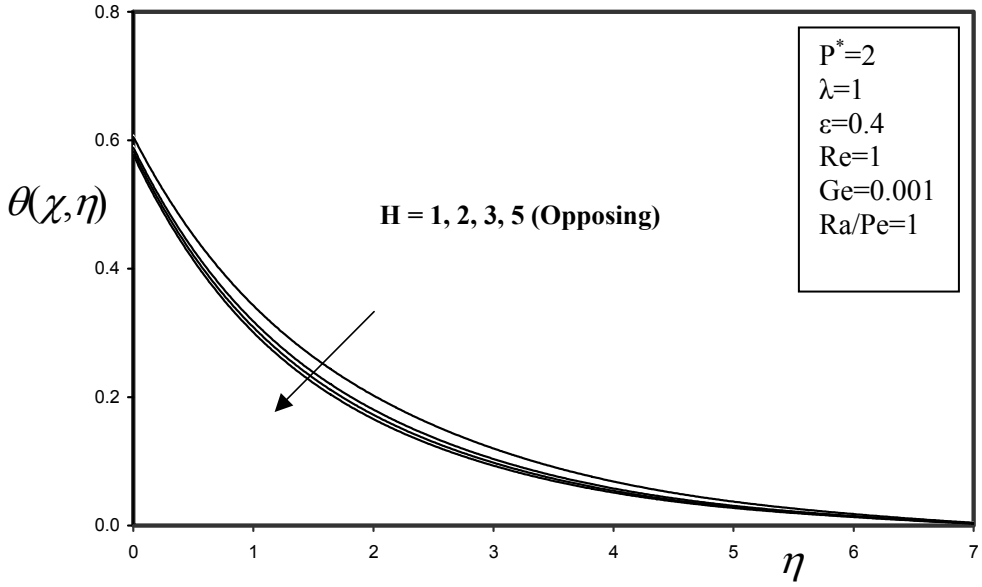

Fig 11 Dimensionless temperature profiles for different H
(mixed convection-B)

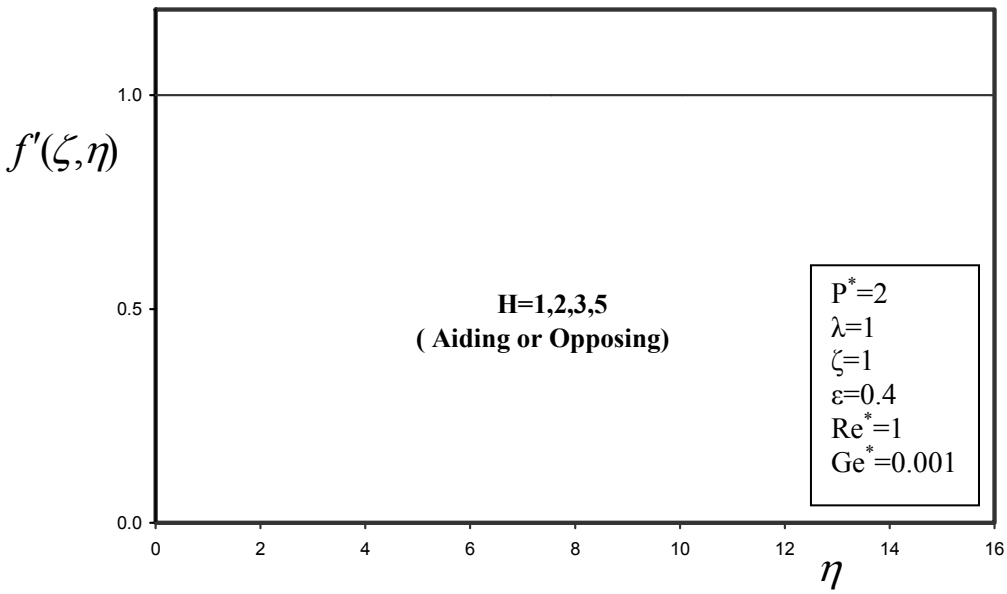

Fig 12 Dimensionless velocity profiles for different H
(Forced convection)

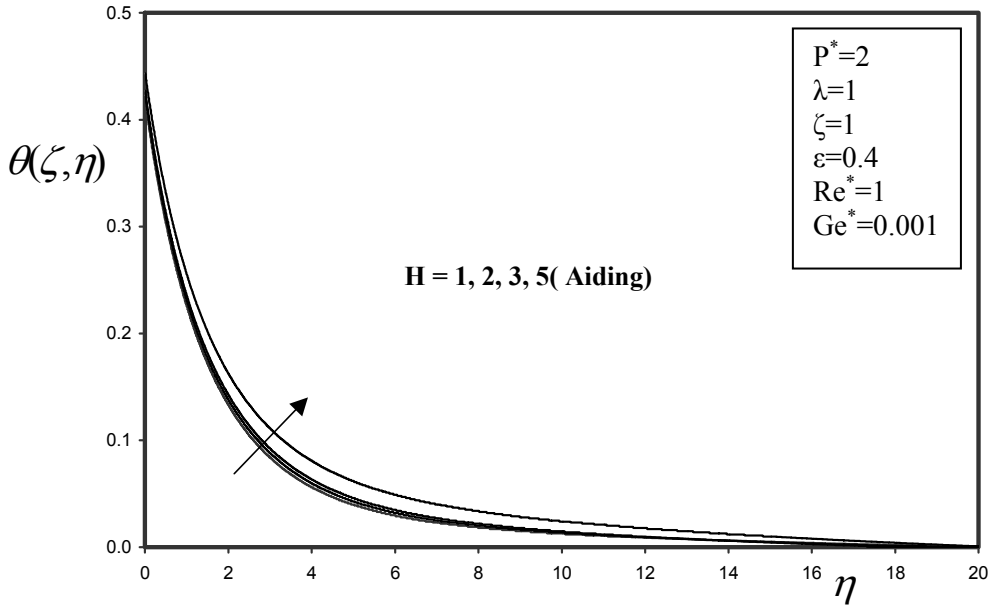

Fig 13 Dimensionless temperatureprofiles for different H
(Forced convection)

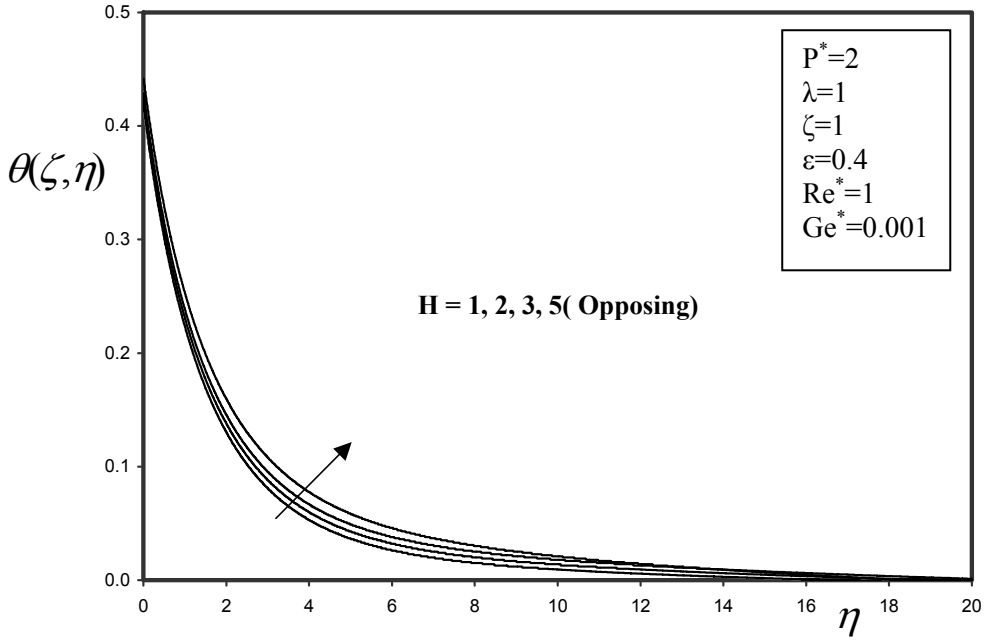

Fig 14 Dimensionless temperatureprofiles for different H
(Forced convection)

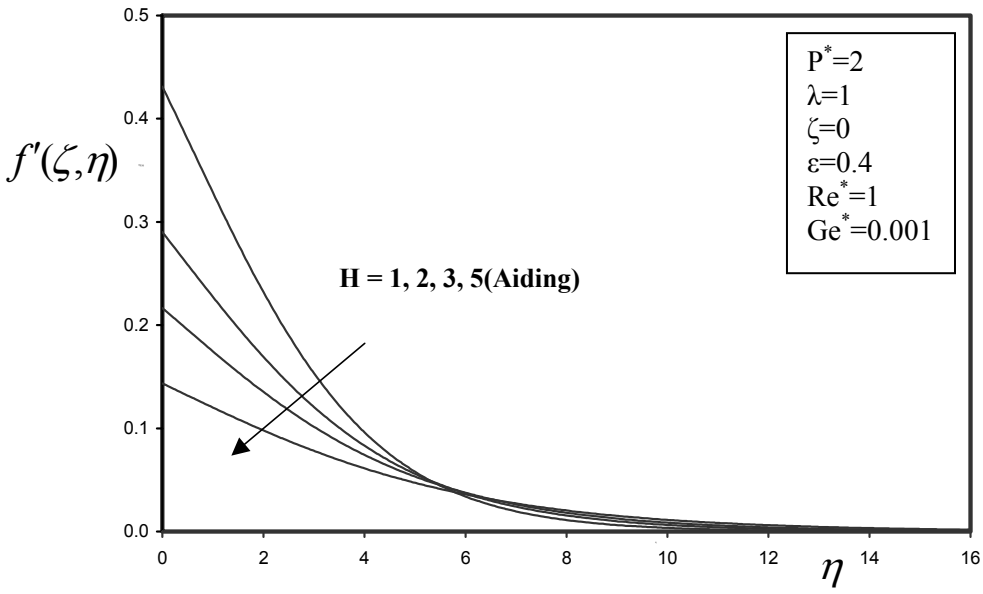

Fig 15 Dimensionless velocity profiles for different H
(Free convection)

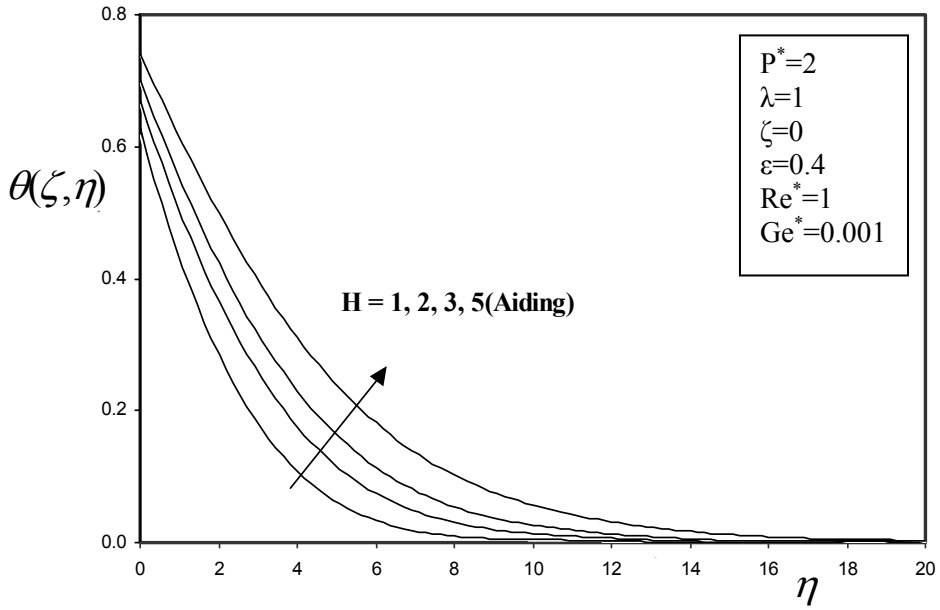

Fig 16 Dimensionless temperature profiles for different H
(Free convection)

3. Viscous dissipation effects:

The effect of viscous dissipation term is included in the energy equations through Ge^*, Ge numbers. Results for velocity and temperature profiles are presented in figures (5.14-5.21) for mixed convection heat transfer aiding and opposing flows for different values of Ge^*, Ge numbers for the two cases. These figures show that increasing Ge^*, Ge numbers had increased the velocity for the buoyancy aiding flow and decreased it for the buoyancy opposing flow. The effect of viscous dissipation again is to heat the fluid due to the work done by the viscous forces, which leads to arise in the fluid temperature, and so decrease the heat transfer rate from the cylinder surface for both buoyancy aiding and opposing flows. increasing the temperature of the fluid leads to increase the buoyancy force which leads to increase the velocity in the aiding flow and decrease it in the opposing flow.

Figures (5.22-5.25) show the effect of Ge^* number on the velocity and the temperature profiles for forced convection heat transfer problem. Where Ge^* number has no effect on the velocity profiles, but it increases the fluid temperature and decrease the heat transfer rate because of the excess heating of the fluid.

Figure (5.26) and figure (5.27) show the effect of Ge^* number on the velocity and the temperature profiles for free convection heat transfer problem. These figures show that increasing Ge^* number had increased the velocity and decreased the heat transfer rate in the flow. This effect is similar to the effect of viscous dissipation on the mixed convection aiding flow.

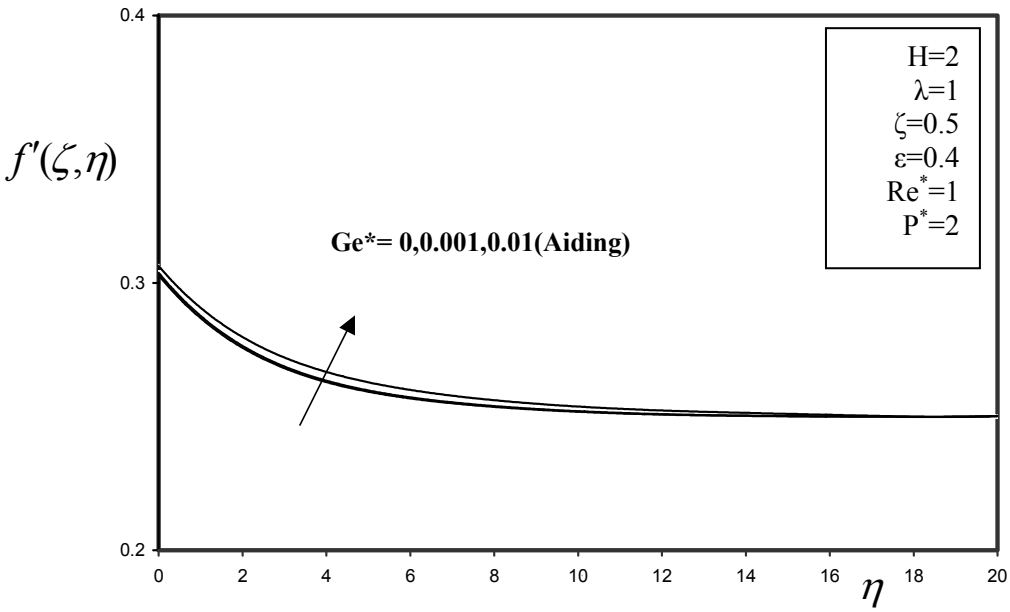

Fig 17 Dimensionless velocity profiles for different Ge*
(mixed convection-A)

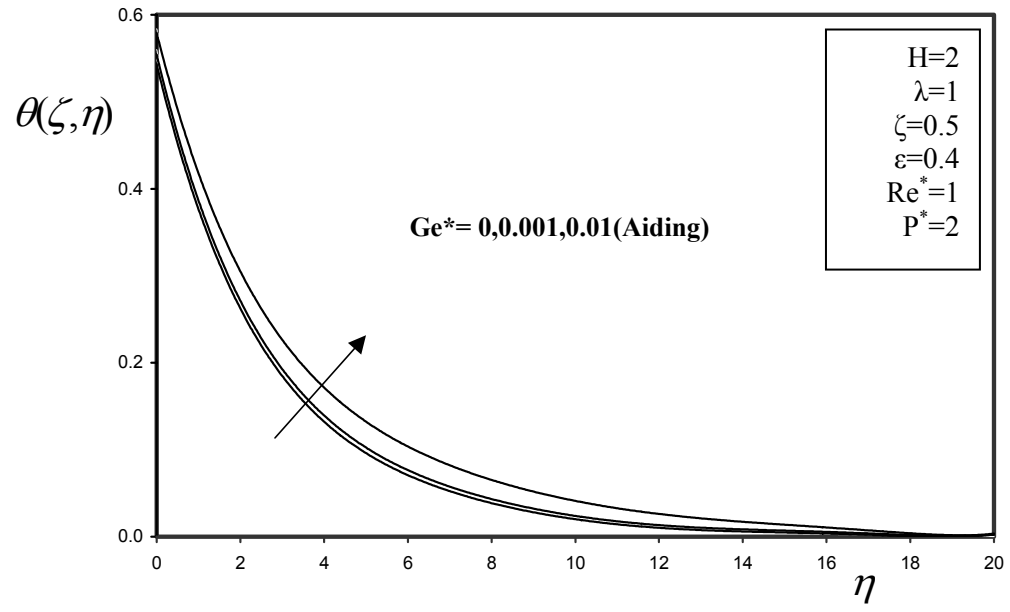

Fig 18 Dimensionless temperature profiles for different Ge*
(mixed convection-A)

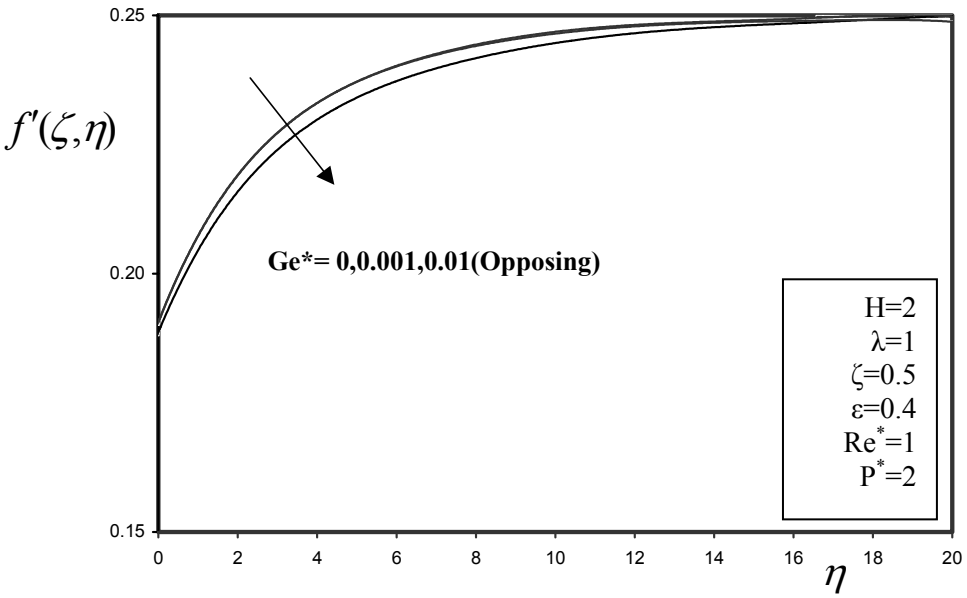

Fig 19 Dimensionless velocity profiles for different Ge*
(mixed convection-A)

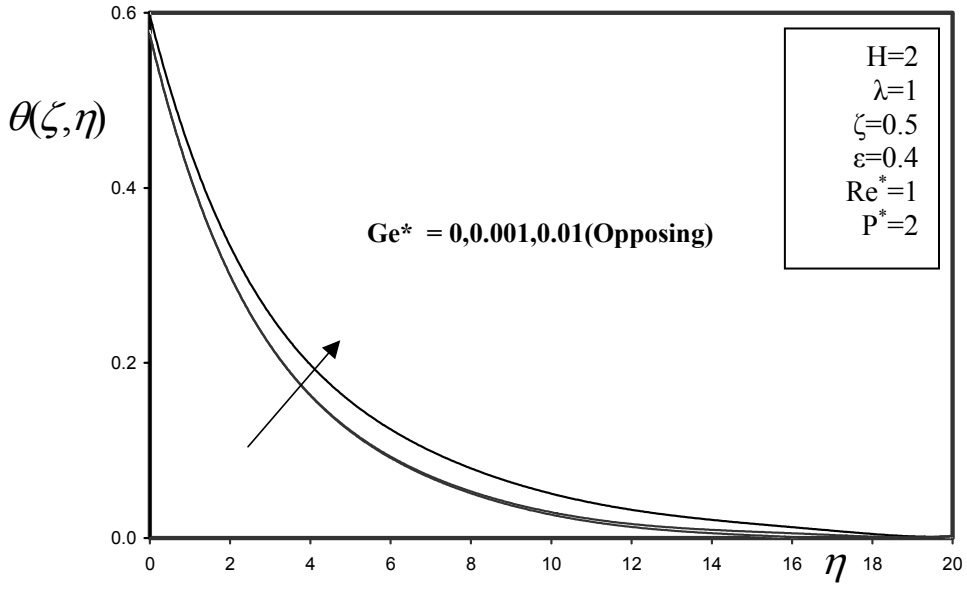

Fig 20 Dimensionless temperature profiles for different Ge*
(mixed convection-A)

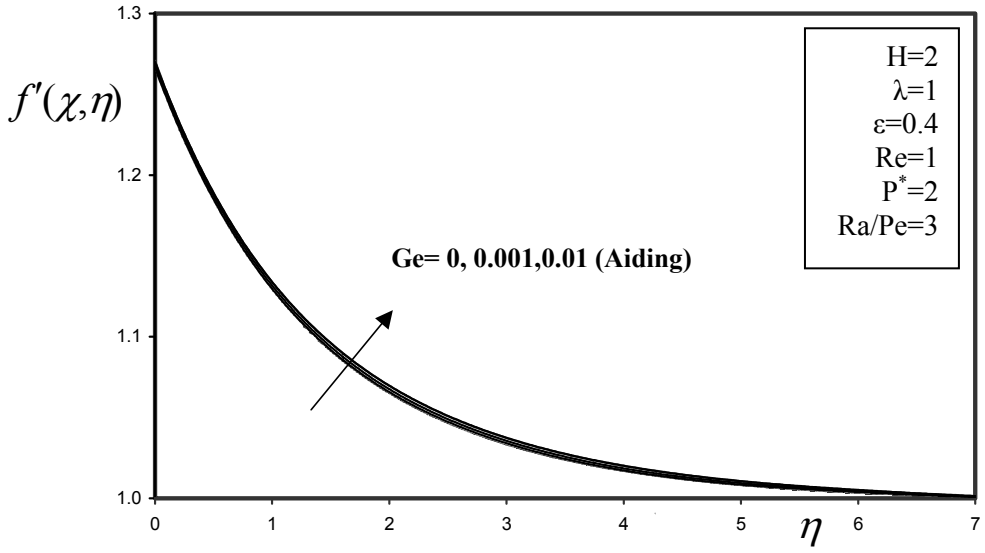

Fig 21 Dimensionless velocity profiles for different Ge
(mixed convection-B)

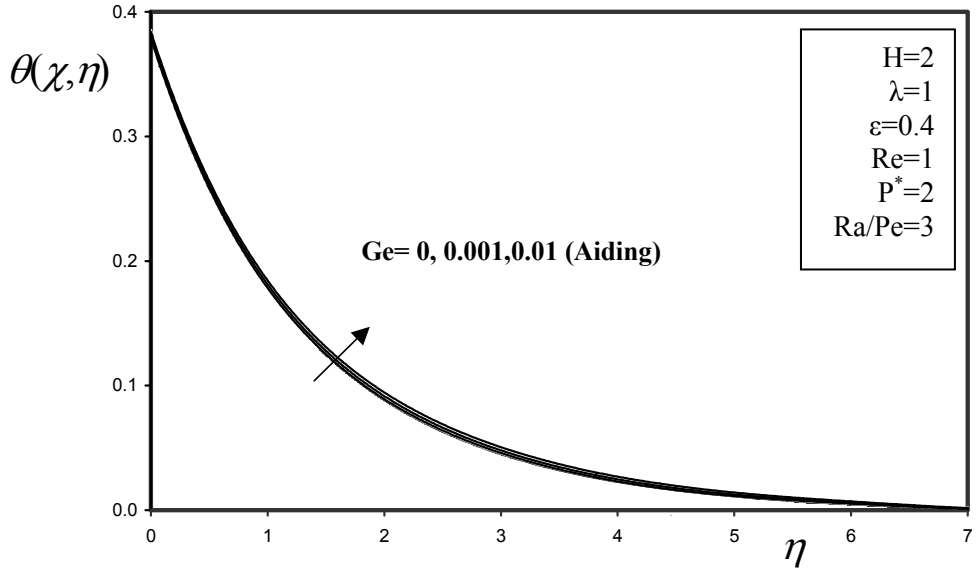

Fig22Dimensionless temperature profiles for different Ge
(mixed convection-B)

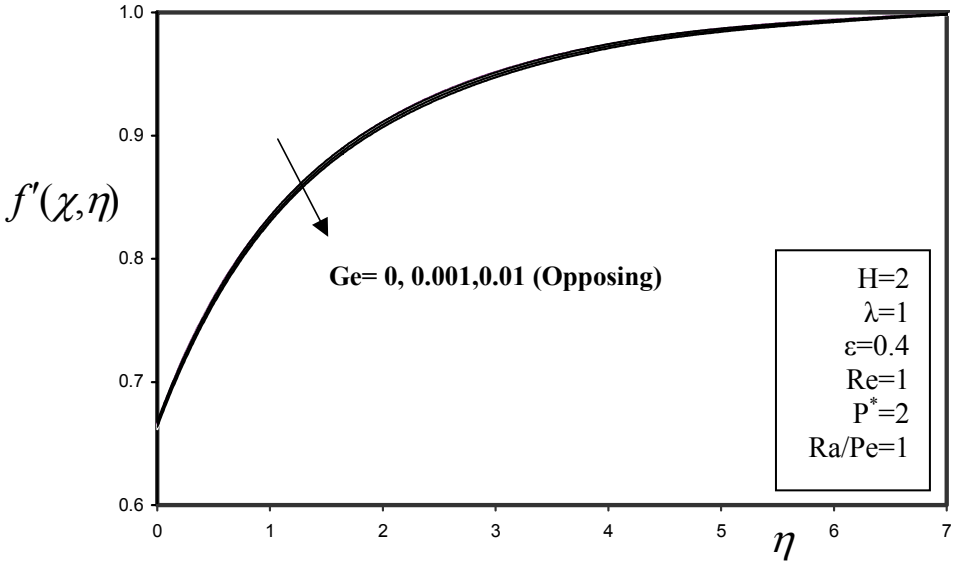

Fig 23 Dimensionless velocity profiles for different Ge (mixed convection-B)

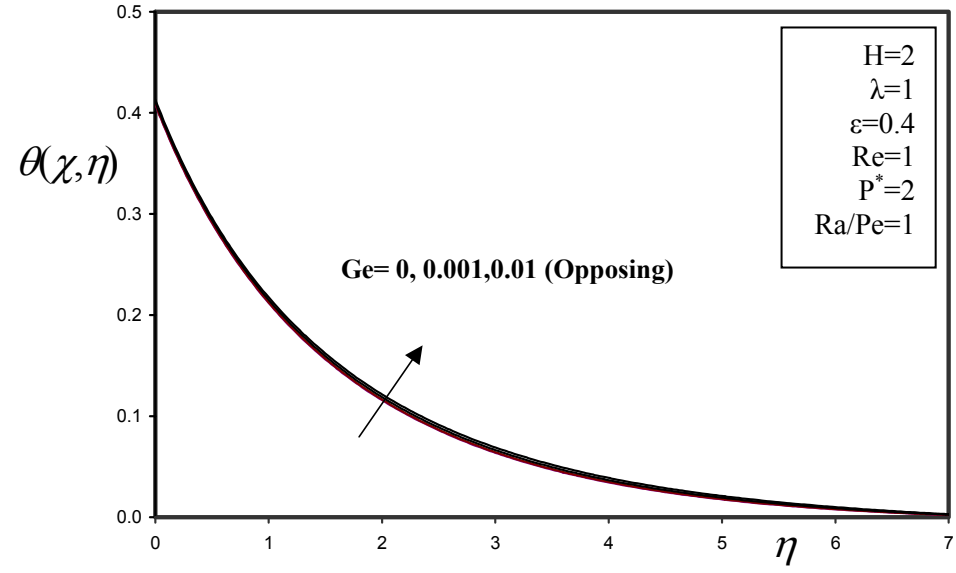

Fig 24 Dimensionless temperature profiles for different Ge (mixed convection-B)

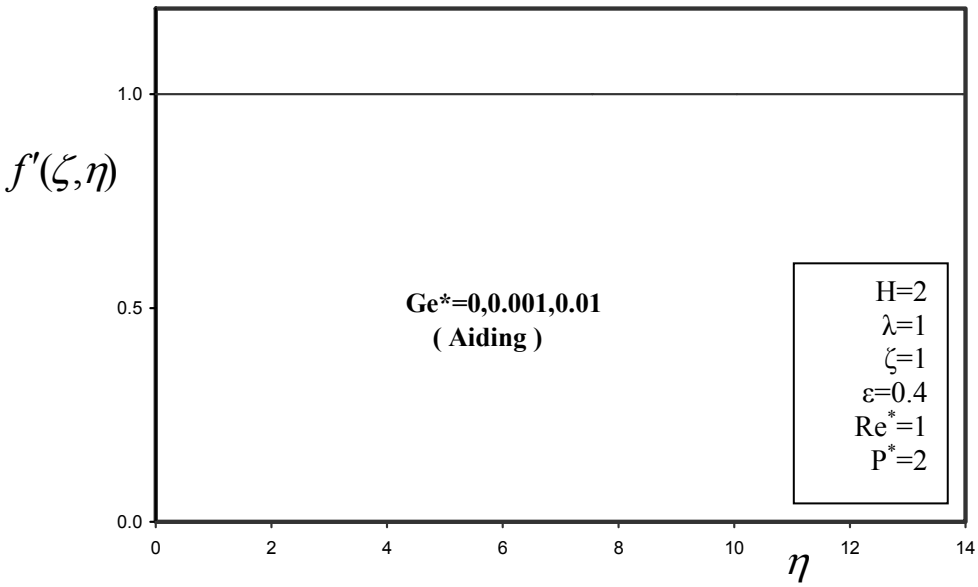

Fig 25 Dimensionless velocity profiles for different Ge*
(Forced convection)

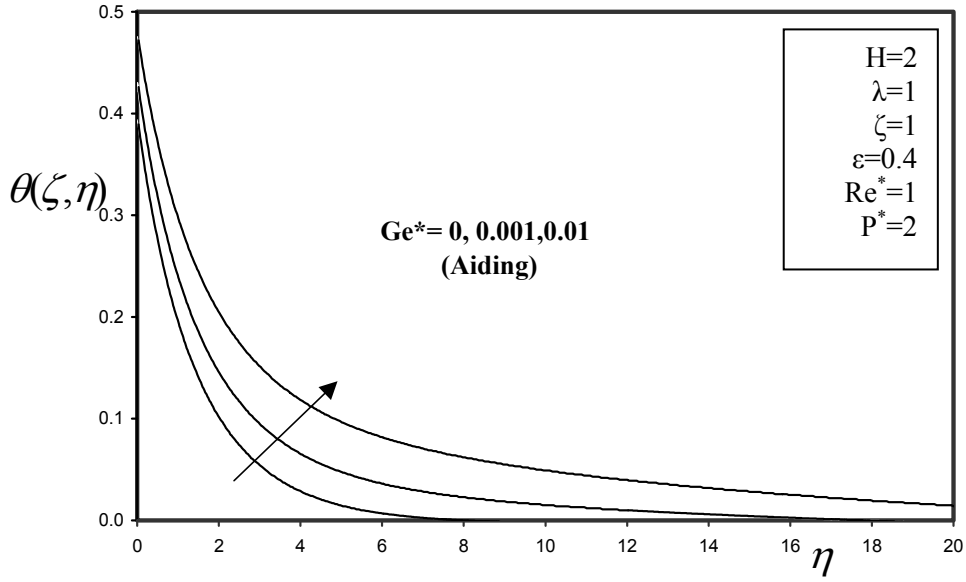

Fig 26 Dimensionless temperature profiles for different Ge*
(Forced convection)

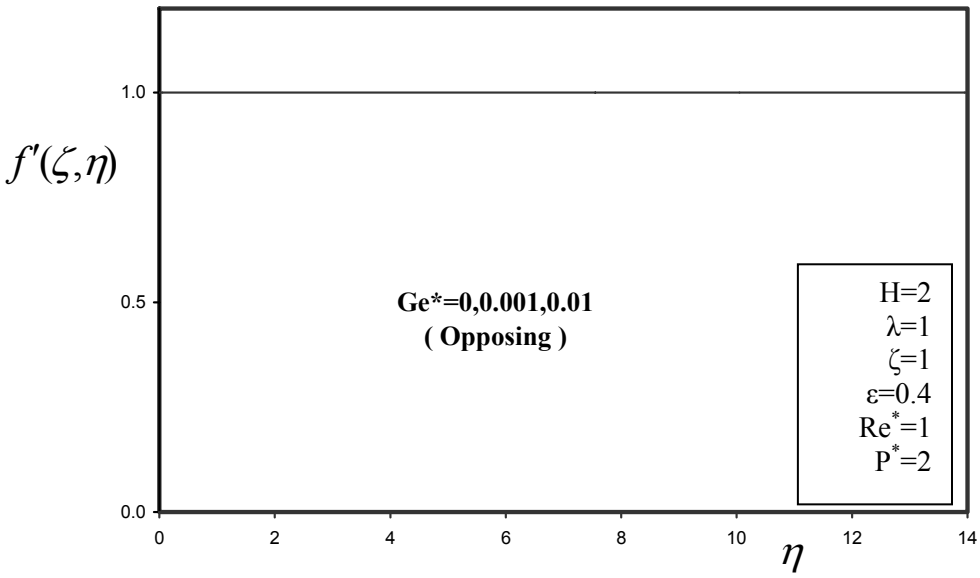

Fig 27 Dimensionless velocity profiles for different Ge*
(Forced convection)

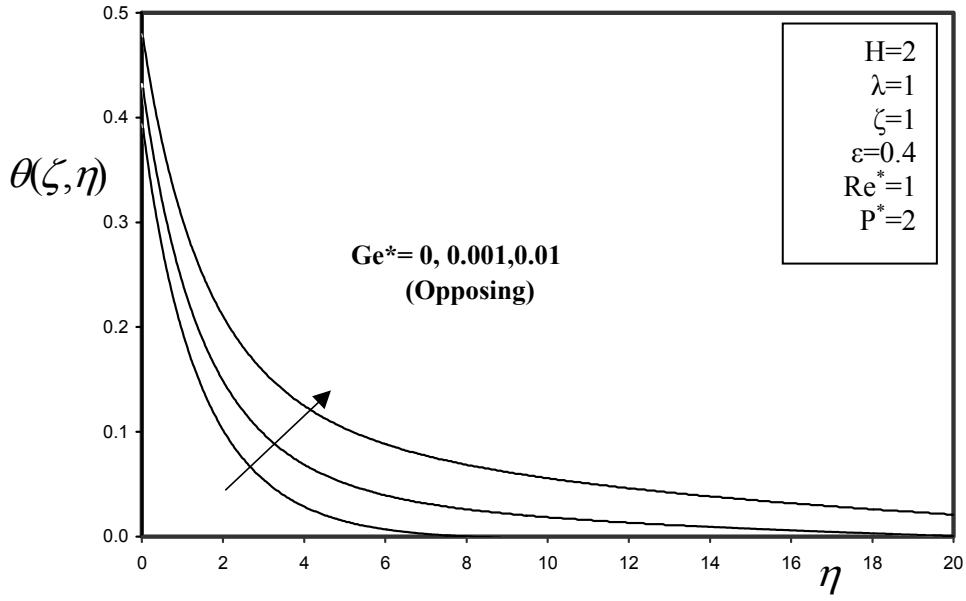

Fig 28 Dimensionless temperature profiles for different Ge*
(Forced convection)

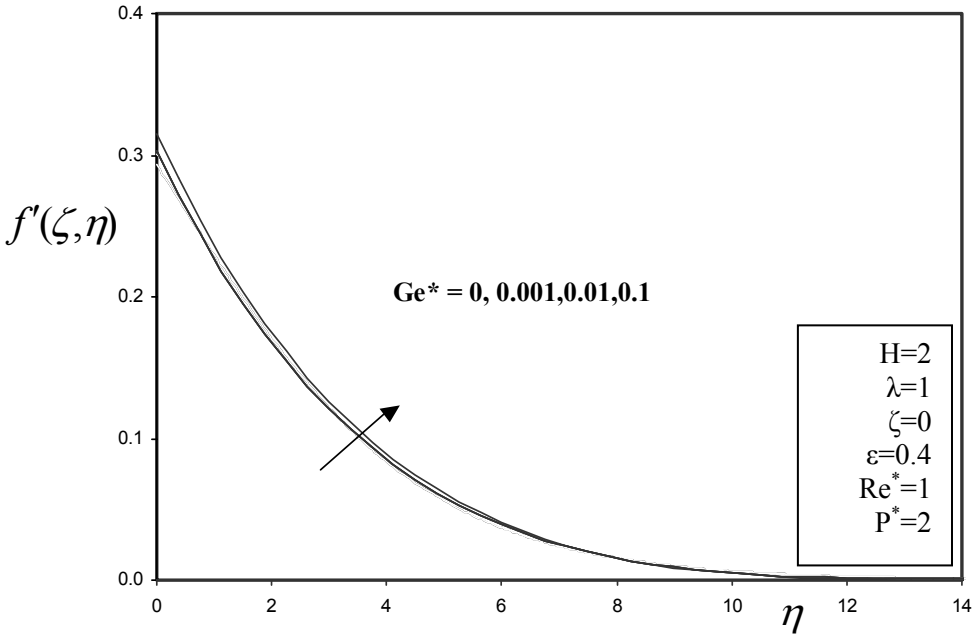

Fig 29 Dimensionless velocity profiles for different Ge*
(Free convection)

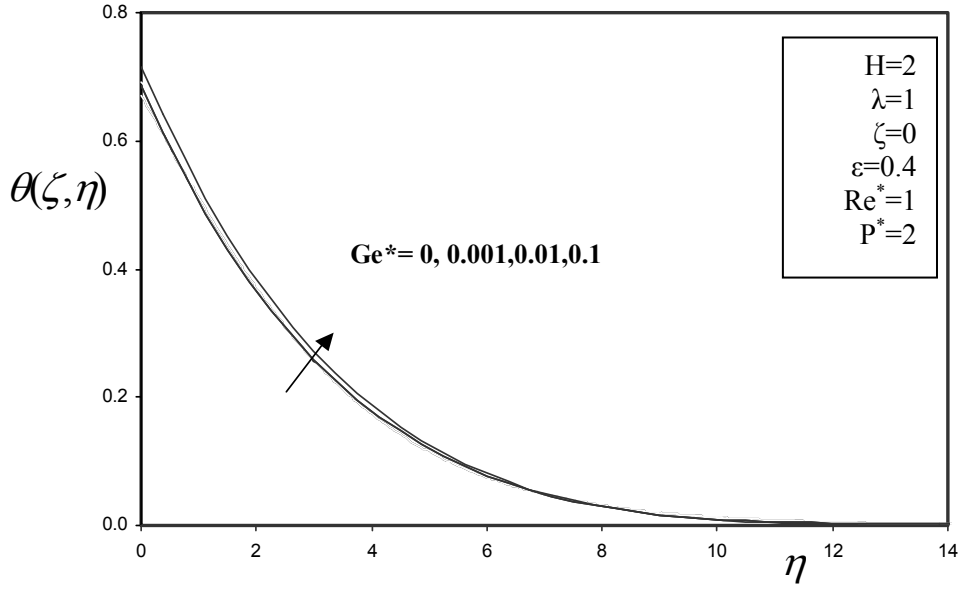

Fig 30 Dimensionless temperature profiles for different Ge*
(Free convection)

4. Surface curvature effects:

The curvature effects in the case of flow along vertical cylinder are introduced by the parameter λ. The physical values of λ depend on the radius of the cylinder (r_o) and Pe_x. The radius of the cylinder r_o must be small compared to x for the assumption of infinite cylinder to be valid with boundary layer approximation (for x>0)(Aldoss et al., 1996). The magnitude of λ is proportional to the ratio of the boundary layer thickness to the cylinder radius. Consequently, small values of λ correspond to relatively thin boundary layer and small deviations from the flat plate problem, whereas large values of λ correspond to relatively to thick boundary layer and large deviation from the flat plate problem. The case of vertical flat surface can be studied by setting λ=0 in the governing equations.

The effect of λ on both velocity and temperature profiles is shown in figures (5.28-5.39). Where the effects of λ on the velocity and temperature profiles for the mixed convection heat transfer (aiding and opposing flows) are shown in figures (5.28-5.35), from these figures it is seen that for the buoyancy aiding flow as λ increases the velocity decreases, but the magnitude of the velocity after a certain limit will increase and the heat transfer rate from the cylinder surface increases. For the effects of λ on the buoyancy opposing flow as shown in figures, as λ increases the velocity increases and the velocity magnitude after a certain limit decreases, the heat transfer rates from the surface of the cylinder increase.

Figures (5.36-5.39) show the effects of λ on forced convection heat transfer rates where it is seen that as λ increases the heat transfer rates increase. This observation is in a good agreement of the fact that large λ corresponds to larger surface area and this tend to increase the heat transfer rates from the surface. It is noted that for pure free convection heat transfer λ is not appropriate as a curvature parameter; because λ has in

its definition Pe_x. Where the effect of cylinder curvature in case of pure free convection is reported by (Minkowyez and cheng, 1976 and Aldoss et al,1996).

5.

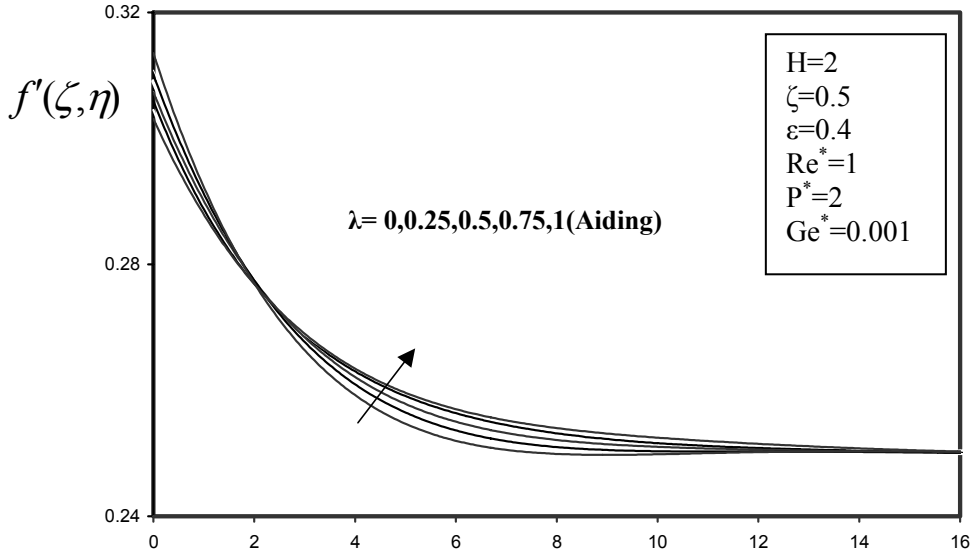

Fig 31 Dimensionless velocity profiles for different λ
(mixed convection-A)

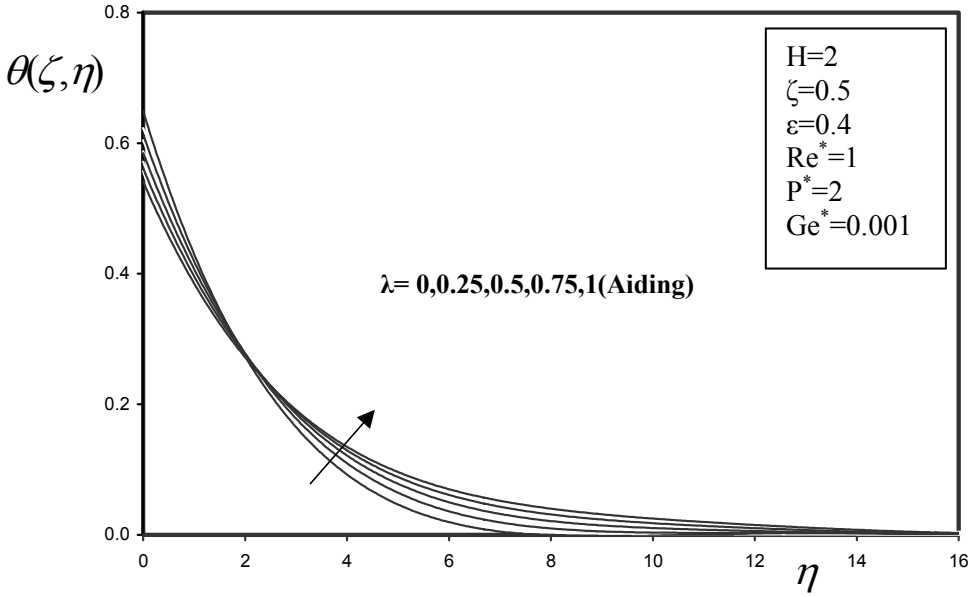

Fig 32 Dimensionless temperatureprofiles for different λ
(mixed convection-A)

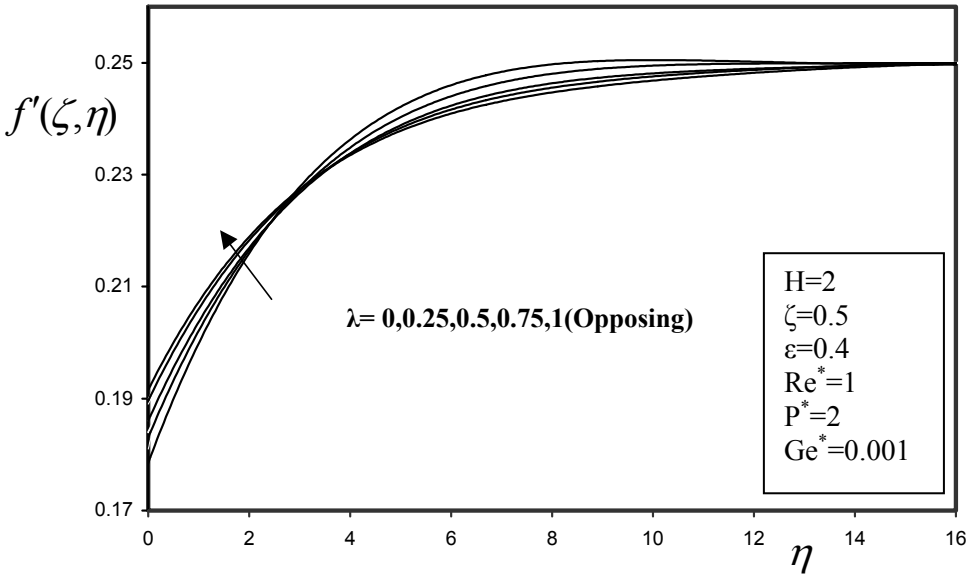

Fig 33 Dimensionless velocity profiles for different λ
(mixed convection-A)

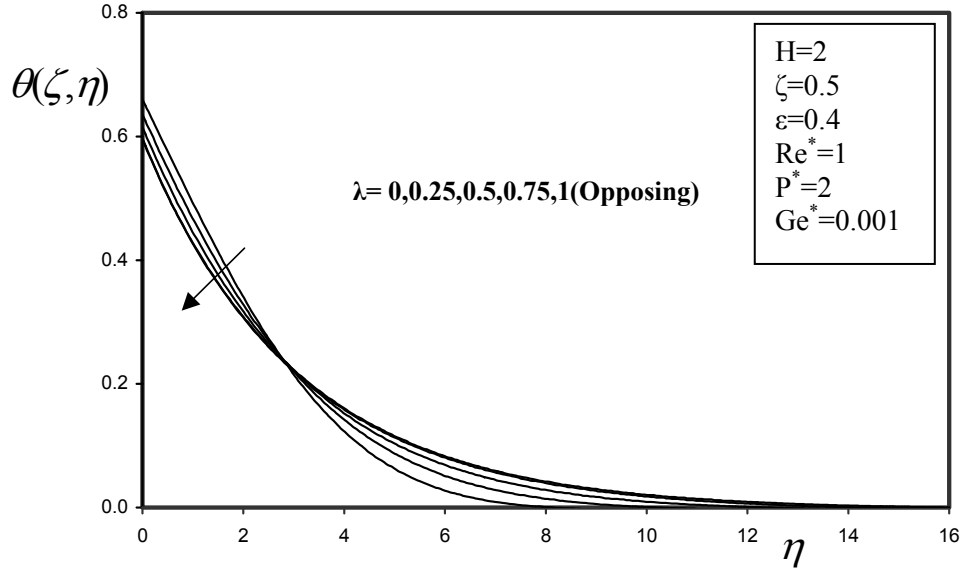

Fig 34 Dimensionless temperatureprofiles for different λ
(mixed convection-A)

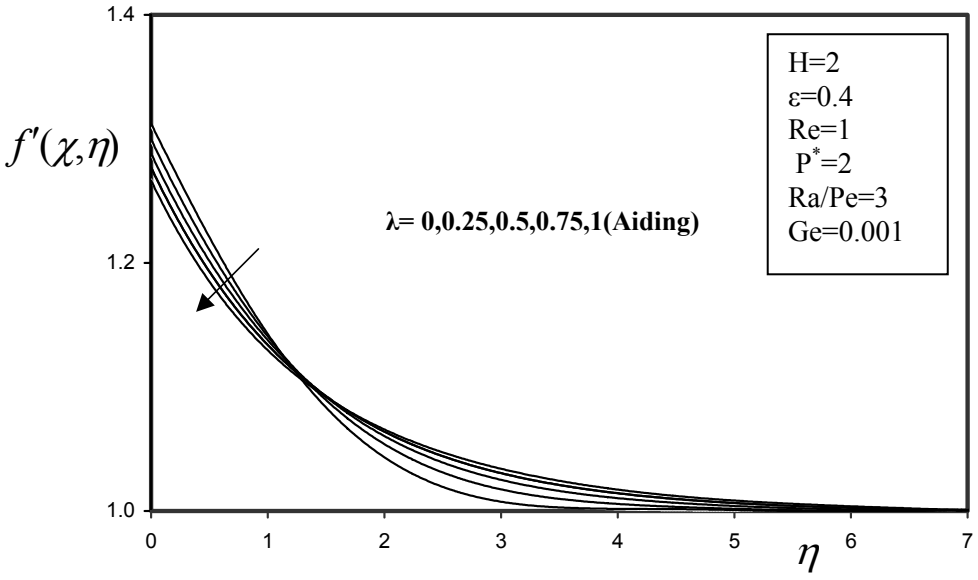

Fig 35 Dimensionless velocity profiles for different λ
(mixed convection-B)

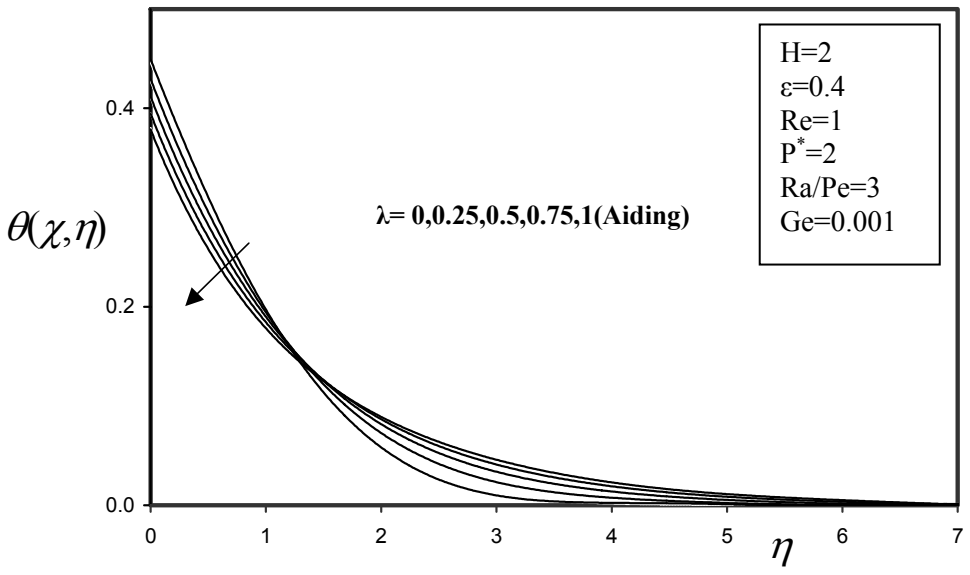

Fig 36 Dimensionless temperature profiles for different λ
(mixed convection-B)

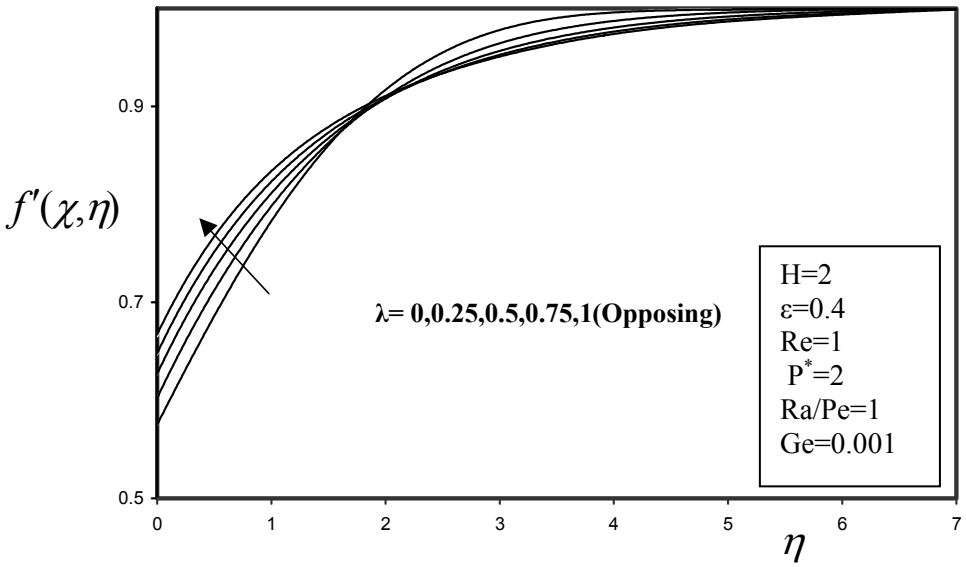

Fig 37 Dimensionless velocity profiles for different λ
(mixed convection-B)

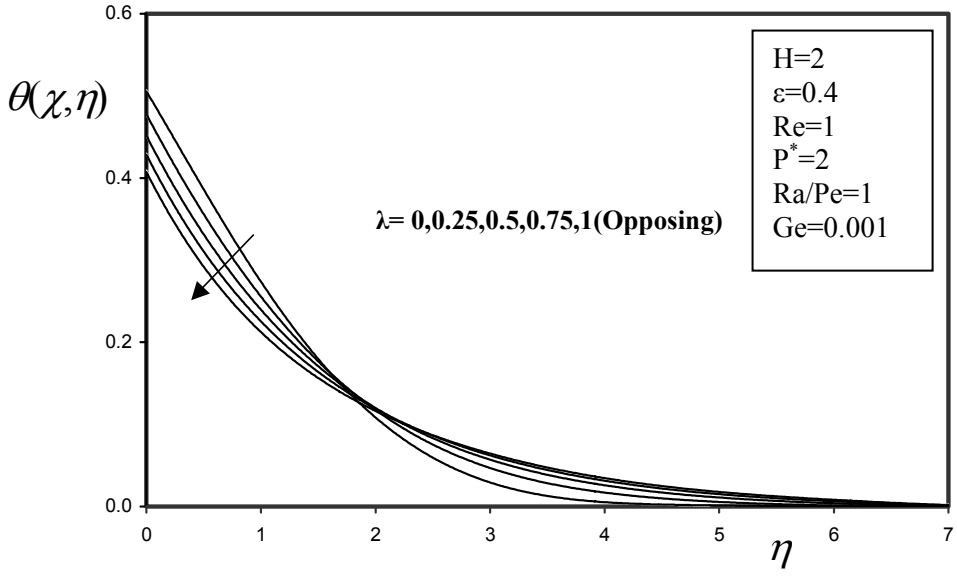

Fig 38 Dimensionless temperature profiles for different λ
(mixed convection-B)

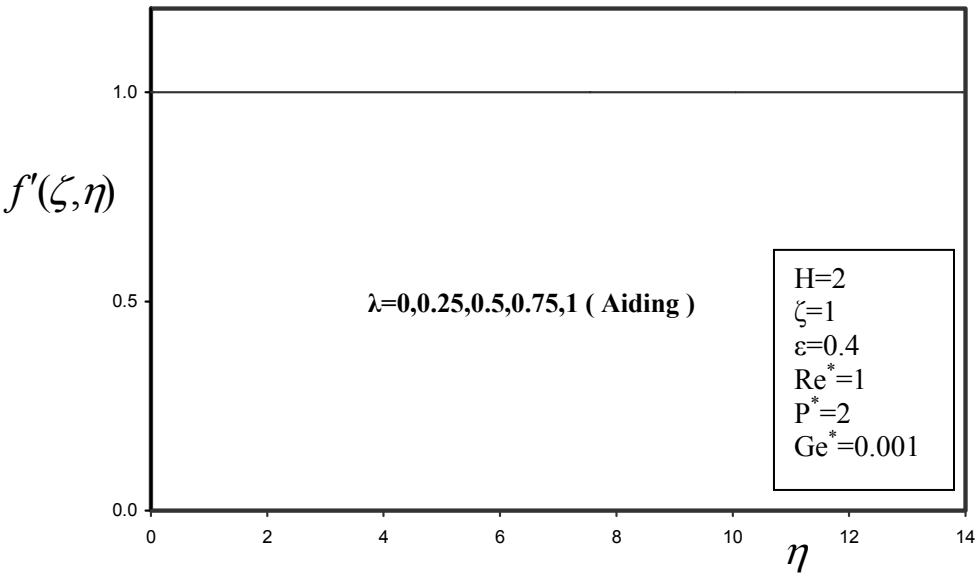

Fig 39 Dimensionless velocity profiles for different λ
(Forced convection)

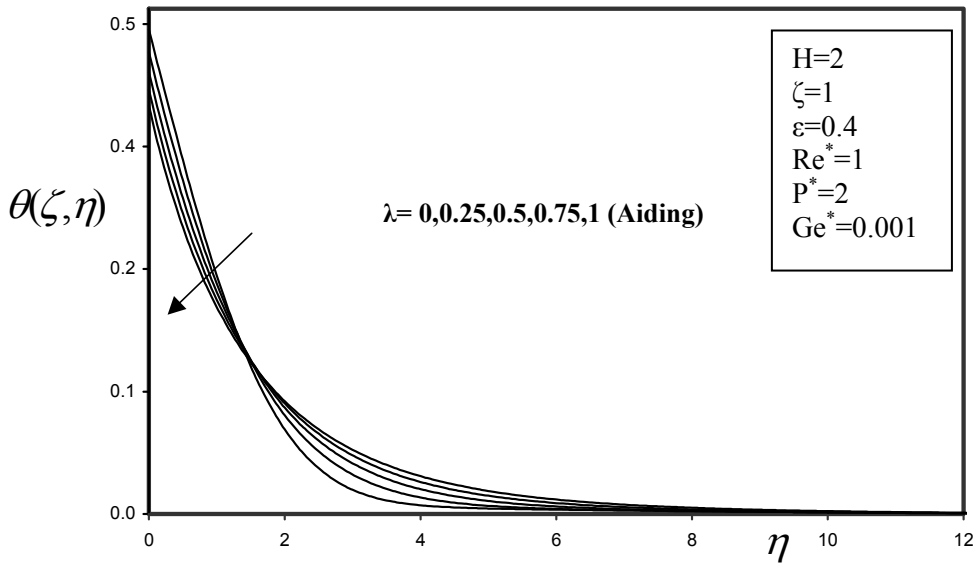

Fig 40 Dimensionless temperature profiles for different λ
(Forcedconvection)

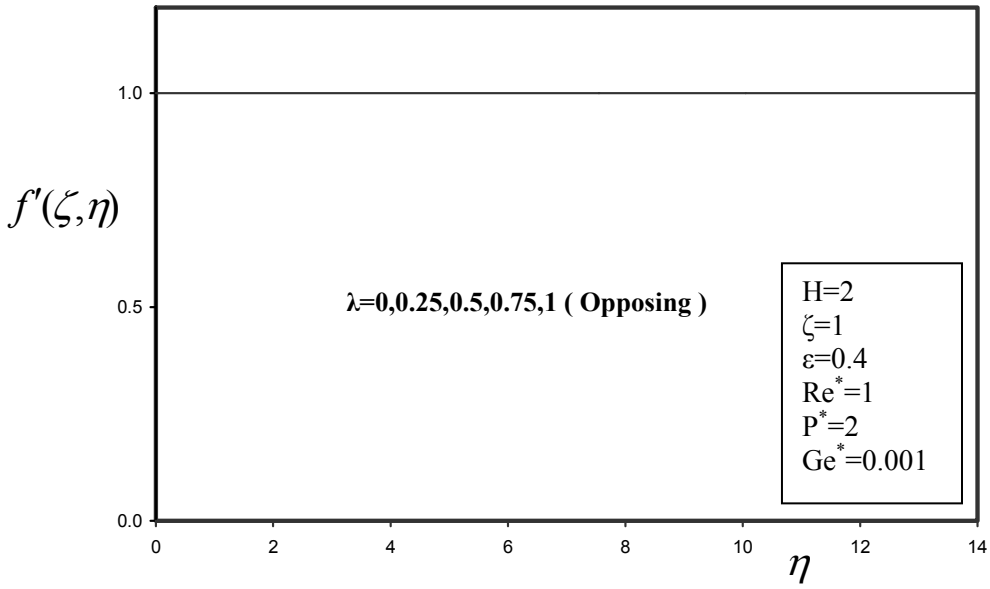

Fig 41 Dimensionless velocity profiles for different λ
(Forced convection)

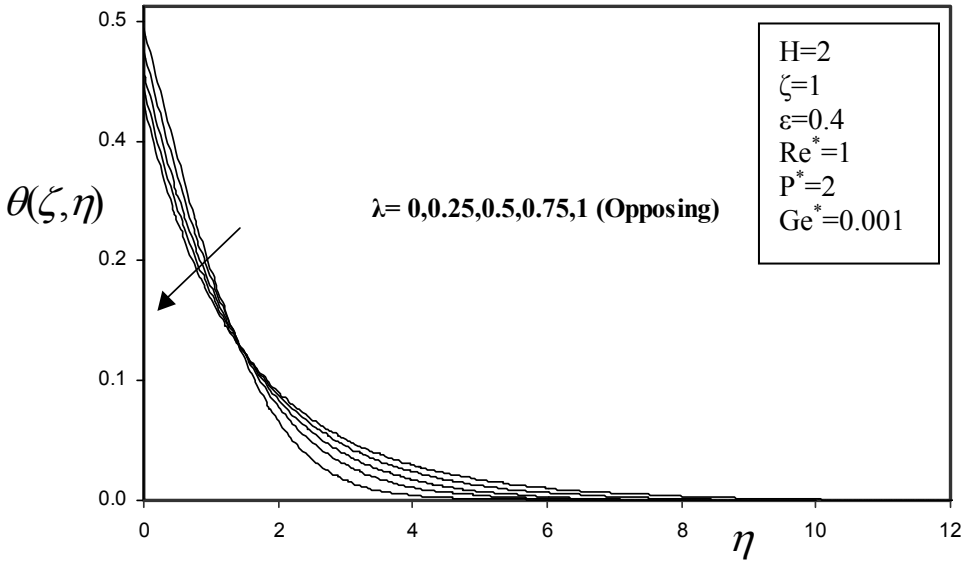

Fig 42 Dimensionless temperature profiles for different λ
(Forced convection)

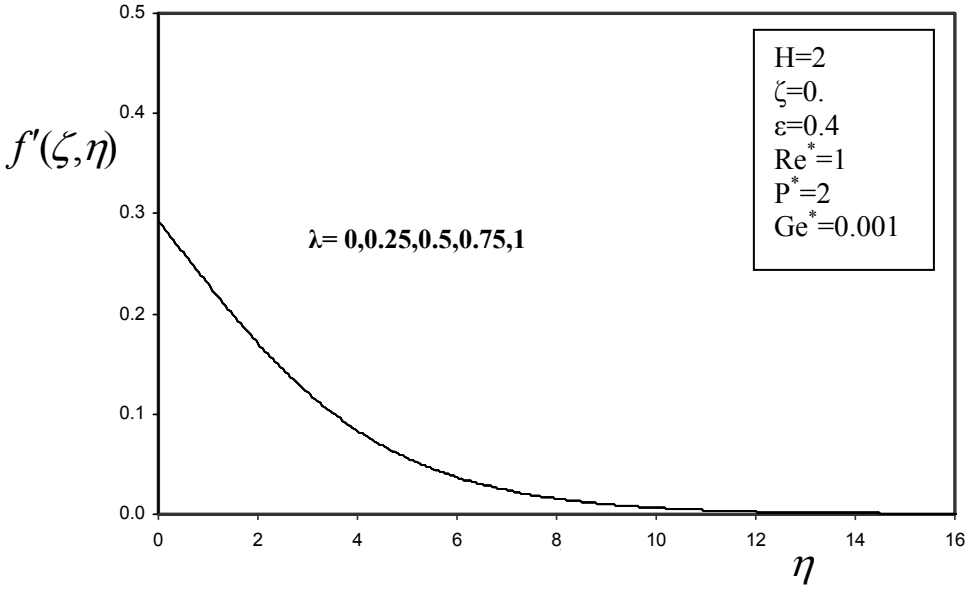

Fig 43 Dimensionless velocity profiles for different λ
(Free convection)

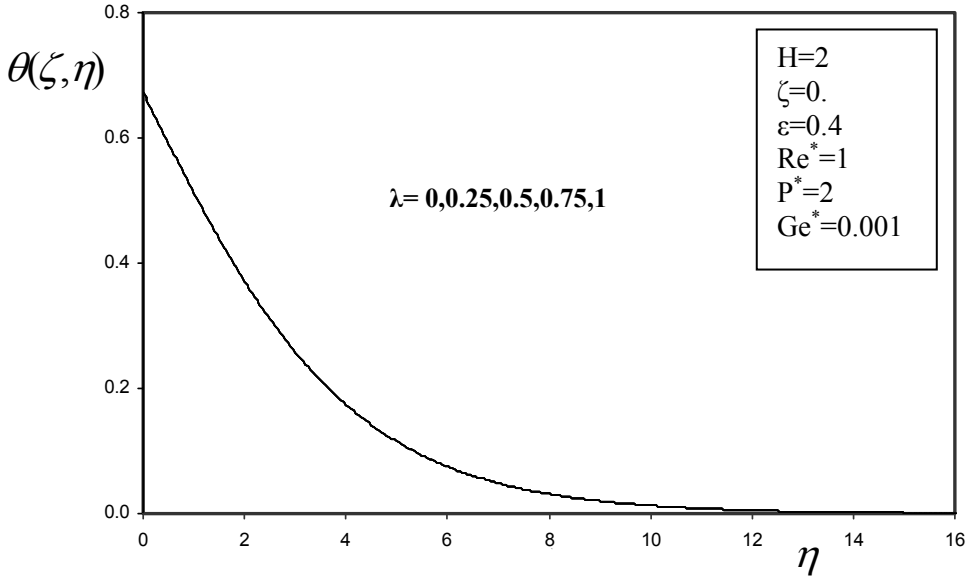

Fig 44 Dimensionless temperature profiles for different λ
(Free convection)

5. Inertial force effect:

The parameters Re^*, Re are found to characterize the effect of the inertial forces on the flow. Where the inertial term K' is proportional to pore diameter. Therefore. The inertia effects depend strongly on the pore size. For porous medium with small pores and low porosities, the permeability is small, and thus, shows negligible inertia effects. On the other hand, for porous media with large pores and properties, Re^*, Re can be quite large. Even for normal temperature difference for the same geometry.

Since in actual applications u_∞ can be assumed to be of order one O(1), $\nu = O(10^{-4})$ and $K' = O(10^{-7})$.then the parameters Re^*, Re become O(0.001). So that the values of Re^*, Re (0,1,..10) are enough to test the effect of inertia (Aldoss et al.,1996).

Results for temperature and velocity profiles are presented in figures (5.42-5.49) for mixed convection heat transfer rates (aiding and opposing flows), from these figures it is seen that, for the buoyancy aiding flow, as the inertia force increases the velocity and heat transfer rate decreases. But for the buoyancy opposing flow, it can be seen that an increase in the inertia force will increase the velocity and decrease the boundary layer thickness, which is contrary to the case of aiding flow.

For forced convection heat transfer (aiding and opposing flows), figures (5.50-5.53) show that increasing inertia force decreases the rate of heat transfer as a result of increasing the boundary layer thickness.

And the result for natural convection dominate regime are presented in figure (5.54) and figure (5.55), where figure (5.54) shows that increasing inertia force, decreases the velocity and increases the temperature inside the boundary layer, that means lower heat transfer rate at higher values of inertia force as shown in figure (5.55).

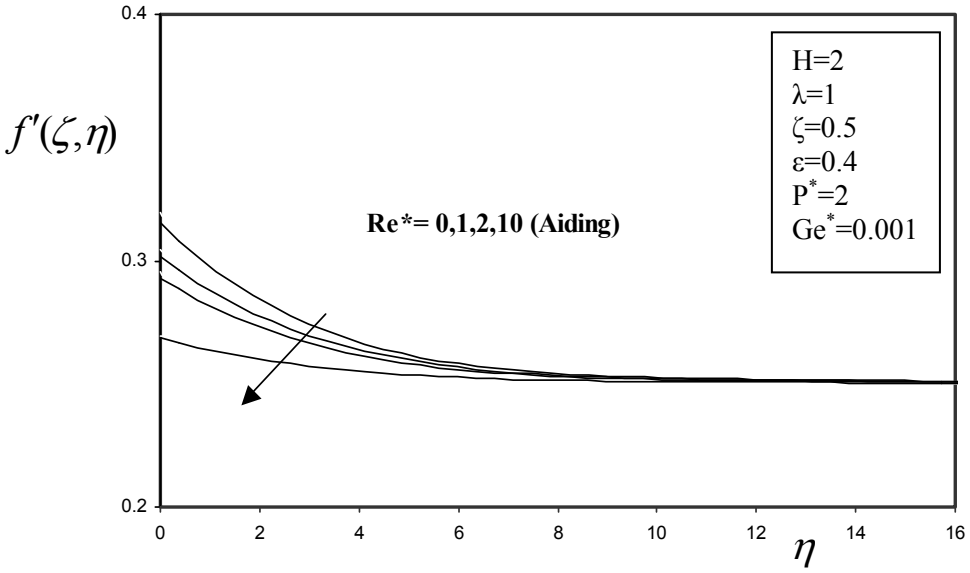

Fig 45 Dimensionless velocity profiles for different Re*
(mixed convection-A)

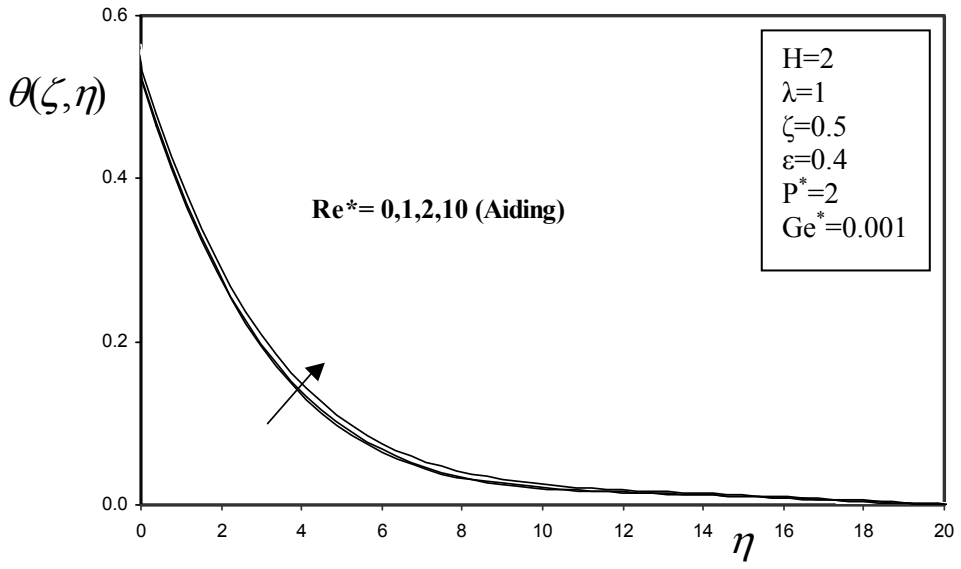

Fig 46 Dimensionless temperature profiles for different Re*
(mixed convection-A)

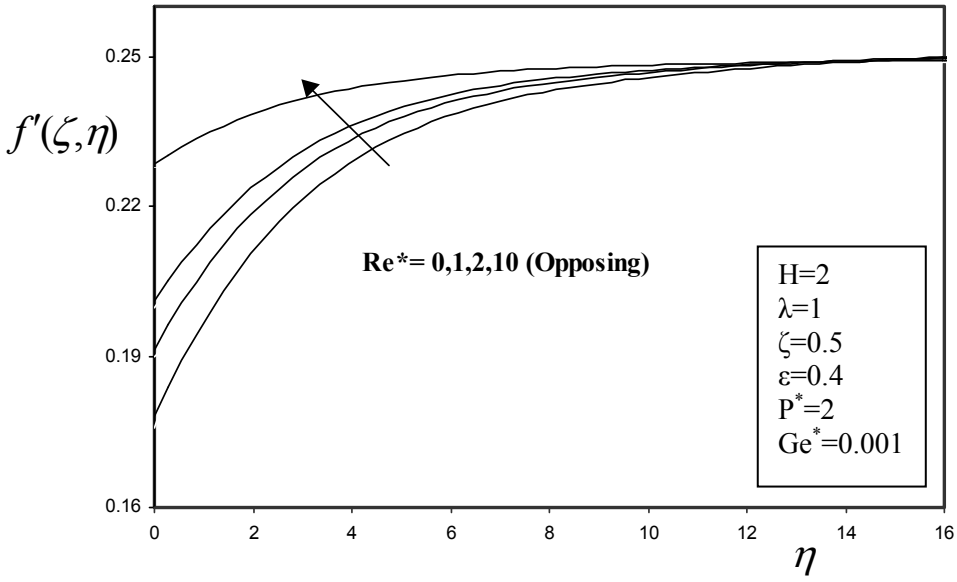

Fig 47 Dimensionless velocity profiles for different Re*
(mixed convection-A)

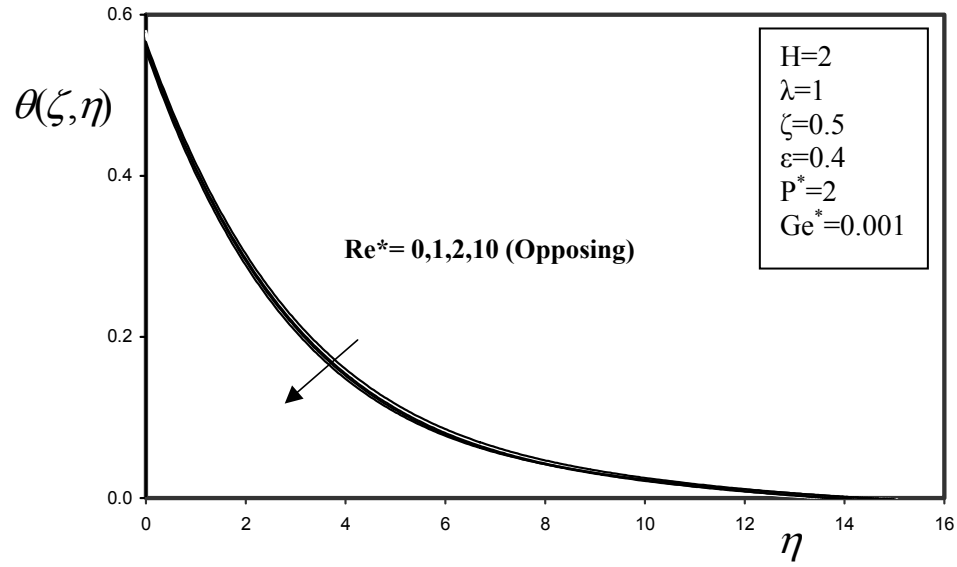

Fig 48 Dimensionless temperature profiles for different Re*
(mixed convection)

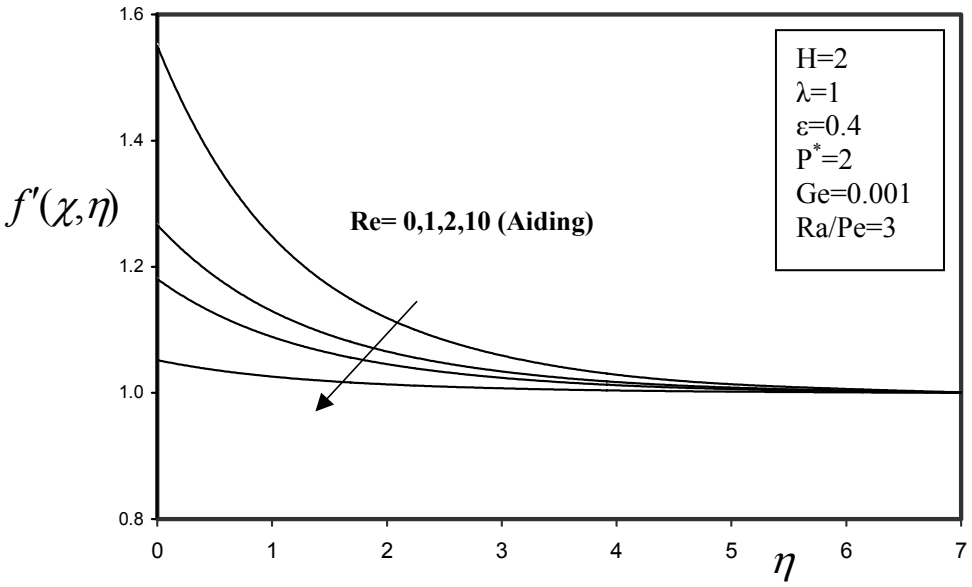

Fig 49 Dimensionless velocity profiles for different Re
(mixed convection-B)

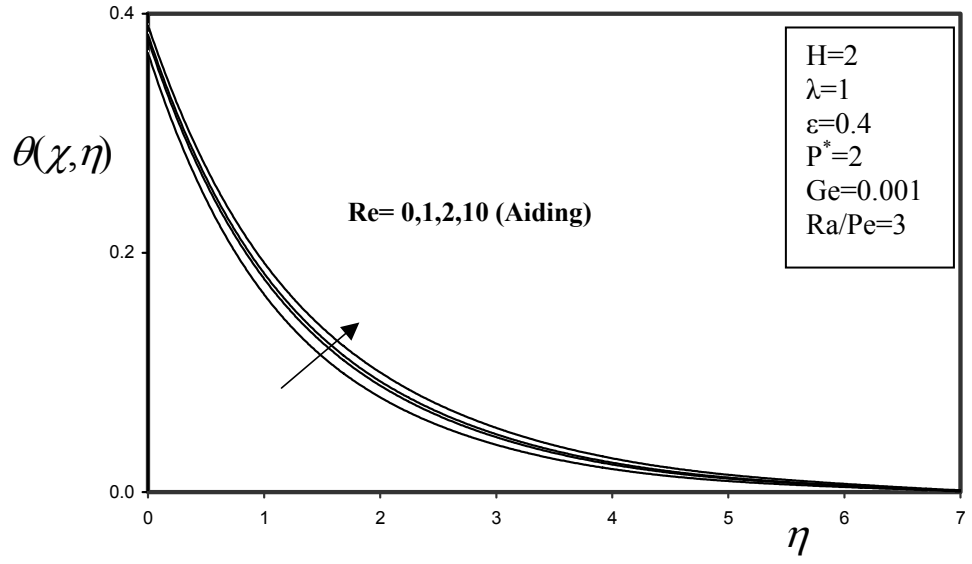

Fig 50 Dimensionless temperature profiles for different Re
(mixed convection-B)

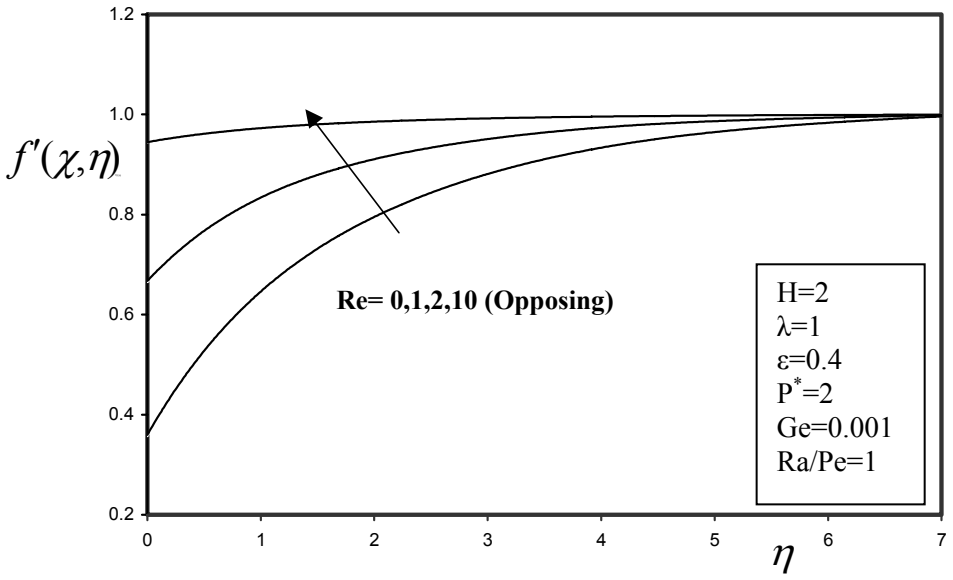

Fig 51 Dimensionless velocity profiles for different Re
(mixed convection-B)

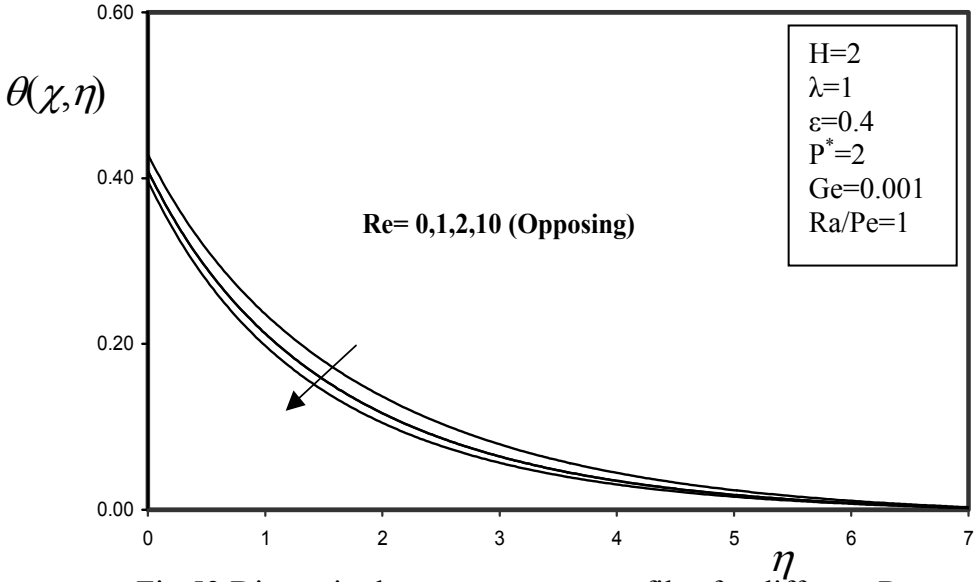

Fig 52 Dimensionless temperature profiles for different Re
(mixed convection-B)

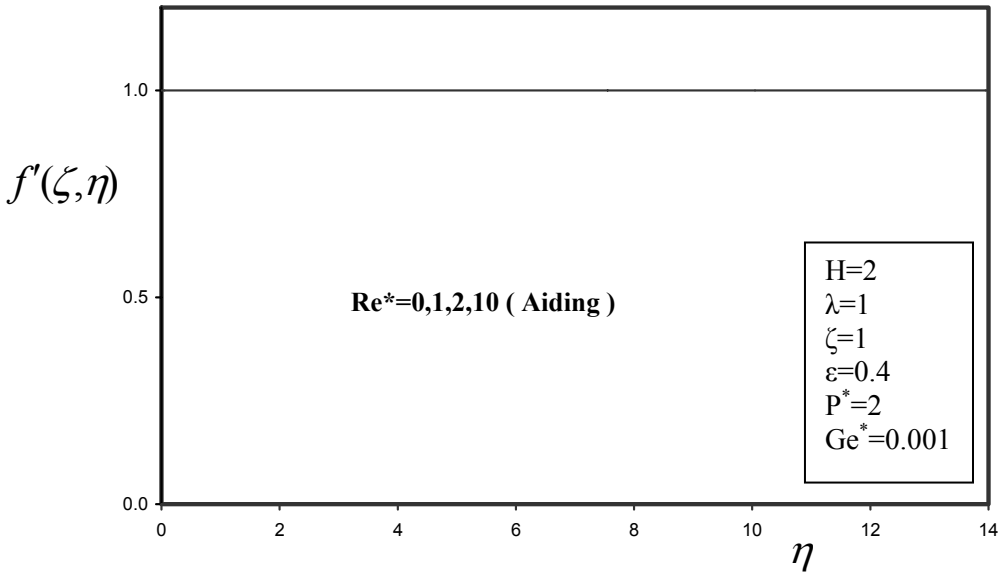

Fig 53 Dimensionless velocity profiles for different Re*
(Forced convection)

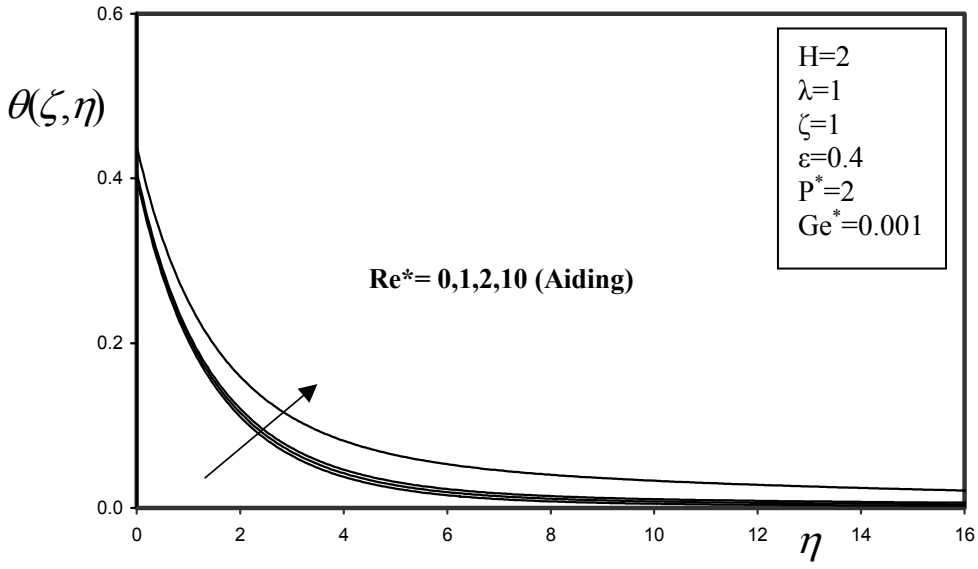

Fig 54 Dimensionless temperature profiles for different Re*
(Forced convection)

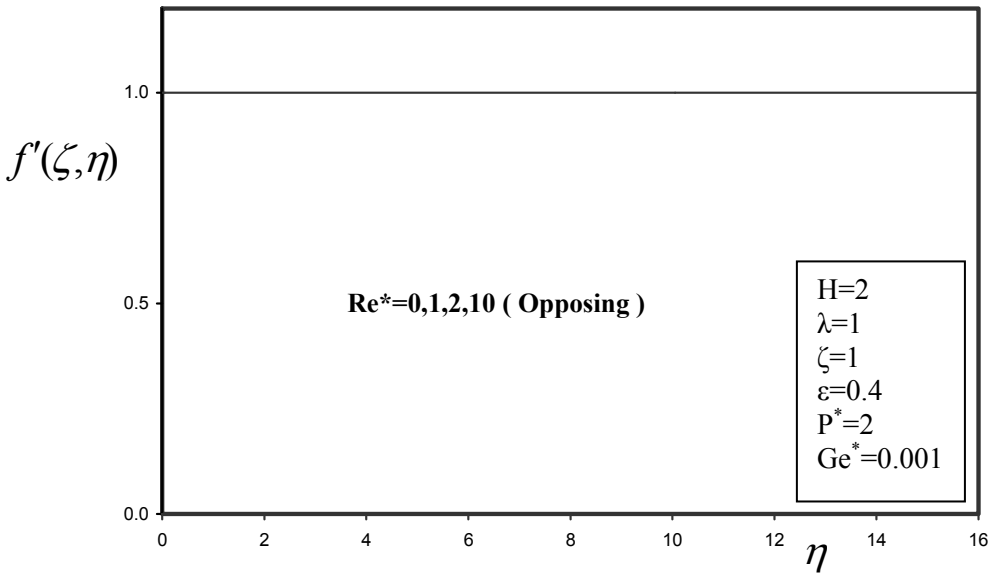

Fig 55 Dimensionless velocity profiles for different Re*
(Forced convection)

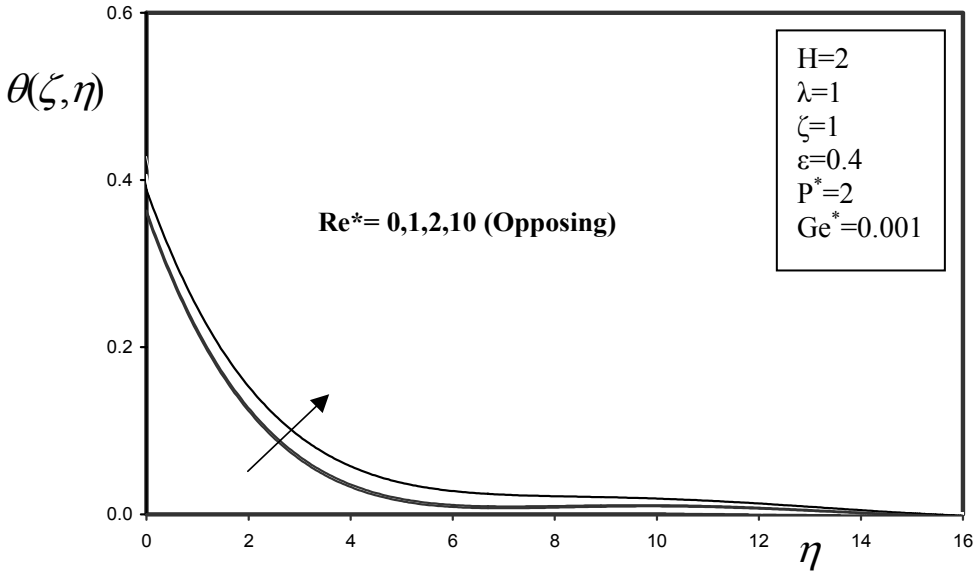

Fig 56 Dimensionless temperature profiles for different Re*
(Forced convection)

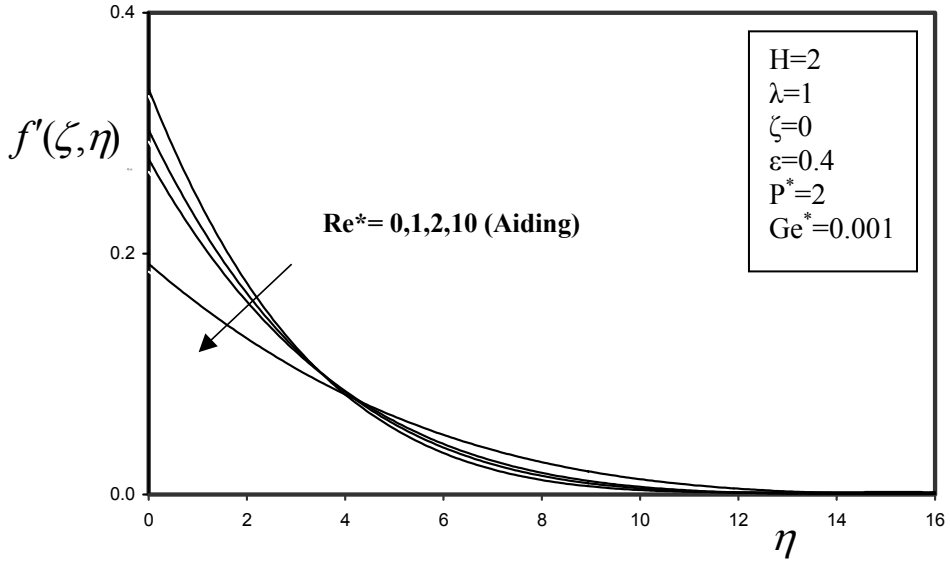

Fig 57 Dimensionless velocity profiles for different Re*
(Free convection)

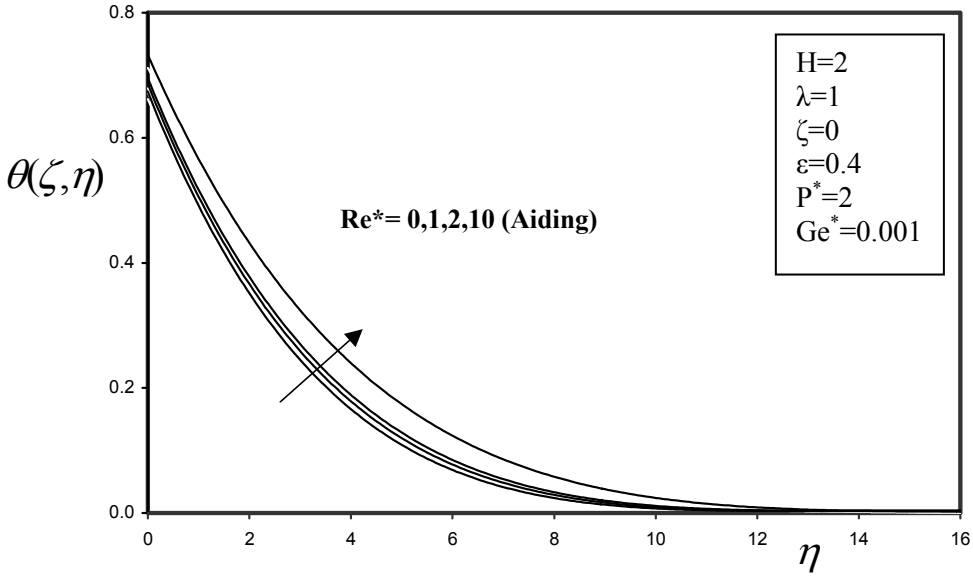

Fig 58 Dimensionless temperature profiles for different Re*
(Free convection)

6. Mixed convection parameter effects:

The nonsimilarity parameter ζ in case A, measures the strength of mixed convection where the limit $\zeta=0$ corresponds to pure natural convection while the other limit $\zeta=1$ corresponds to pure forced convection. Thus. The values of ζ from zero to one cover all the possible strength of mixed convection including free and forced convections.

The effect of ζ on the velocity and the temperature of the flow are demonstrated in figures (5.56-5.59), for the buoyancy aiding and the buoyancy opposing flows in the first case. It can be seen that an increase in ζ will increase the heat transfer rate and the thermal boundary layer thickness will decrease. This result is agreement with the fact, as ζ increases the velocity will increase. Thus. The heat transfer rate by convection will increase.

For the case B, the strength of mixed convection had measured by (Ra_x/Pe_x). Where the limit $Ra_x/Pe_x = 0$ corresponds to pure forced convection while the other limit $Ra_x/Pe_x \rightarrow \infty$ corresponds to pure natural convection.

The effect of the mixed convection parameter (Ra_x/Pe_x) on the MHD- mixed convection buoyancy aiding and opposing flows on both velocity and temperature profiles are shown in figures (5.60-5.63). For the buoyancy aiding flow, increasing the mixed convection parameter had increased the velocity inside the boundary layer due to favorable buoyancy effects and consequently increased the heat transfer rate from the surface of the cylinder. While increasing the mixed convection parameter for the opposing flow had decreased the velocity inside the boundary layer due to increasing effect of the buoyancy force in opposite direction, and the heat transfer rates from the surface of cylinder will decrease.

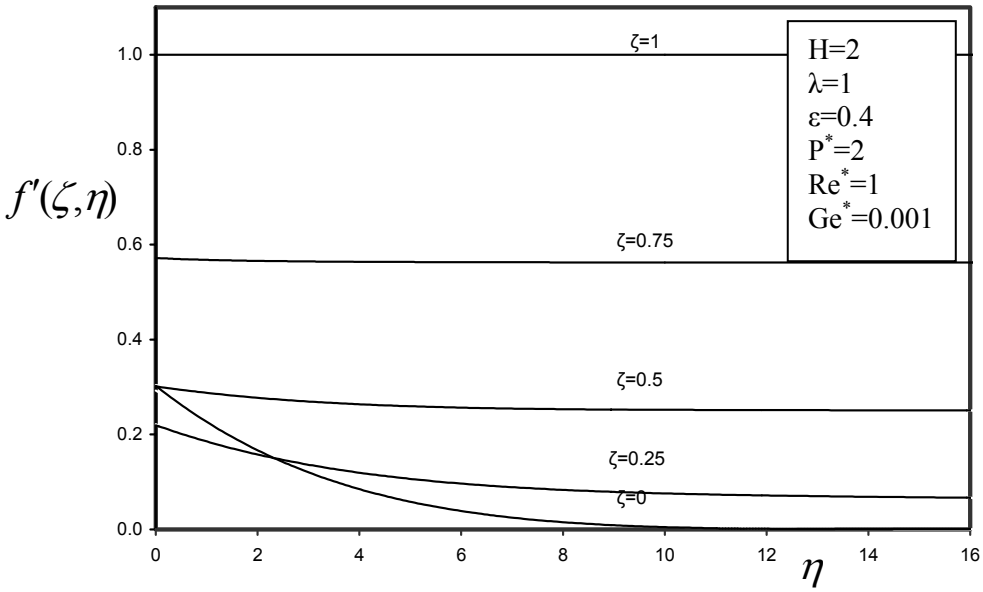

Fig 59 Dimensionless velocity profiles for different ζ
(Aiding)

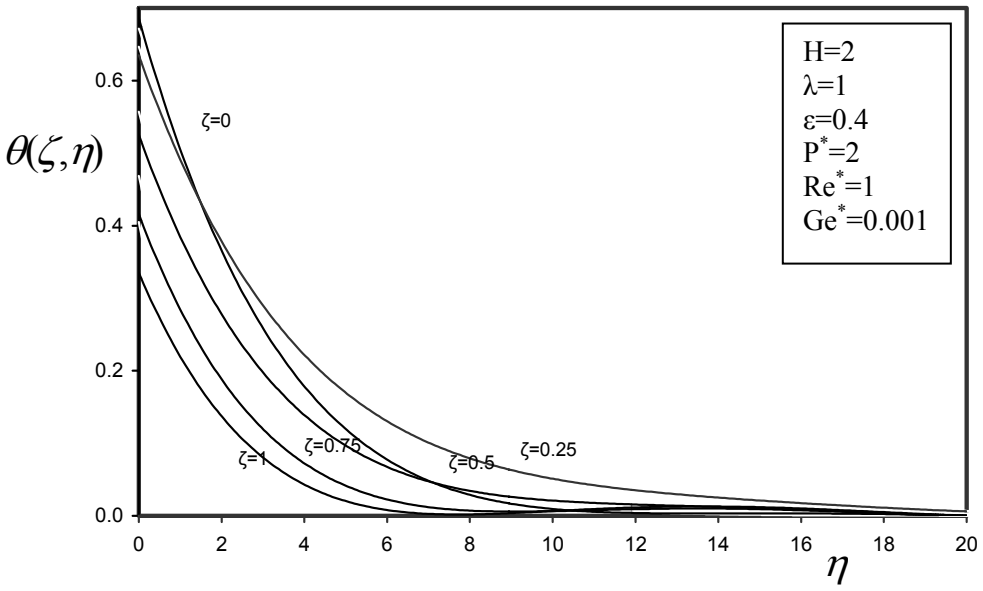

Fig 60Dimensionless temperature profiles for different ζ
(Aiding)

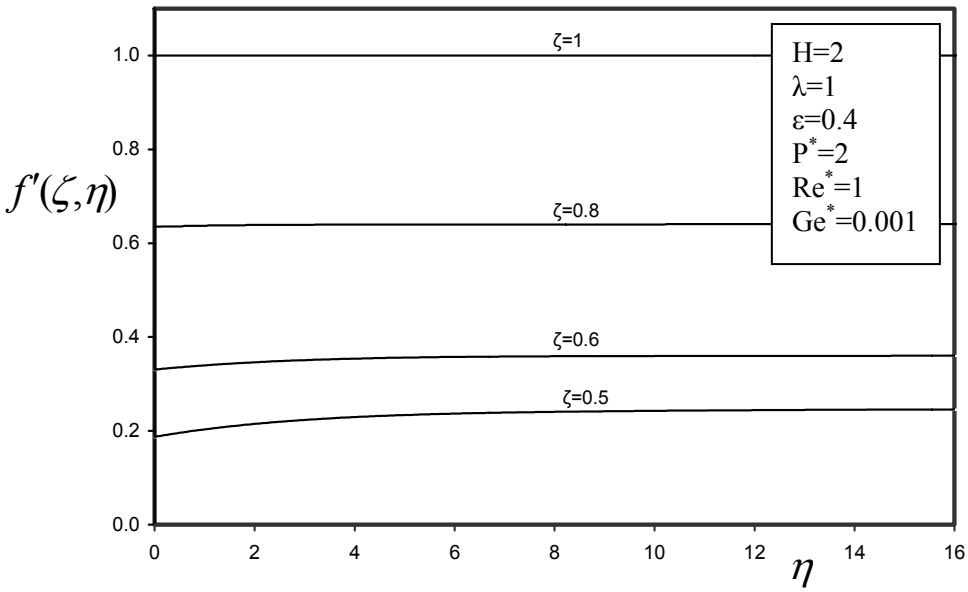

Fig 61 Dimensionless velocity profiles for different ζ
(Opposing)

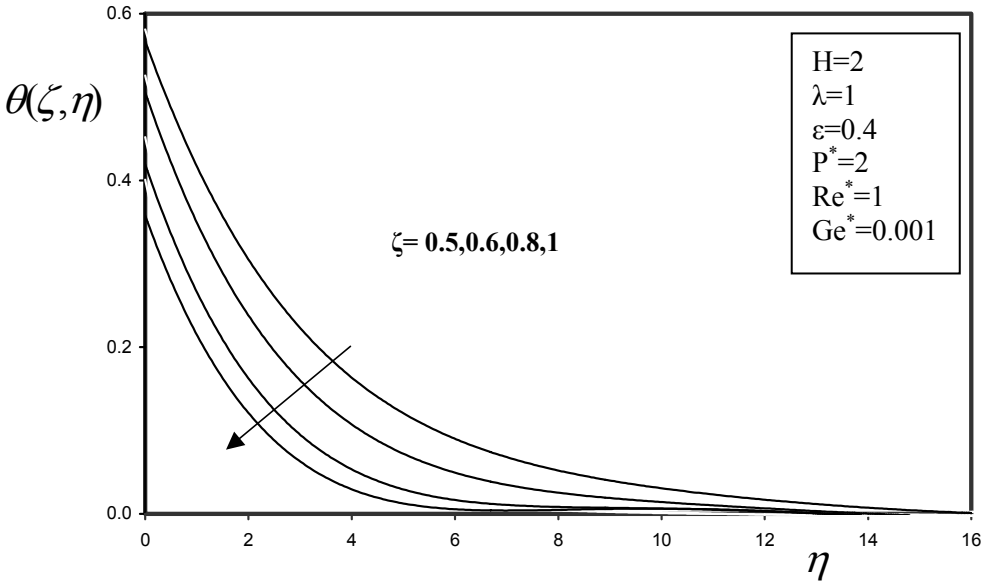

Fig 62 Dimensionless temperature profiles for different ζ
(Opposing)

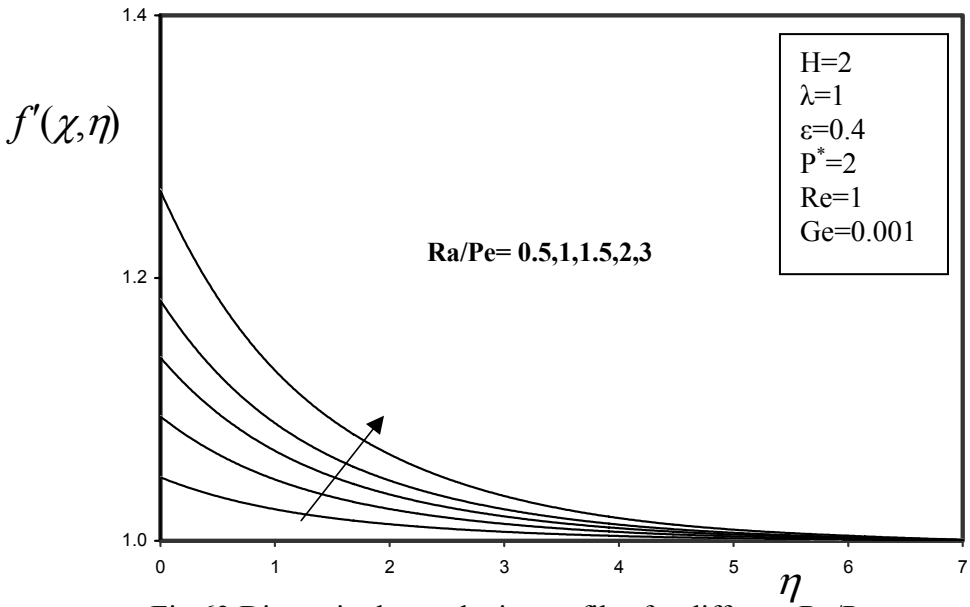

Fig 63 Dimensionless velocity profiles for different Ra/Pe (Aiding)

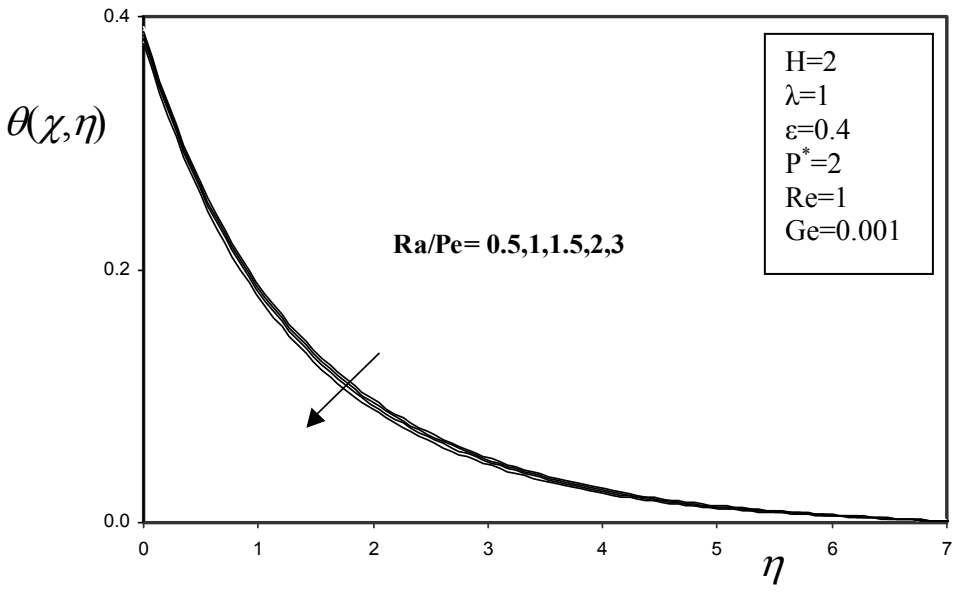

Fig 64 Dimensionless temperature profiles for different Ra/Pe (Aiding)

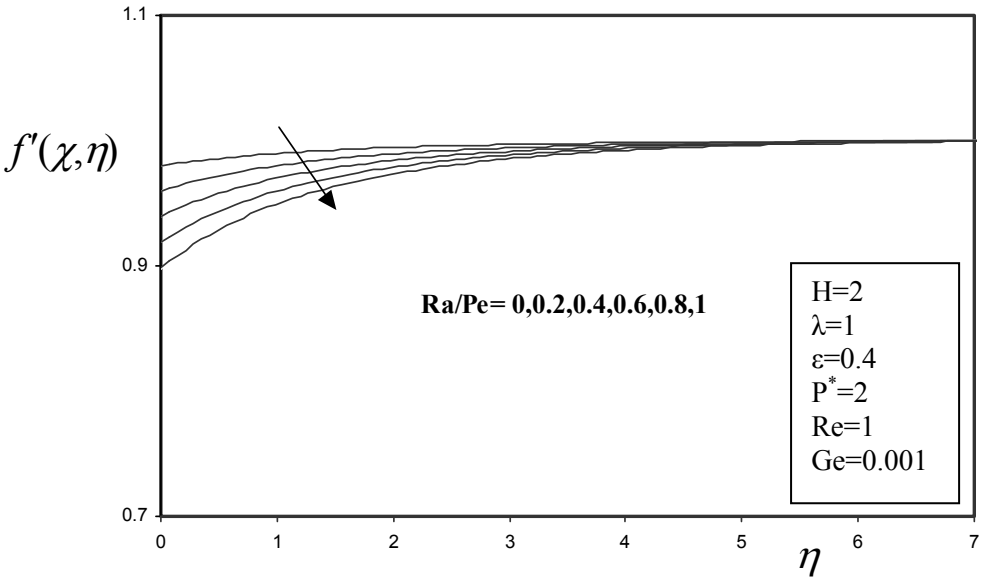

Fig 65 Dimensionless velocity profiles for different Ra/Pe (Opposing)

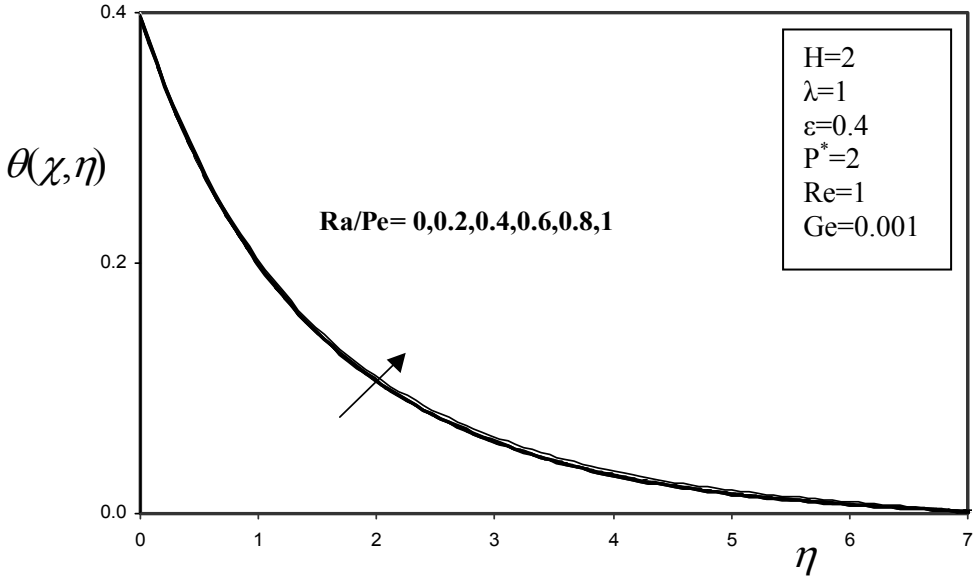

Fig 66 Dimensionless temperature profiles for different Ra/Pe (Opposing)

7. Conjugate conduction parameter effects:

The conjugate-conduction heat transfer parameter is described the effects of heat transfer by conduction in one dimension inside a solid wall on the boundary conditions of heat transfer inside the boundary layer.

Figures (5.66-5.77) show the effects of the conjugate conduction numbers on the velocity and the temperature profiles for the buoyancy aiding and the buoyancy opposing flows. . For the buoyancy aiding flow increasing the conjugate numbers had decreased the velocity and the temperature inside the boundary layer, while increased and decreased the velocity and the temperature respectively, for the buoyancy opposing flow.

The effects of increasing the conjugate numbers are found to decrease the heat transfer rates by conduction on the surface of cylinder and hence decreased its temperature. The effect of the buoyancy force will decrease inside the boundary layer and the velocity of the fluid decreased for the buoyancy aiding flow and increased for the buoyancy opposing flow respectively.

8. Surface skin friction and surface heat transfer rates:

In the present study, the effects of the different parameters on the local coefficient friction and on the local Nusselt numbers for the buoyancy aiding and opposing flows are drawn: Figures (5.78-5.85) show the effects of H on the local coefficient of friction and heat transfer rates for the buoyancy aiding and opposing flows. These figures show that increasing H had decreased the local coefficient of friction for the buoyancy aiding and opposing flows. While, increasing H had decreased the heat transfer rates for the buoyancy aiding flow and increased it up to a certain limit, after which the magnetic field effects had decreased the local Nusselt

numbers for the buoyancy opposing flow. For the buoyancy aiding flow, the effects of H are found to retard the motion of fluid and heat it at same time, while for the buoyancy opposing flow effects of H are found to reduce effect of the buoyancy forces.

The effect of the viscous dissipation on the local coefficient of friction and local Nusselt numbers are drawn in figures (5.86-5.93). Increasing Ge^*,Ge had increased the local coefficient of friction and decreased the local Nusselt numbers respectively for the buoyancy aiding flow. While, decreased them for the buoyancy opposing flow. The effect of the viscous dissipation again is to heat the fluid inside the boundary layer and hence the buoyancy force becomes more effective in increasing or decreasing the velocity inside the boundary layer.

Figures (5.94-5.101) show the effects of P^* on the local coefficient of friction and local Nusselt numbers. These figures show that For the buoyancy aiding flow increasing the conjugate numbers had decreased the local coefficient of friction and local Nusselt numbers, this behavior is due to reducing the effects of the buoyancy forces as the heat transfer rates inside the solid surface decreased. While, for the buoyancy opposing flow increasing the conjugate numbers had increased the local Nusselt numbers up to a certain limit, after which the effects of the conjugate parameters had decreased the local Nusselt numbers. This behavior again subjected to reduce the effects of the buoyancy forces on the flow, where the velocity of the flow had increased inside the boundary layer.

The effect of the modify inertial forces are drawn in figures (5.102-5.109) . these figures show increasing the inertial forces had decreased the heat transfer rates for the buoyancy aiding flow. While, increased it up to a certain limit for the buoyancy opposing flow after which, the heat transfer rates had increased.

The effects of the curvature is introduced by the parameter $\lambda = \frac{2x}{r_o Pe_x^{1/2}}$, where λ=0 corresponds to case of vertical flat surface. Figure(5.106-5.109) show the effects of λ on the local coefficient of friction and local Nusselt numbers for the buoyancy aiding and opposing flows. . It can be see that increasing λ had decreased the local coefficient of friction and increased the heat transfer rates for the buoyancy aiding flow. And increasing λ had decreased the local coefficient of friction and increased the heat transfer rates for the buoyancy opposing flow. This behavior of the curvature effect is in a good agreement of the fact that larger λ corresponds to larger surface area and this tend to increase the heat transfer rates from the surface.

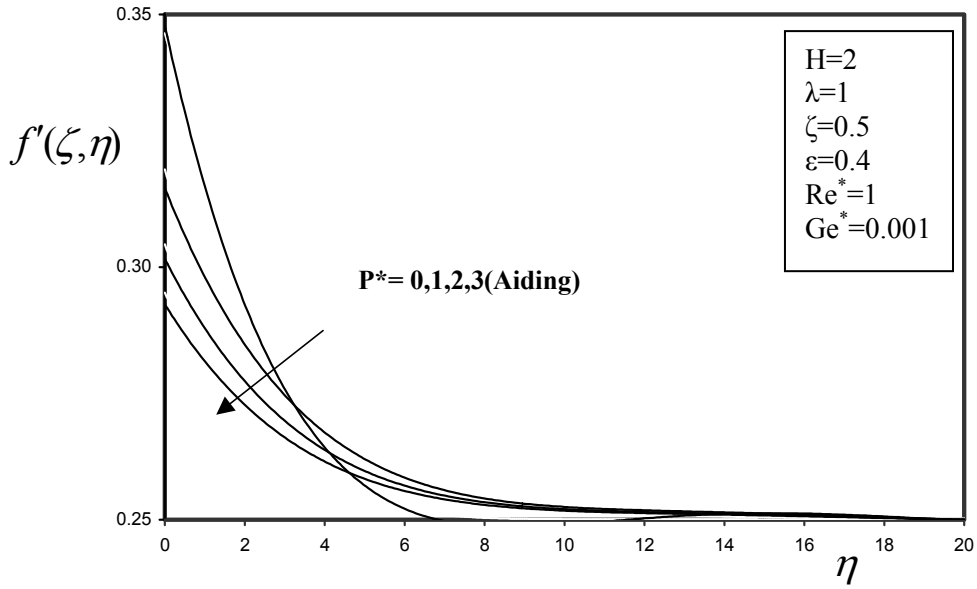

Fig 67 Dimensionless velocity profiles for different p*
(Mixed convection-A)

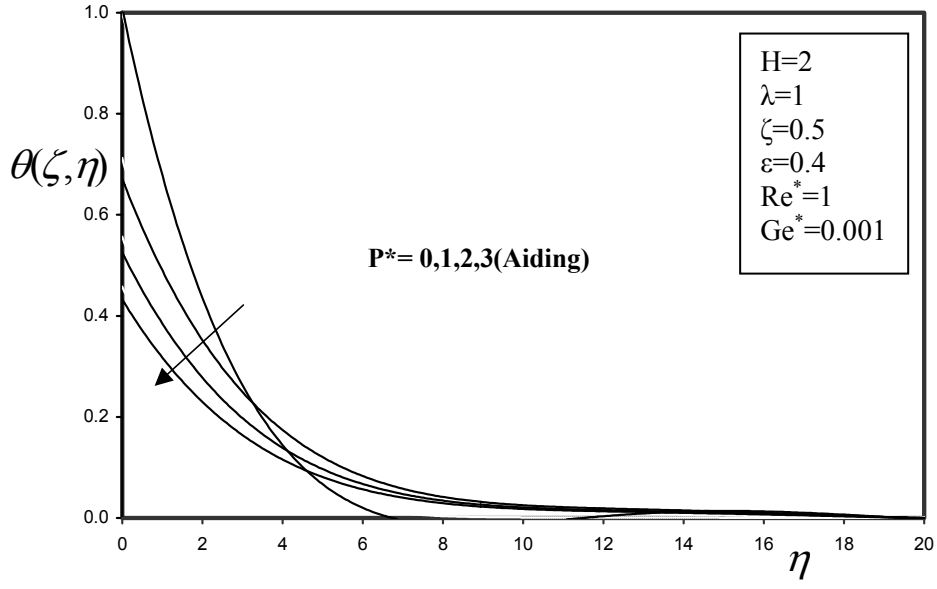

Fig 68 Dimensionless temperature profiles for different p*
(Mixed convection -A)

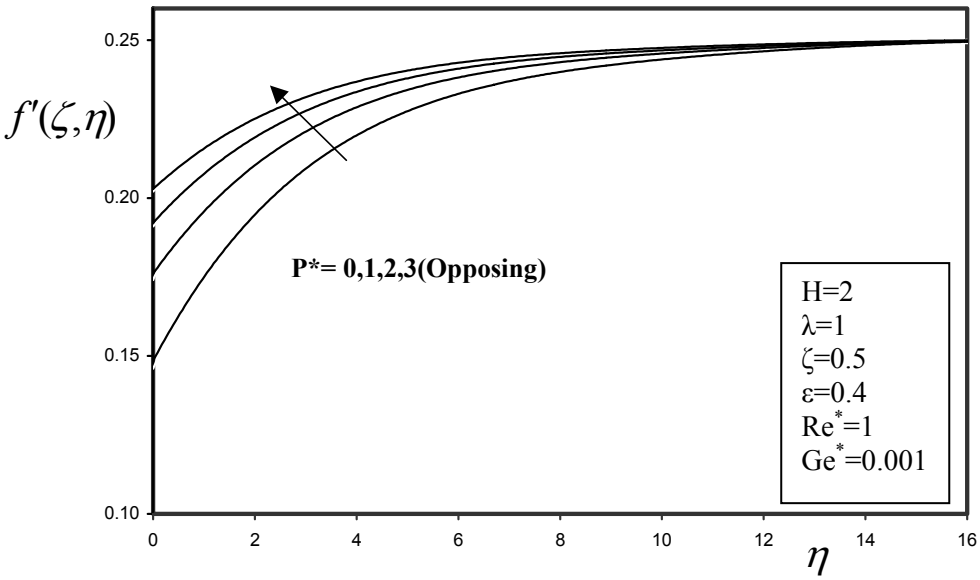

Fig 69 Dimensionless velocity profiles for different p*
(Mixed convection -A)

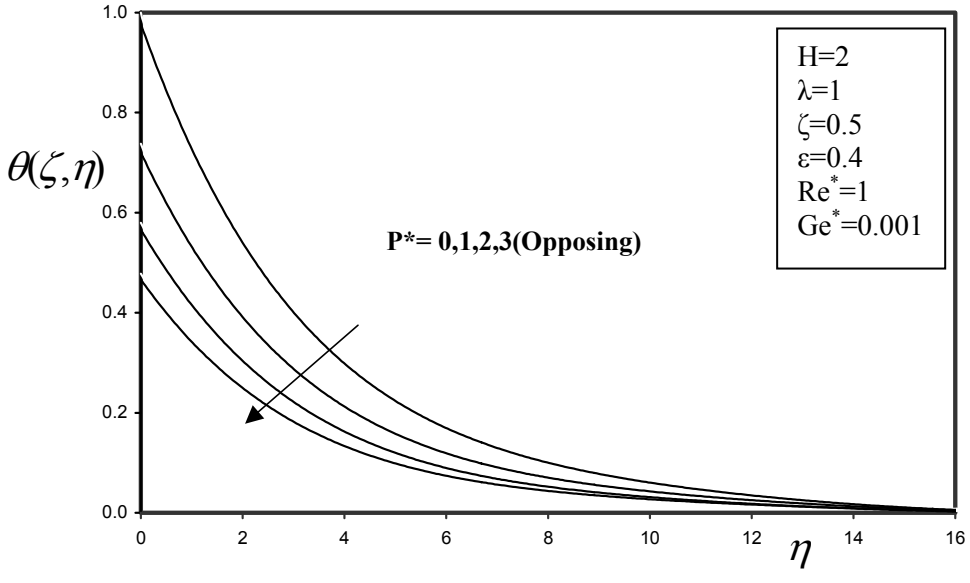

Fig 70 Dimensionless temperature profiles for different p*
(Mixed convection -A)

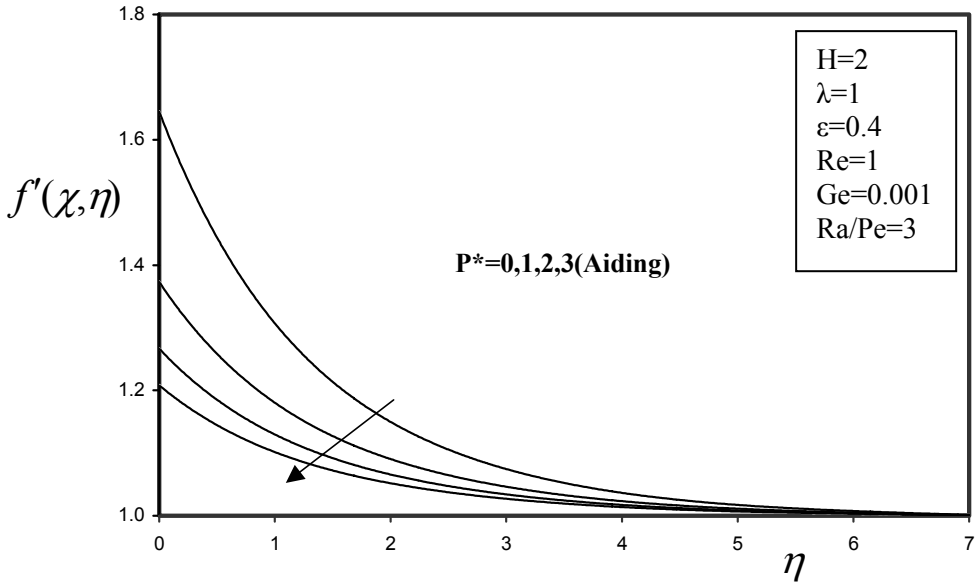

Fig 71 Dimensionless velocity profiles for different p*
(Mixed convection-B)

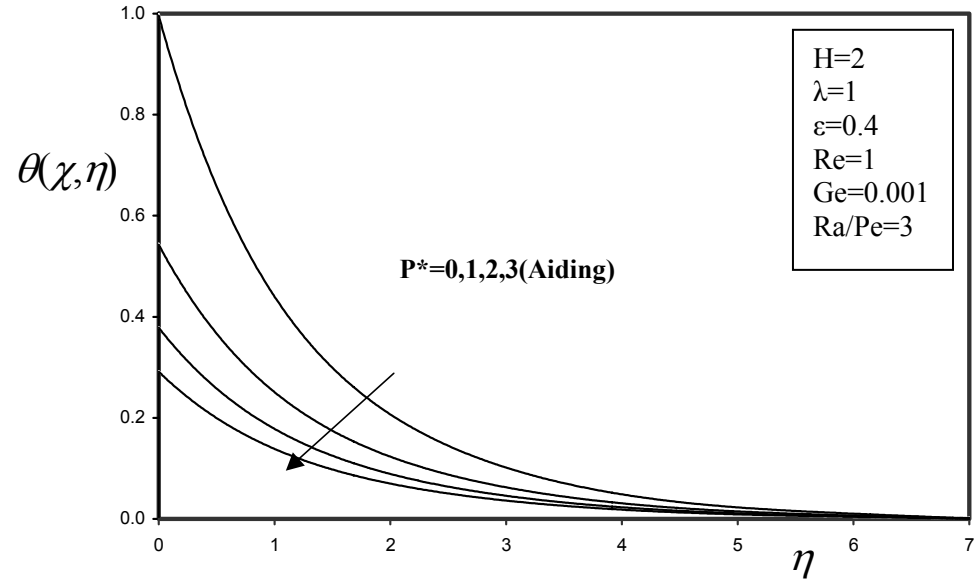

Fig 72 Dimensionless temperature profiles for different p*
(Mixed convection-B)

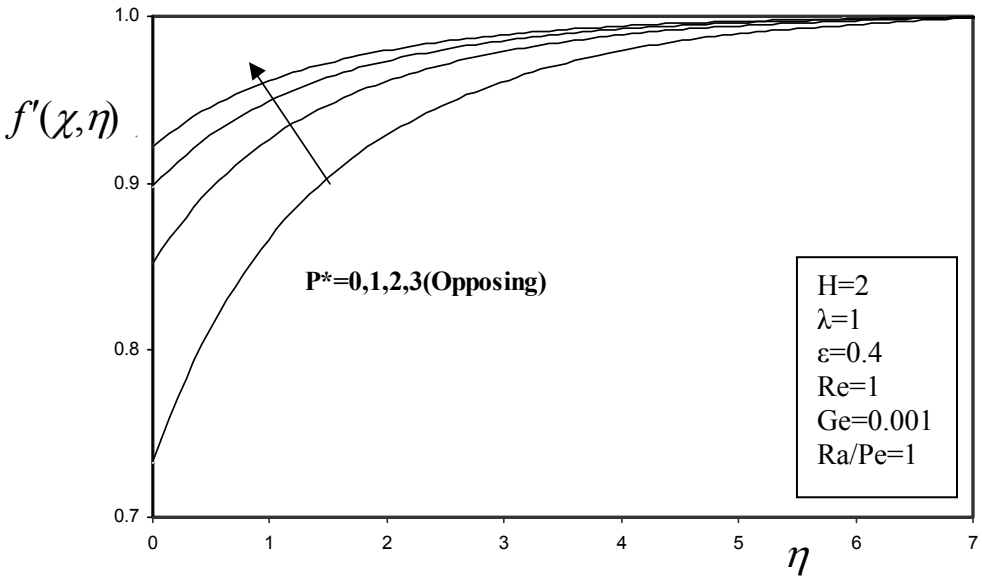

Fig 73 Dimensionless velocity profiles for different p*
(Mixed convection -B)

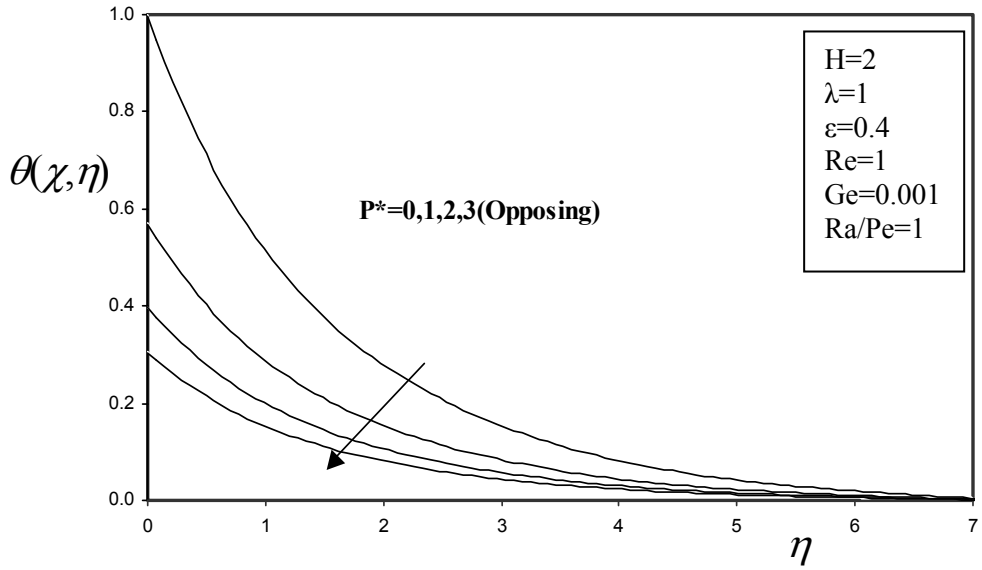

Fig 74 Dimensionless temperature profiles for different p*
(Mixed convection -B)

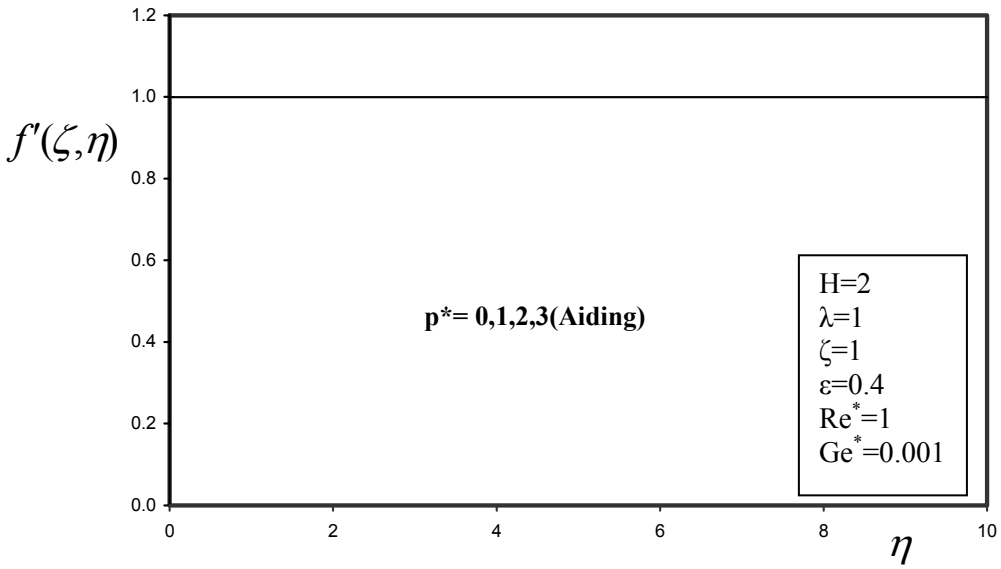

Fig 75 Dimensionless velocity profiles for different p*
(Forced convection-B)

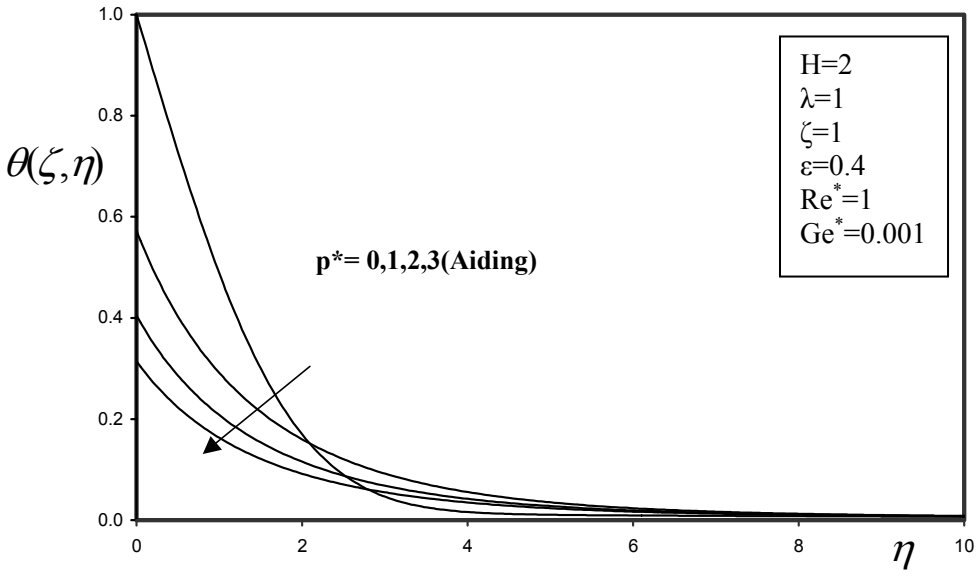

Fig 76 Dimensionless temperature profiles for different p*
(Forced convection)

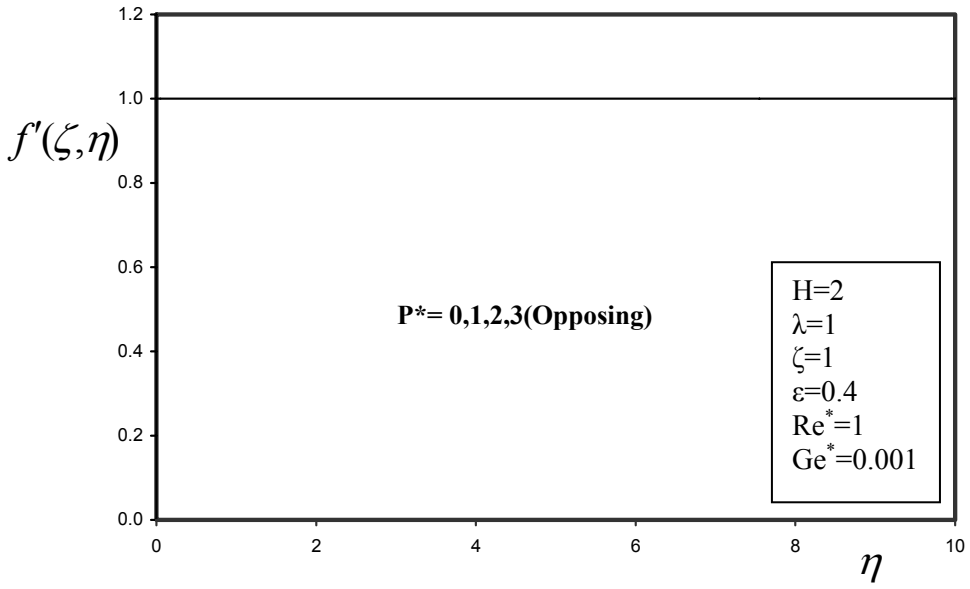

Fig 77 Dimensionless velocity profiles for different p*
(Forced convection)

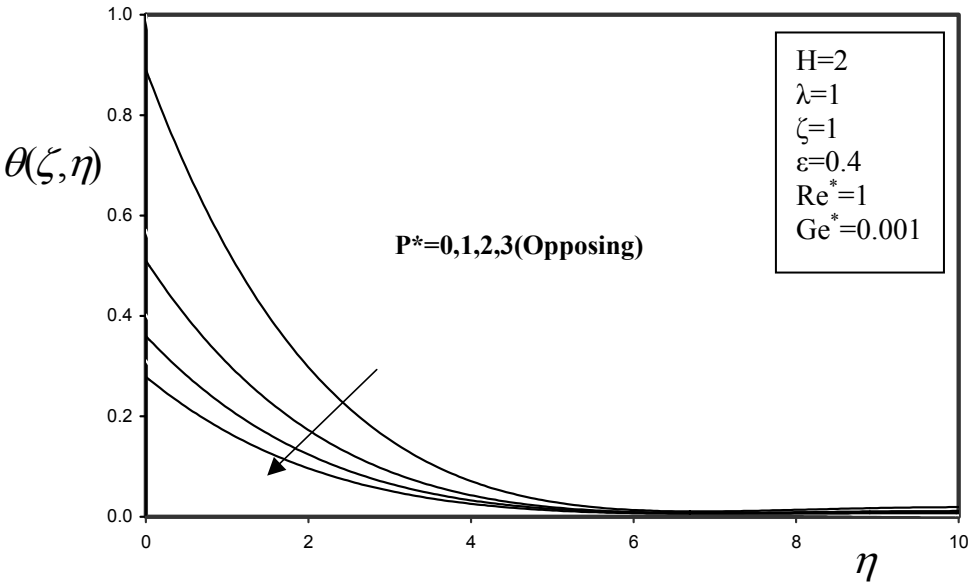

Fig 78 Dimensionless temperature profiles for different p*
(Forced convectiom)

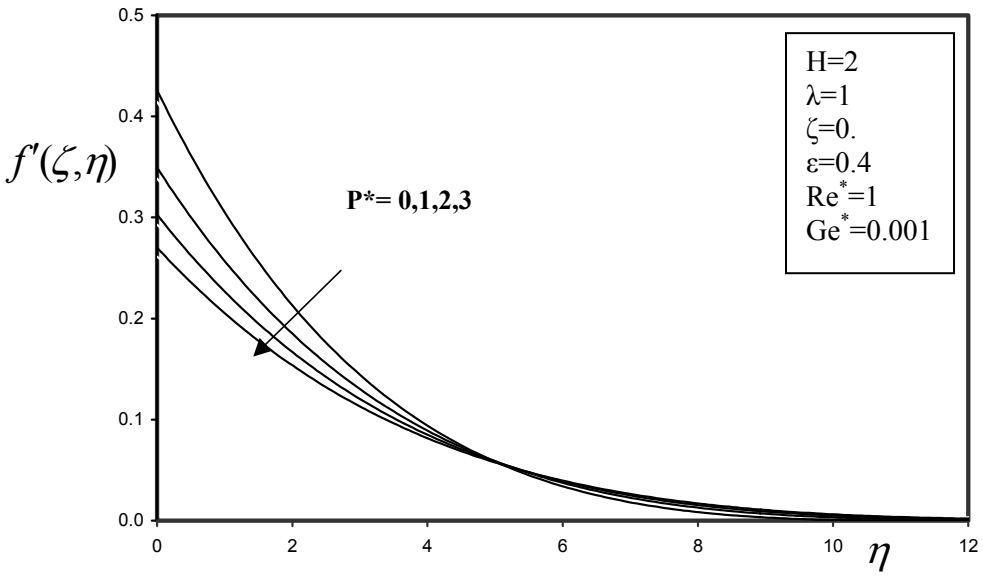

Fig 79 Dimensionless velocity profiles for different p*
(Natural convection)

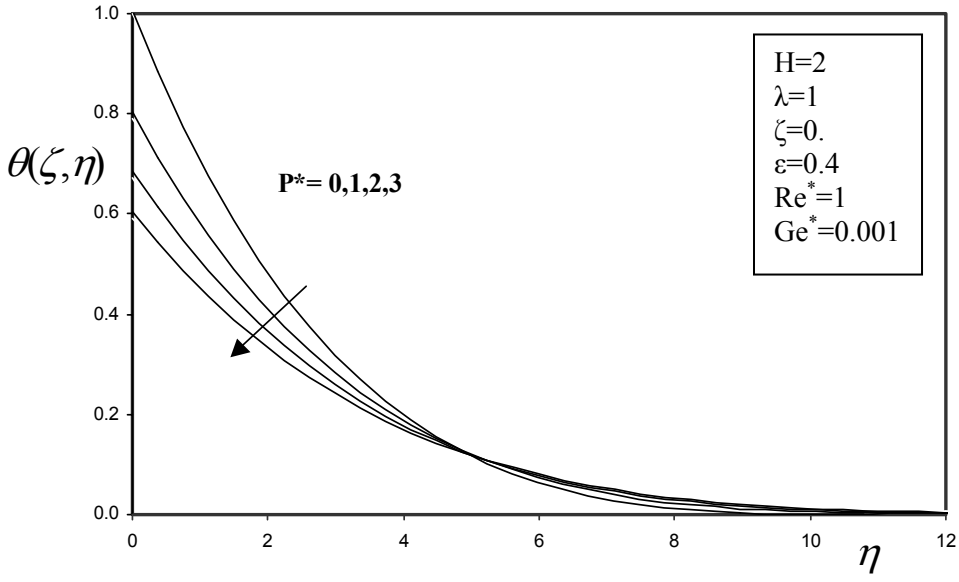

Fig 80 Dimensionless temperature profiles for different p*
(Natural convection)

Effect of H on local skin friction and local Nusselt number (A)

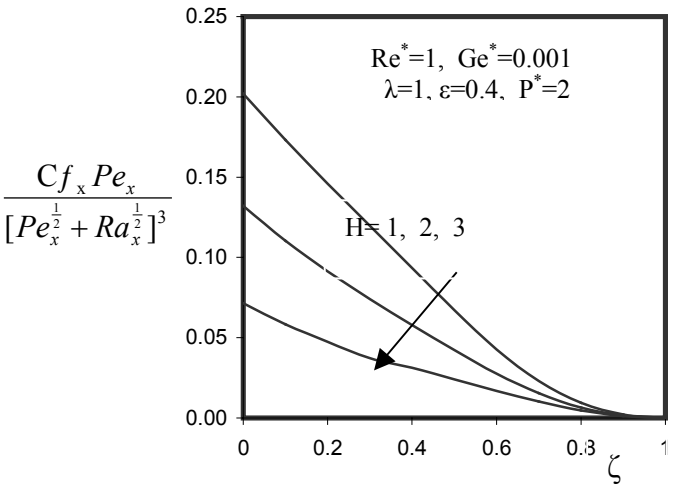

Fig 81(Aiding)

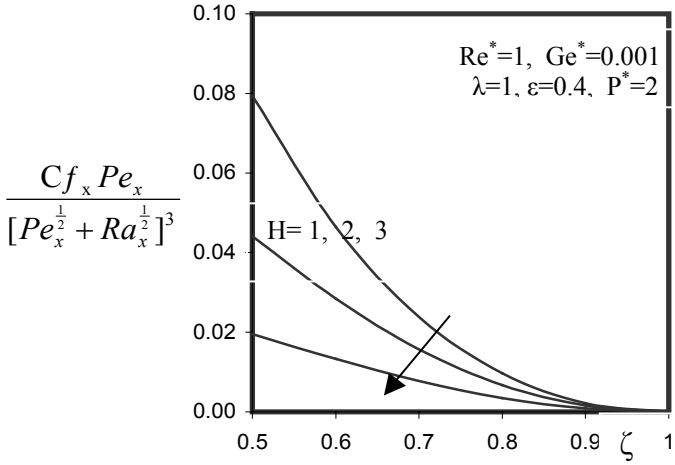

Fig 82 (Opposing)

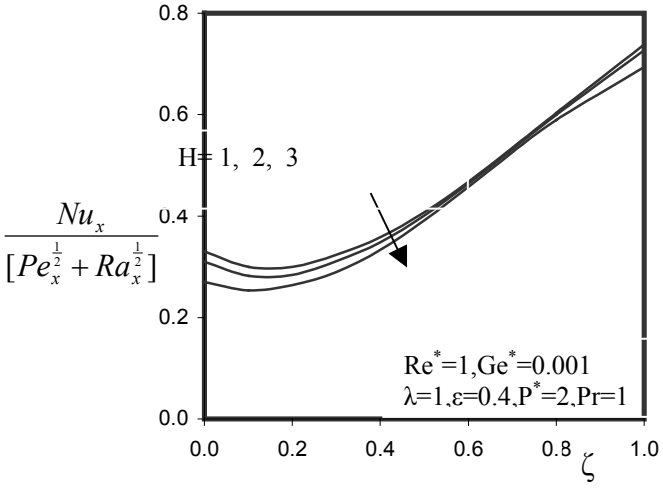

Fig 83 (Aiding)

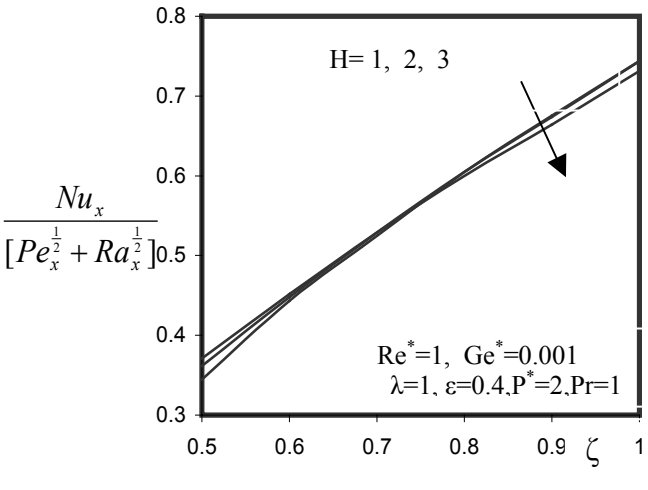

Fig 84 (Opposing)

Effect of H on local skin friction and local Nusselt number (B)

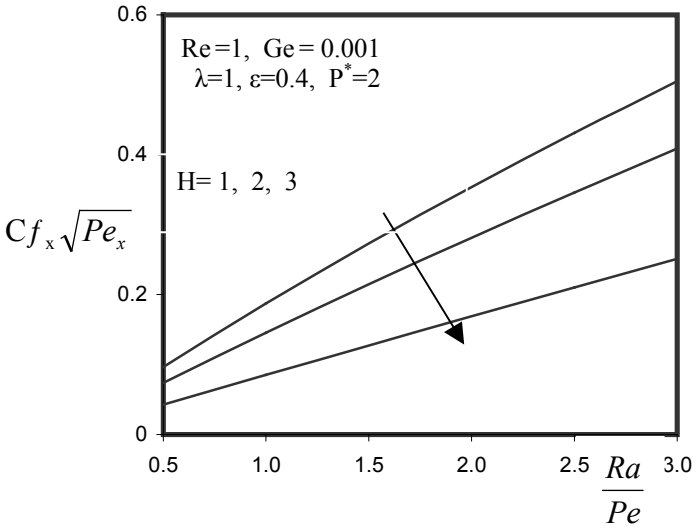

Fig 85 (Aiding)

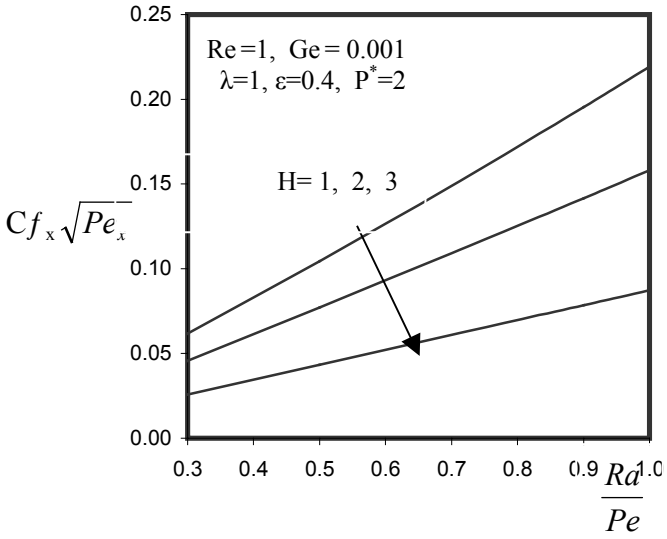

Fig 86 (Opposing)

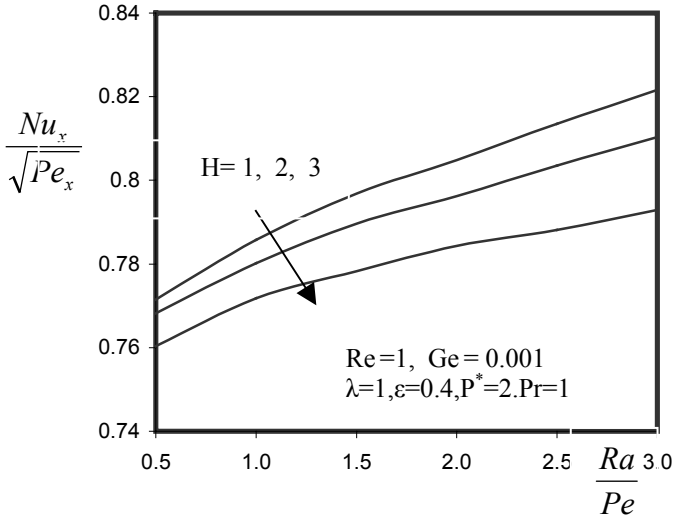

Fig 87 (Aiding)

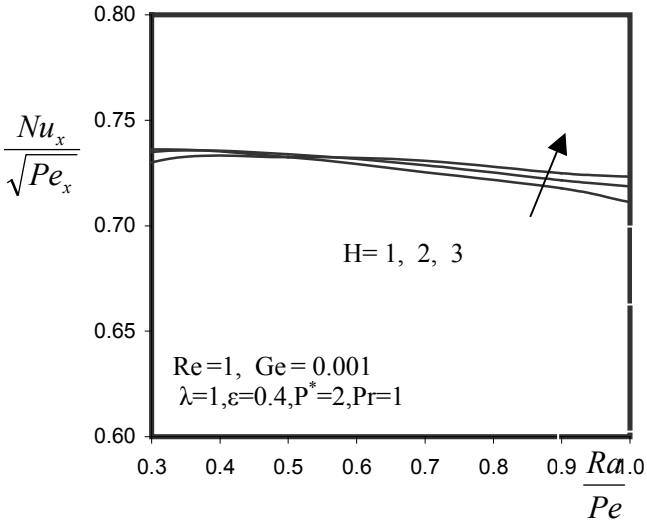

Fig 88 (Opposing)

Effect of Ge^* on local skin friction and local Nusselt number (A)

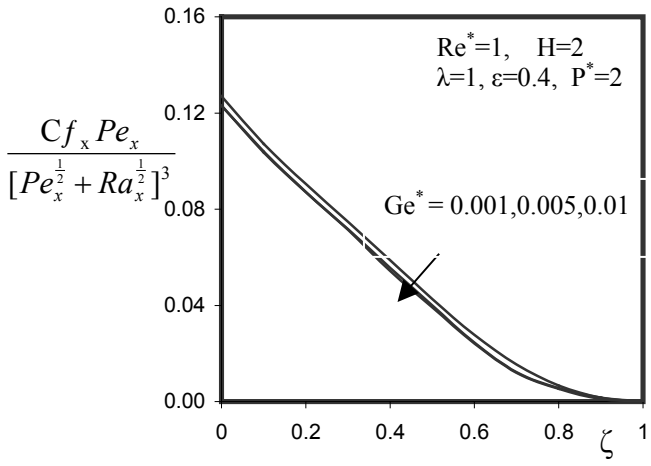

Fig 89 (Aiding)

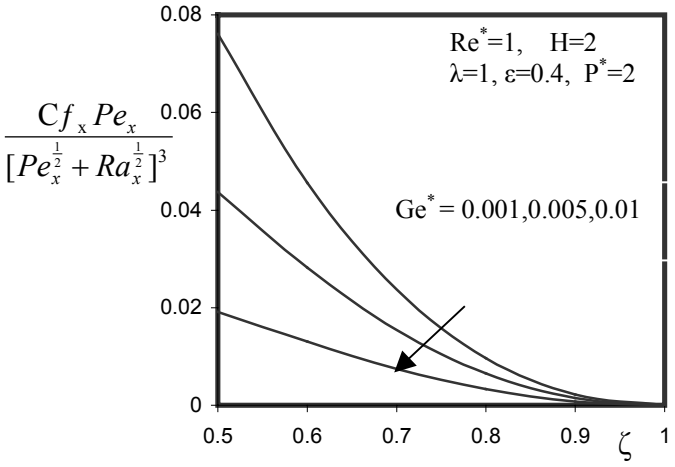

Fig 90 (Opposing)

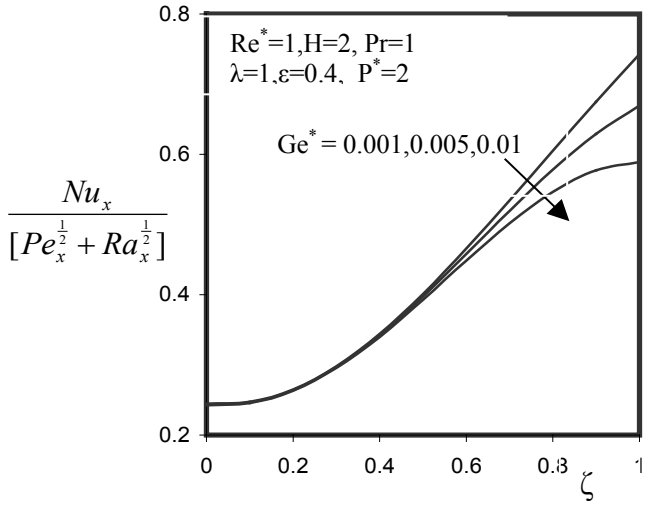

Fig 91(Aiding)

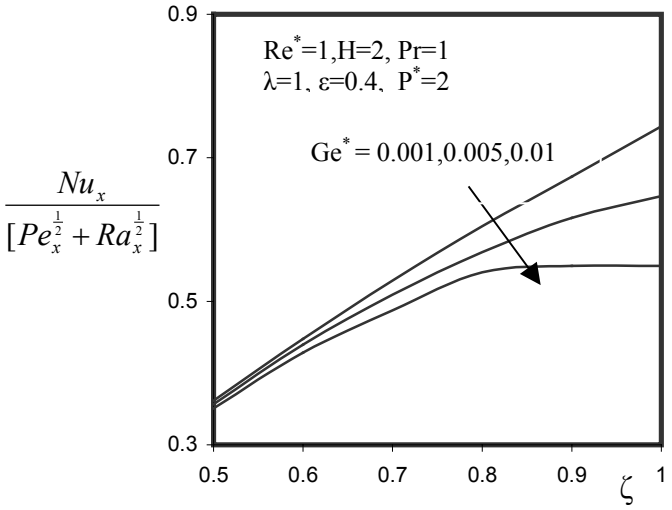

Fig 92(Opposing)

Effect of Ge on local skin friction and local Nusselt number (B)

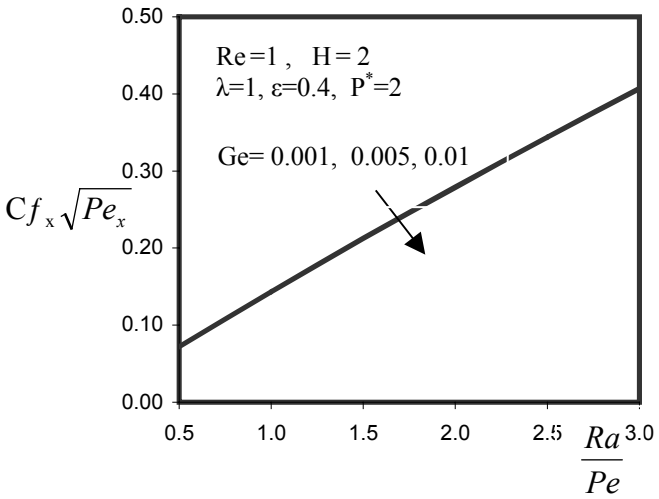

Fig 93 (Aiding)

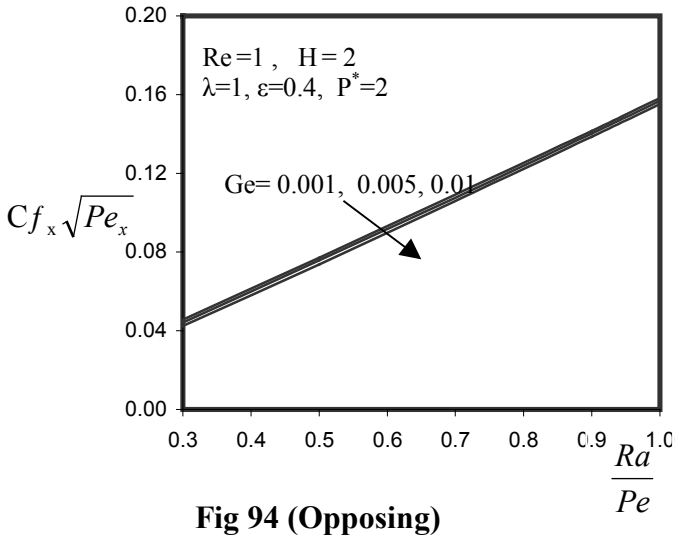

Fig 94 (Opposing)

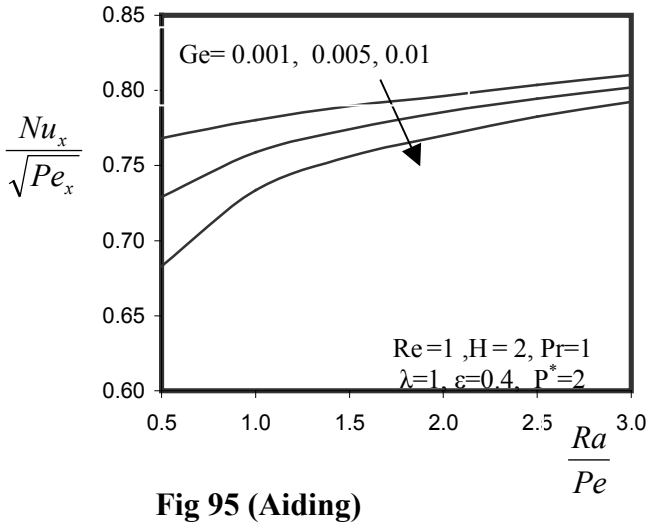

Fig 95 (Aiding)

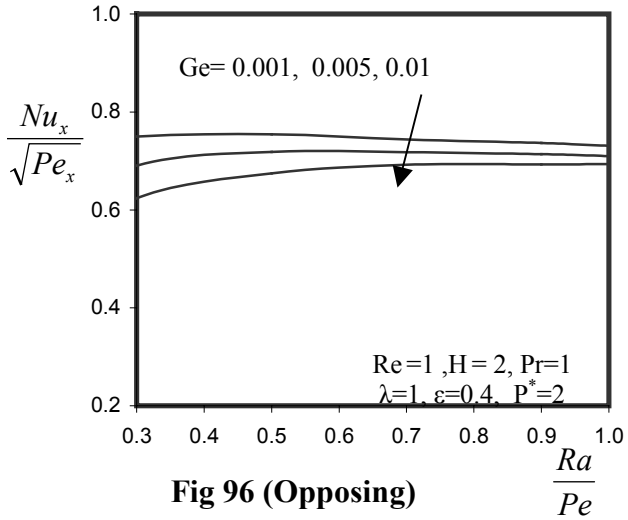

Fig 96 (Opposing)

Effect of P^* on local skin friction and local Nusselt number (A)

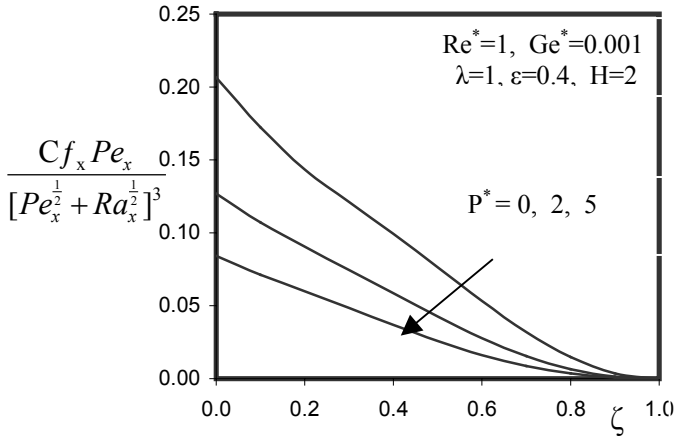

Fig97 (Aiding)

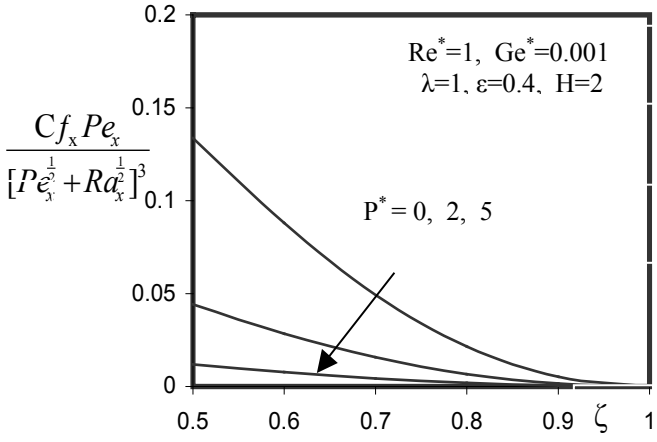

Fig 98 (Opposing)

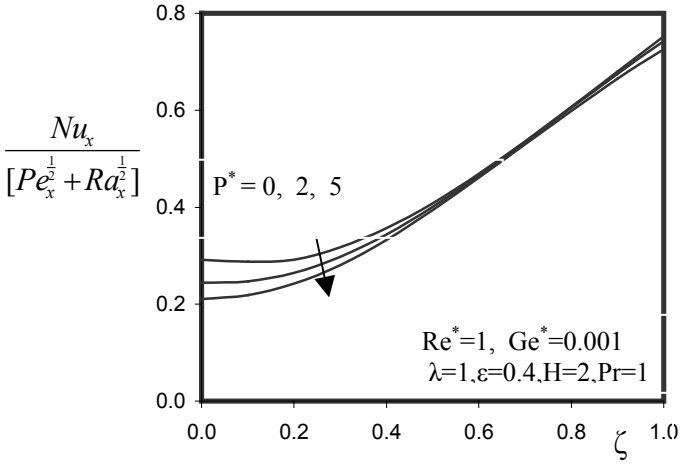

Fig 99 (Aiding)

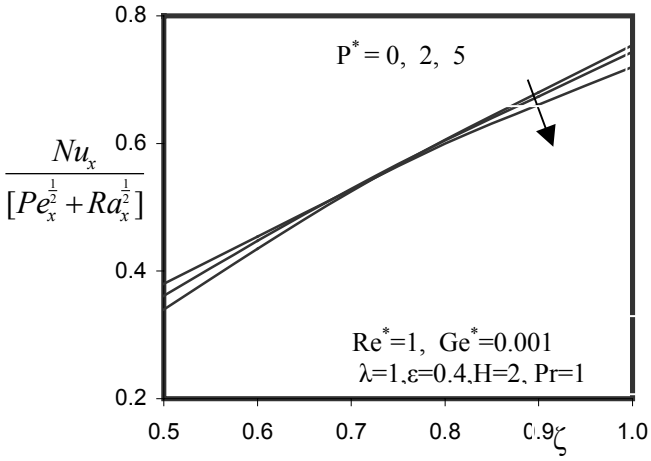

Fig 100 (Opposing)

Effect of P^* on local skin friction and local Nusselt number (B)

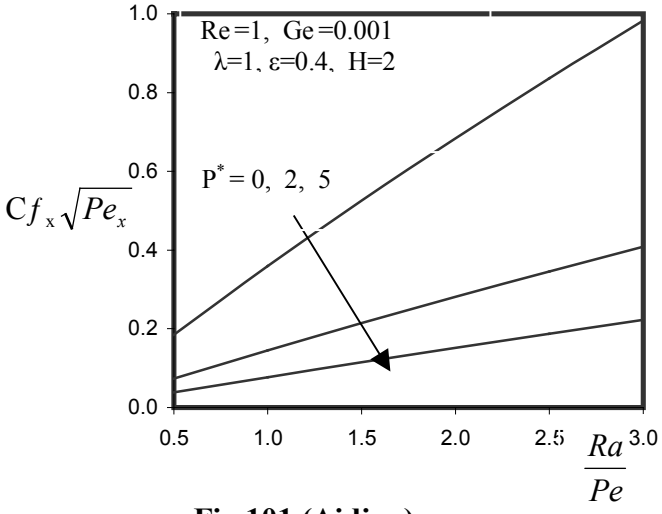

Fig 101 (Aiding)

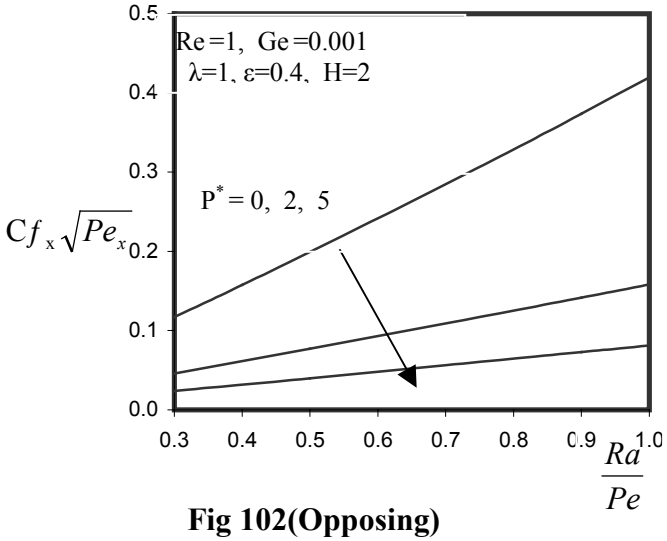

Fig 102(Opposing)

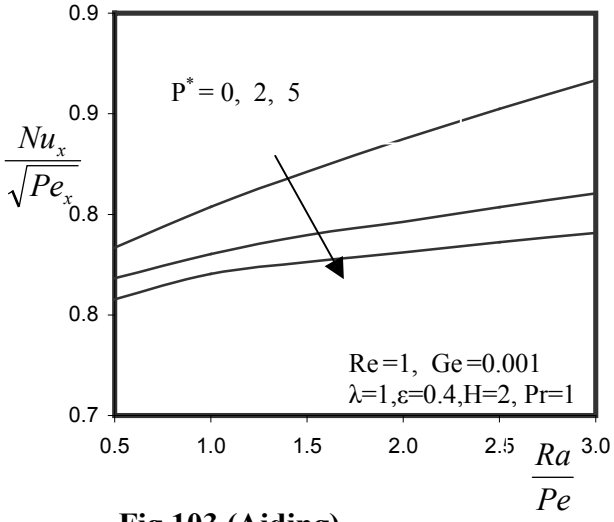

Fig 103 (Aiding)

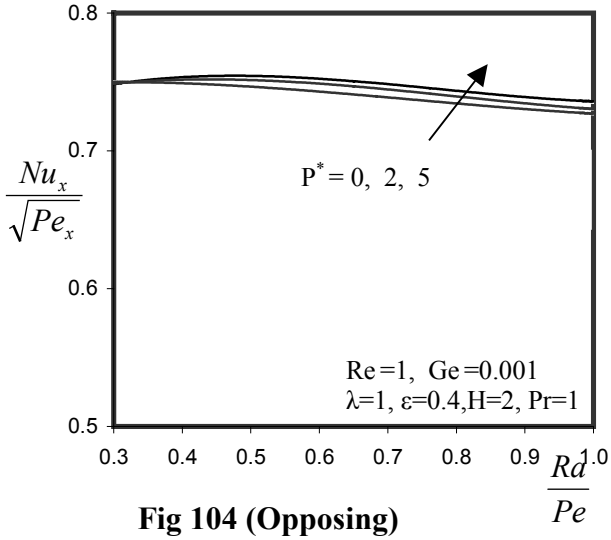

Fig 104 (Opposing)

Effect of Re^* on local skin friction and local Nusselt number (A)

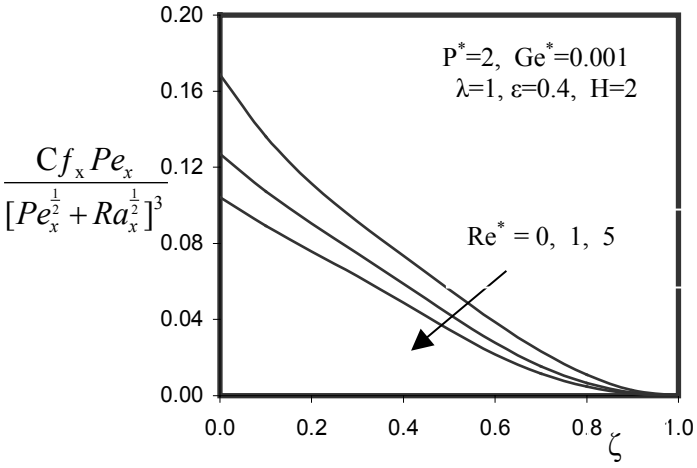

Fig 105 (Aiding)

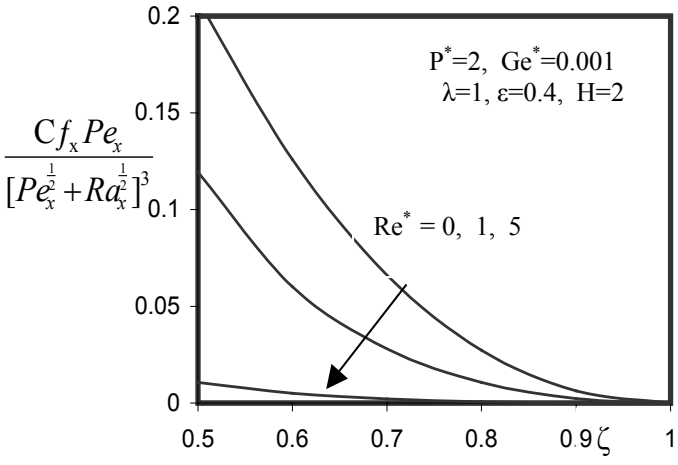

Fig 106 (Opposing)

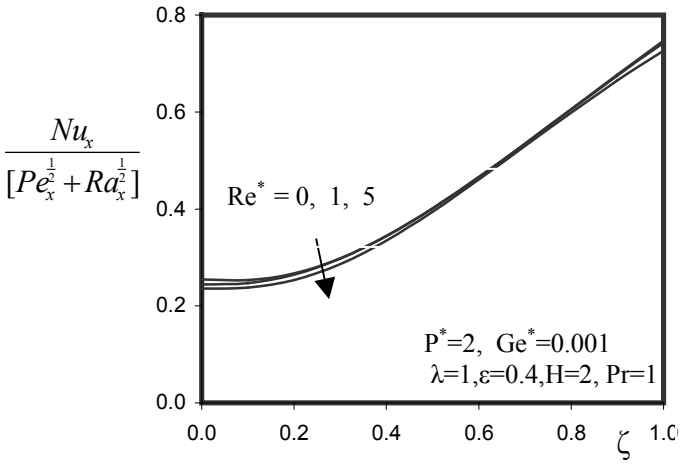

Fig 107 (Aiding)

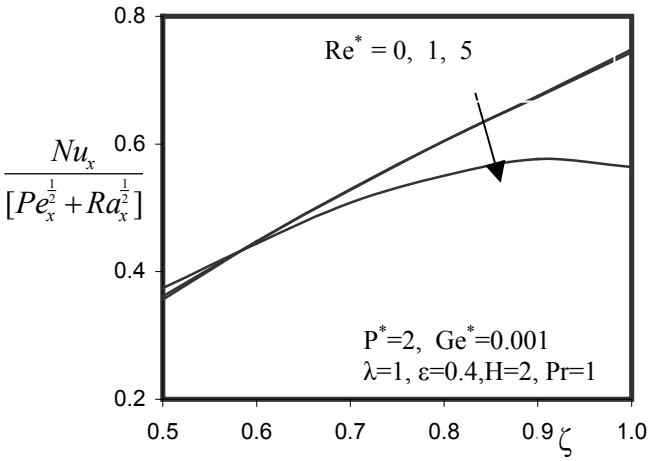

Fig 108 (Opposing)

Effect of λ on local skin friction and local Nusselt number (A)

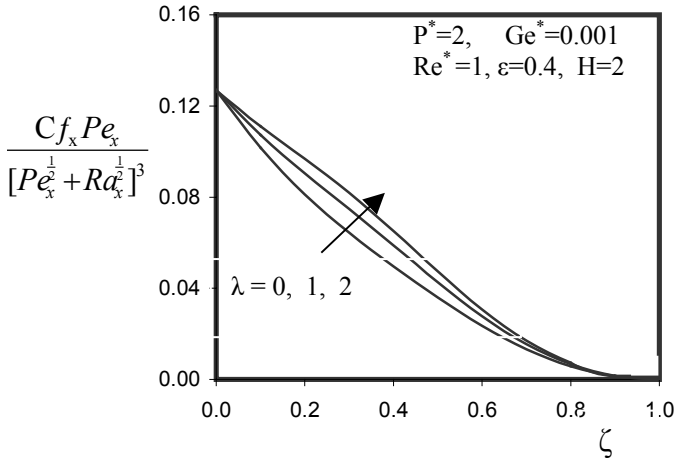

Fig 109 (Aiding)

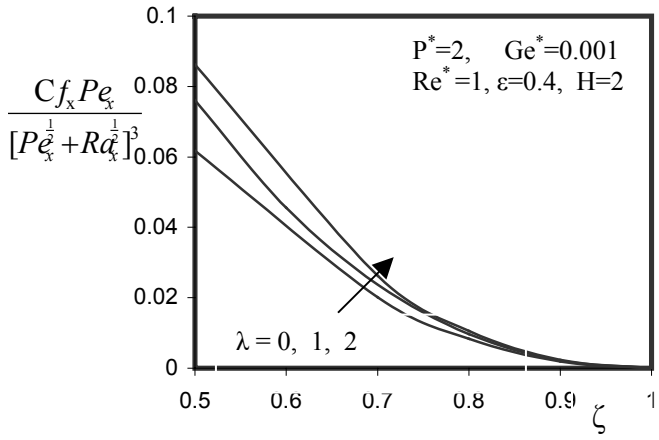

Fig 110 (Opposing)

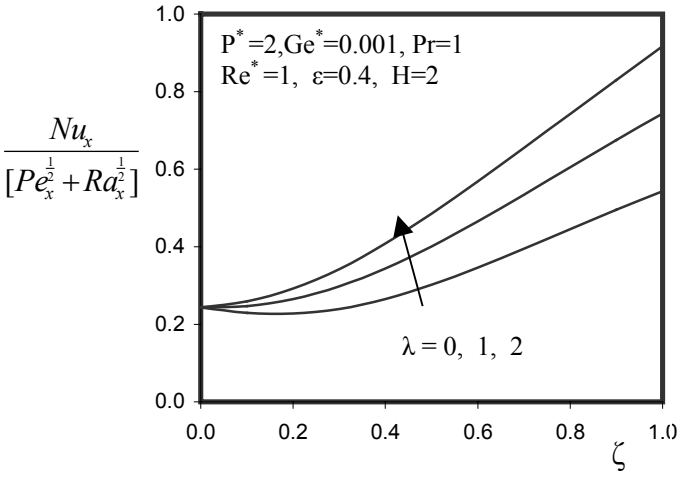

Fig 111 (Aiding)

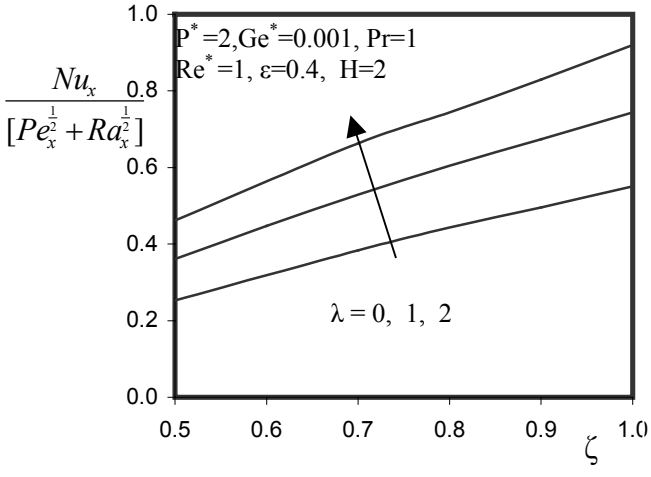

Fig 112(Opposing)

Effect of λ on local skin friction and local Nusselt number (B)

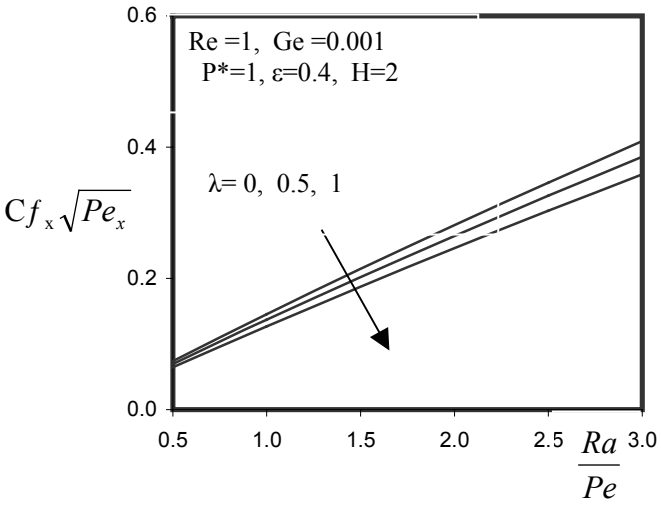

Fig 113 (Aiding)

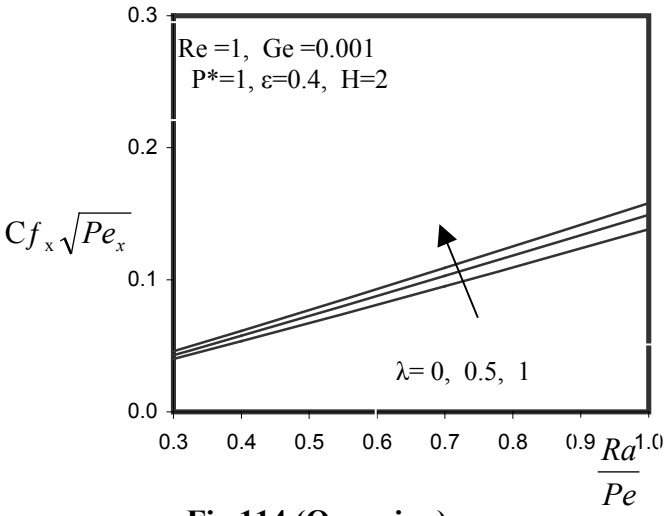

Fig 114 (Opposing)

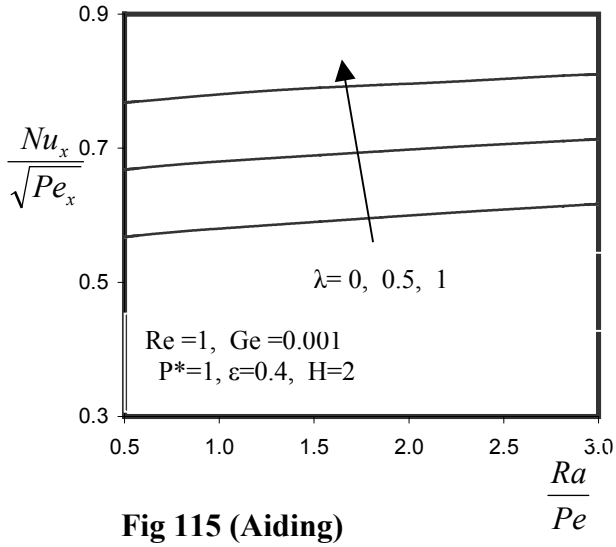

Fig 115 (Aiding)

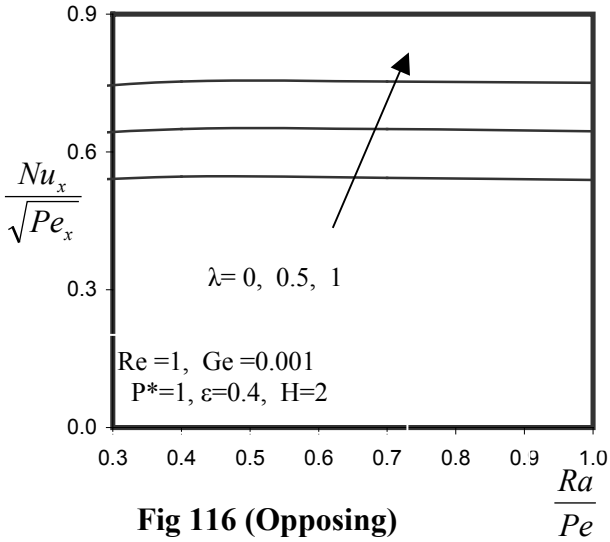

Fig 116 (Opposing)

9. Comparison with other works:

In order to assess the accuracy of the numerical method Keller Box method as described by Cebeci and Bradshow (1977). The results, which had obtained by using Keller method in this study had compared with some results, which had obtained by Hsieh et al. (1993).

By comparing the values of the surface heat transfer $-\theta'(\zeta,0)/\theta(\zeta,0)$ in this study to the values of the surface heat transfer $-\theta'(\zeta,0)$ at (Hsieh et al., 1993). for constant wall temperature on the entire mixed convection regime (aiding flow). The results in table 5.1 show that there are a good agreement in these results with small difference may, however, be attributed to the different methods used, round off errors in the programs (precision).

Table 5.1 shows the comparison of the surface heat transfer for the case of a vertical plate (λ=0), constant wall temperature ($\theta(\zeta,0)=1$), no conjugate conduction effect ($\overset{*}{P}=0$), and for the Darcy model ($\overset{*}{\mathrm{Re}}=0$) and in absent of effect the magnetic field (H=1).

Table 5.2 and table 5.3 show the values of the local Nusselt number, which had obtained in this study for the case of the flow over a vertical flat plate without effects of the conjugate conduction condition on the flow.

In table 5.1 if the Rayleigh number is taken as Ra_x=100 and the corresponding Peclet number to be Pe_x=100. the Nu_x value for mixed convection (Ra_x=100, Pe_x=100). is 7.19376. But for pure forced convection (Pe_x=100, Ra_x=0), the Nu_x value is found to be 5.6. For the case of pure free convection (Ra_x=100, Pe_x=0), the Nu_x value is found to be 4.44. From these result it is found that the predicted value of the local Nusselte number for mixed convection is higher than that for pure forced and pure free convection.

Table 1. Comparison between the $Nu_x/[Pe_x^{1/2}+Ra_x^{1/2}]$ calculated by the present method and that of Hsieh et al.(1993). for the case of:

$[\lambda=0,\ \theta(\zeta,0)=1\ ,\ \overset{*}{P}=0\ ,\ \overset{*}{\mathrm{Re}}=0\ ,\ H=1\ ]$

ζ	Present method	Hsieh et al. (1993)	Error (%)
0	0.443114	0.4438	0.155
0.1	0.403044	0.4035	0.113
0.2	0.372798	0.3732	0.108
0.3	0.354623	0.355	0.106
0.4	0.350118	0.3506	0.137
0.5	0.359688	0.3603	0.170
0.6	0.382325	0.3832	0.228
0.7	0.415963	0.4174	0.344
0.8	0.45819	0.4603	0.458
0.9	0.506798	0.5098	0.589
1	0.560022	0.5642	0.741

Table 2. Values of local Nusselt number $[-\theta'(\zeta,0)]$ at different values of ζ and at selected values of the magneticnumber H and viscous dissipation number Ge^* for the case of vertical plate without conjugate effect.[λ=0, P^*=0].

ζ	Darcy Model Re^*=0				Non-Darcy Model Re^*=1			
	H=1 Ge^*=0	H=2 Ge^*=0	H=1 Ge^*=0.001	H=2 Ge^*=0.001	H=1 Ge^*=0	H=2 Ge^*=0	H=1 Ge^*=0.001	H=2 Ge^*=0.001
0	0.443749	0.313778	0.443114	0.313463	0.365758	0.292063	0.365237	0.291754
0.1	0.403521	0.288226	0.403044	0.287982	0.340191	0.270994	0.33979	0.270753
0.2	0.373184	0.276016	0.372798	0.275791	0.321051	0.26148	0.320717	0.261255
0.3	0.35499	0.278485	0.354623	0.278207	0.31158	0.265737	0.311243	0.265454
0.4	0.350551	0.29508	0.350118	0.294653	0.314962	0.28412	0.314524	0.283659
0.5	0.360293	0.323698	0.359688	0.322987	0.332846	0.314953	0.332156	0.314133
0.6	0.383232	0.361611	0.382325	0.360436	0.364271	0.355394	0.363099	0.353936
0.7	0.417339	0.406302	0.415963	0.404435	0.406229	0.402545	0.404229	0.400043
0.8	0.460238	0.455818	0.45819	0.452981	0.45525	0.454074	0.451924	0.449951
0.9	0.509763	0.508769	0.506798	0.504626	0.508532	0.508322	0.503177	0.501788
1	0.564191	0.564191	0.560022	0.558354	0.564191	0.564191	0.555852	0.554184

Table 3. Values of local Nusselt number [$-\theta'(\zeta,0)$] for different values of Ra_x/Pe_x and at selected valuesof theMagnetic number H and viscous dissipation number Ge for the case of vertical plate without conjugate effect.[λ=0, P^*=0].

Ra_x/Pe_x	Darcy Model Re=0				Non-Darcy Model Re=1			
	H=1 Ge=0	H=2 Ge=0	H=1 Ge=0.001	H=2 Ge=0.001	H=1 Ge=0	H=2 Ge=0	H=1 Ge=0.001	H=2 Ge=0.001
0.5	0.647399	0.607315	0.644249	0.603568	0.592235	0.585701	0.586975	0.57965
1	0.720588	0.647399	0.718492	0.645195	0.617158	0.605557	0.614132	0.602195
1.5	0.786738	0.685018	0.784953	0.683314	0.639678	0.62403	0.637381	0.62155
2	0.847583	0.720588	0.845926	0.719121	0.660278	0.641326	0.658341	0.63928
2.5	0.90424	0.754415	0.902646	0.753083	-6.79E-01	-6.58E-01	-6.78E-01	-6.56E-01
3	0.95748	0.786738	0.955906	0.785488	0.697017	0.673001	0.695423	0.671379

CONCLUSIONS AND RECOMMENDATIONS

1. Conclusions:

In this study, the MHD-mixed convection heat transfer along vertical slender, hollow cylinder embedded in a saturated porous medium with conjugate-conduction heat transfer in a solid surface included in the boundary conditions and viscous dissipation effects included in the energy equation had analyzed using formulations with one nonsimilar variable ζ ending to the following conclusions:

1. Increasing the magnetic influence numbers had decreased the heat transfer rates for the buoyancy aiding flow, while for the buoyancy opposing flow, increasing the magnetic influence numbers had increased the heat transfer rates up to certain limit after which the heat transfer rates had decreased.

2. Increasing the viscous dissipation parameter had decreased the heat transfer rates for the buoyancy aiding and the buoyancy opposing flows.

3. Increasing the curvature numbers had increased the heat transfer rates for the buoyancy aiding and the buoyancy opposing flows. Where for $\lambda=0$, the problem reduced to flow over a vertical plate.

4. Increasing the inertia numbers had decreased the heat transfer rates for the buoyancy aiding flow. While increasing the inertia terms for the buoyancy opposing flow had increased the heat transfer rates up to certain limit after which the heat transfer rates had decreased.

5. Increasing the conjugate conduction numbers had decreased the heat transfer rates for the buoyancy aiding flow. And increase it up to certain limit and then the heat transfer rates will decrease again.

6. For the case A (entire regime): as the mixed convection parameter ζ, increases the values of Nusselt numbers will increase. This is due to the fact the values of Nusselt numbers of mixed convection regime are higher than those of the pure forced convection or pure free convection limits.

7. For the case B (mixed convection regime): as the mixed convection parameter (Ra_x/Pe_x) increases, the effects of the free convection will increase, thus enhancing the heat transfer rates. Whereas for the buoyancy opposing flow the heat transfer rates will decrease as the mixed convection parameter (Ra_x/Pe_x) increases.

2. Recommendations:

In the present work, the conjugate mixed convection heat transfer along vertical slender, hollow cylinder with MHD effects has been investigated. The following suggestions for further investigation based on the previous work are recommended:

1. Studying the effect of changing the boundary conditions to be constant heat flux at the cylinder surface.

2. Studying the effect of the conjugate conduction heat transfer parameter in the solid to be in two dimensions instead of one dimension.

3. Studying the problem with effect of radiation from the surface of the cylinder.

4. Studying the problem with variations of both velocity and temperature fields in time.

5. Studying the mass diffusion may be included within the governing equations.

6. Studying the effect of injection or withdrawal of fluid from the cylinder.

REFRENCES

Aldoss, T. K., Al-Namir, M. A., Jarrah, M. A., and Al-Sha'er, B. J. (1995). **Magnetohydrodynamic mixed convection from a vertical plate embedded in a porous medium.** Numerical Heat Transfer, part A,28:635-645.

Aldoss, T. K., Jarrah, M. A., and Al-Sha'er, B. J. (1996). **Mixed convection from a vertical cylinder embedded in a porous medium: Non-Darcy Model.** Int.J.Heat Transfer,vol.39.No.6.pp.1141-1148.

Anderson, A., John, C., and Tannehill, R. H.(1984). **Computational Fluid Mechanics and Heat Transfer, Chaps. 3-7.** Newyork: McGraw -Hill Co.

Bejan, A. (1972). **Convection heat transfers, chap. 10.** NewYork.

Cebeci, T. and Bradshaw, P., (1977,a). **Momentum transfer in boundary layers**, **chaps. 7** and 8. Hemisphere, Washington-D.C.

Cebeci, T. and Bradshaw, P., (1984,b). **Physical and Computational Aspects of Convective Heat Transfer.** New York: Springer Co.

Chandra, B., and Gosh, N. (2001). **MHD flow of a visco-elastic fluid through porous medium.** International Journal of Numerical Methods for Heat and Fluid, 11:682-698.

Duwairi, H. M., and Damseh, R. A. (2004,a). **Magnetohydrodynamic natural convection heat transfer from radiate vertical porous surfaces.** Heat and Mass Transfer, 40:787-792.

Duwairi, H. M., and Damseh, R. A. (2004,b**). MHD-Buoyancy aiding and opposing flows with viscous dissipation effects from radiate vertical surfaces.** The Canadian Journal of Chemical Engineering,volume 82,

Duwairi, H. M., and Duwairi, R. M. (2004). **Thermal radiation effects on MHD-Rayleigh flow with constant surface heat flux.** Heat Mass Transfer,41:51-57.

Duwairi,H. M., and Al-Araj, S.(2004). **MHD-mixed convection heat transfer along radiate vertical cylinder.**(1st Conference of thermal Engineering, 31/5-4/6-2004, Lebanon).

Garandet, J. P., Alboussiere, T., and Moreau, R.(1992). **Buoyancy driven convection in a rectangular enclosure with a transverse magnetic field.** Int. J. Heat Mass Transfer, vol. 35, pp. 741-749.

Henoch, C. W., and Meng, J. C. S. (1991). **Magnetohydrodynamic turbulen boundary layer control using external direct current crossed surface poles.** KSME, 5(3):115-121.

Hsieh, J. C., Chen, T. S., and Armaly, B. F. (1993). **Mixed convection along a nonisothermal vertical flat plate embedded in a porous medium: the entire regime.** Int. J. Heat Mass Transfer, vol 36, No 7. pp. 1819-1825.

Hsu, C. T., and Cheng, P. (1985). **The Brinkman model for natural convection a bpout a semi-infinite vertical flat plate in a porous medium.** Int.J.Heat Mass Transfer, vol. 28, pp.683-697.

Holman, J. A. (1990). **Heat Transfer, Ch12.** Newyork: McGraw -Hill Co.

Hossain, M. A.(1992). **Viscous And Joule Heating Effects on MHD-free convection flow with variable plate temperature.** Int. J. Heat Mass Transfer, vol. 35, pp. 3485-3487.

Huang, M. J.,and Chen, C. K.(1984). **Vertical circular pin with conjugated forced convection conduction .** Haw, J, Heat Transfer. 106:458-5-461.

Jha, B. K. (2001). **Natural convection in unsteady MHD couette flow. Heat and Mass Transfer,** vol. 37, pp: 329-331.

Jilani, G., Jayaraj, S., and Ahmad, M. (2002). **Conjugate forced convection-conduction heat transfer analysis of a heat generation vertical cylinder.** International Journal of Heat and Mass Transfer, 45:331-341.

Karvinen, R.(1978). **Some new results for conjugated heat transfer in a rate plate.** Int, J, Heat Mass Transfer.21:1261-1264.

Kaviany, M. (1991). **Principles of heat transfer in porous media.** Springer-Verlag.

Keller, H. B.(1978). **Numerical methods in boundary layer theory.** Ann, Rev, Fluid Mech.10:417-433.

Kim, S., and Lee, C. (2000). **Numerical investigation of cross-flow around a circular cylinder at a low-Reynolds number flow under an electromagnetic force.** Experiments in Fluids. 28:252-260.

Kimura, S., and Pop, I. (1991,a). **Non-Darcian effects on conjugate natural convection between horizontal concentric cylinders filled with a porous medium.** Fluid Dynamics Res. 7:241-254.

Kimura, S., and Pop, I. (1991,b). **Conjugate natural convection between horizontal concentric cylinders filled with a porous medium.** Warrne-undstoffubertr.85-91.

Kimura, S., and Pop, I. (1992). **Conjugate free convection from a circular cylinder in a porous medium.** Int.J. Heat Mass Transfer.36:3105-3113.

Kimura, S., and Pop, I. (1994**). Conjugate convection from a sphere in a porous medium.** Int.J. Heat Mass Transfer.37:2178-2192.

Kimura, S., Kiwata, T., Okajima, A., and Pop, I.(1997). **Conjugate natural convection in porous media.** Adv.Water Resources.20:111-126.

Lesnic, D. , Ingham, D. B., and Pop, I. (1995). **Conjugate free convection from a horizontal surface in a porous medium.** J. Appl. Math Mech. (ZAMM) 75: 715-722.

Luikov, A. V.(1974). **Conjugate convective heat transfer problems.** Int.I.Heat Mass Transfer.17:257-265.

Luikov, A. V., Aleksashenko, V. A., and Aleksashenko, A. A.(1971). **Analytical methods of solution of conjugate problems in convective heat transfer.** Int.I.Heat Mass Transfer.14:1047-1056.

Minkowycz, W. J., and Cheng, P. (1976). **Free convection about a vertical cylinder embedded in a porous medium.** Int. J. Heat Mass Tranfer. 19: 805-813.

Murthy, P. V., and Singh, P.(1997). **Effect of viscous dissipation on non-Darcy natural convection regime.** Int. J. Heat Mass Transfer.40:1251-1260.

Nield, D. A. (1991). **The limitations of the Brinkman-Forchheimer equation in modeling flow in a saturated porous medium and at an interface.** Int.J.Heat and fluid flow. Vol. 12,pp.269-272.

Nield, P. A., and Bejan, A.(1999). **Convection in Porous Media,(2nd ed.).** New York:Springer-verlag .

Oosthuizen, P. H., and Naylor, D.(1999). **An Introduction to Convective Heat Transfer Analysis, Ch.1.** New York:McGraw-Hill.

Plumb, O. A., and Huenefeld, J. C. (1981). **Non-Darcy natural convection from heated surface in saturated porous media.** Int.J.Heat Mass Transfer, vol. 24, pp.765-768.

Pop, I., Lesnic, D. , and Ingham, D. B. (1995). **Conjugate mixed convection on a vertical surface in a porous medium.** Int.J. Heat Mass Transfer.38:1917-1525.

Pop, I., and Merkin, J. H.(1995). **Conjugate free convection on a vertical surface in a saturated porous medium.** Fluid Dynam.Res. 16:71-231.

Pop, I., and Na, T. Y. (2000**). Conjugate free convection over a vertical slender hollow cylinder embedded in a porous medium.** Heat and Mass Transfer,36:375-379.

Raptis, A., and Singh, A. K.(1983). **MHD free convection flow past an accelerated vertical plate.** Int. Comm. Heat Mass Transfer, vol. 10, pp: 313-321.

Sacheti, N. C., and Singh, A. K. (1994). **An exact solution for unsteady magnetohydrodynamic free convection flow with constant heat flux.** Int. Comm. Heat Transfer,21:131-142.

Sparrow, E. M., and Cess, R. D., (1961). **Effect of magnetic field On free convection heat transfer.** Int. J. Heat Mass Transfer, vol. 3, pp:267-27.

Sparrow, E. M., and Chyu, M. K. (1982**). Conjugate forced convection conduction analysis of heat transfer in a plate fin.** ASME J. Heat Transfer. 104:204-206.

Tashtoush, B. J. (2000). **Analytical solution for the effect of viscous dissipation on mixed convection in saturated porous media.** Transport in Porous Media, 41:197-209.

Takhar, H., Chamkha, A., and Nath, G.(2000). **Combined heat and mass transfer along a vertical moving cylinder with a free streem.** Heat and Mass Transfer,36:237-246.

Velusamy, K., and Garg, V. K. (1988). **Heat transfer from a cylindrical fin in combined free-forced flow.**Int.I.Heat Fluid Flow.9:233-240.

Vynnycky, M.,and Kimura, S.(1994). **Conjugate free convection due to a vertical plate in a porous medium.** Int.J. Heat Mass Transfer.37:229-236.

Vynnycky, M.,and Kimura, S.(1995). **Transient conjugate free convection due to a vertical plate in a porous medium.** Int.J. Heat Mass Transfer.38:219-231.

White, F. M.(1991**). Viscous Fluid Flow,(2nd ed.).** New York:McGraw-Hill .

APPENDIX A

COEFFICIENT OF MOMENTUM AND ENERGY EQUATION

The values of the coefficients in equations 4.1 and 4.2

$m_1=H$

$m_2 = Re^*$

$m_3 = \pm (1-\zeta)^2$

$m_4 = \lambda \times \zeta$

$m_5 = Ge^* \times [1+\varepsilon \times (H-1)]$

$m_6 = Ge^* \times Re^*$

The coefficients of the linearized momentum equation 4.33:

$(S_k)_j$ (k=1 to 8) are:

$$(S_1)_j = 0$$

$$(S_2)_j = m_1 h_j^{-1} + 2m_2 h_j^{-1} u_j$$

$$(S_3)_j = -\frac{m_3^n}{2}$$

$$(S_4)_j = 0$$

$$(S_5)_j = 0$$

$$(S_6)_j = -m_1 h_j^{-1} - 2m_2 h_j^{-1} u_{j-1}$$

$$(S_7)_j = -\frac{m_3^n}{2}$$

$$(S_8)_j = 0$$

The coefficients of the linearized energy equation 4.33:

$(B_k)_j$ (k=1 to 8) are:

$$(B_1)_j = \frac{1}{4} V_j$$

$$(B_2)_j = m_5^n U_j + \frac{3}{2} m_6^n U_j^2$$

$$(B_3)_j = h_j^{-1} + \eta_{j-1/2} m_4^n h_j^{-1} + \frac{m_4^n}{2} + \frac{1}{4} f_j$$

$$(B_4)_j = 0$$

$$(B_5)_j = \frac{1}{4} V_{j-1}$$

$$(B_6)_j = m_5^n U_{j-1} + \frac{3}{2} m_6^n U_{j-1}^2$$

$$(B_7)_j = -h_j^{-1} - \eta_{j-1/2} m_4^n h_j^{-1} + \frac{m_4^n}{2} + \frac{1}{4} f_{j-1}$$

$$(B_8)_j = 0$$

The values of the coefficients in equations 4.4 and 4.5

m_1=H

m_2 = Re

$$m_3 = \pm \frac{Ra_x}{Pe_x}$$

$m_4 = \lambda$

$m_5 = 0.5$

$$m_6 = \frac{Pe_x}{Ra_x} [1+\varepsilon \times (H-1)] \times \chi$$

$m_7 = \frac{Ra_x}{Pe_x} \times \mathrm{Re} \times \chi$

$m_8 = \chi$

The coefficients of the linearized momentum equation 4.41:

$(S_k)_j$ (k=1 to 8) are:

$$(S_1)_j = 0$$

$$(S_2)_j = m_1 h_j^{-1} + 2m_2 h_j^{-1} U_j$$

$$(S_3)_j = -\frac{m_3^n}{2}$$

$$(S_4)_j = 0$$

$$(S_5)_j = 0$$

$$(S_6)_j = -m_1 h_j^{-1} - 2m_2 h_j^{-1} U_{j-1}$$

$$(S_7)_j = -\frac{m_3^n}{2}$$

$$(S_8)_j = 0$$

The coefficients of the linearized energy equation 4.42:

$(B_k)_j$ (k=1 to 8) are:

$$(B_1)_j = \frac{\alpha_1}{2} V_j + \frac{\alpha}{2} V_{j-1/2}^{n-1}$$

$$(B_2)_j = m_6^n U_j + \frac{3}{2} m_7^n U_j^2 - \frac{\alpha}{2}\theta_j + \frac{\alpha}{2}\theta_{j-1/2}^{n-1}$$

$$(B_3)_j = h_j^{-1} + \eta_{j-1/2} m_4 h_j^{-1} - \frac{\alpha}{2} f_{j-1/2}^{n-1} + \frac{\alpha_1}{4} f_j$$

$$(B_4)_j = -\frac{\alpha}{2}U_j - \frac{\alpha}{2}U_{j-1/2}^{n-1}$$

$$(B_5)_j = -\frac{\alpha_1}{2}V_{j-1} + \frac{\alpha}{2}V_{j-1/2}^{n-1}$$

$$(B_6)_j = m_6^n U_{j-1} + \frac{3}{2}m_7^n U_{j-1}^2 - \frac{\alpha}{2}\theta_{j-1} + \frac{\alpha}{2}\theta_{j-1/2}^{n-1}$$

$$(B_7)_j = -h_j^{-1} - m_4\eta_{j-1/2}h_j^{-1} - \frac{\alpha}{2}f_{j-1/2}^{n-1} + \frac{\alpha_1}{2}f_{j-1}$$

$$(B_8)_j = -\frac{\alpha}{2}U_{j-1} - \frac{\alpha}{2}U_{j-1/2}^{n-1}$$

أنتقال الحرارة المترافق بالحمل المختلط من على أسطوانة رأسية مفرغة
في وسط مسامي مشبع وممغنط

عمل الطالب

ياسر عبدو القبلاوي

المشرف

د. حمزة مصطفى دويري

الملخص

في هذه الدراسة، التأثير المختلط لأنتقال الحرارة لكل من الحمل القسري و الحمل الطبيعي بوجود حقل مغناطيسي على أسطوانة رأسية مفرغة في وسط مسامي مشبع بوجود تأثيرات لزوجة السائل المتضمنة في المعادلات المتحكمة قد درست. بحثت حالتان من مسألة أنتقال الحرارة بالحمل المختلط و هما جريان سائل طفوي اضافي و جريان سائل طفوي معاكس.

المعادلات المتحكمة حلّت بأستخدام طريقة الفرق المحدد(طريقة كيلر)، و قد تمّ الحصول على الحلول بأستخدام نوعين من الأعداد اللابعدية. العدد الأول ζ و الذي يغطي كامل نطاق أنتقال الحرارة المختلط، حيث ζ=٠ تمثل أنتقال الحرارة بالحمل الطبيعي بينما ζ=١ تمثل حالة أنتقال الحرارة بالحمل القسري. العدد اللابعدي الثاني هو χ والذي يغطي أنتقال الحرارة بالحمل المختلط.

درست تأثيرات الأعداد اللابعدية المختلفة على توزع السرعة و الحرارة اللابعديين في المنطقة الحدّية للجريان و أيضا تأثيراتها على عوامل احتكاك السطح الخارجي المحلية وعلى اعداد نسلت المحلية و من ثمّ رسمت تأثيرات هذه الأعداد اللابعدية في كلتا الحالتين.